Metropolitan Area Groundwater Model
Project Summary

Lower Aquifers Model
Layers 4 and 5

Version 1.00, November 2000

Douglas D. Hansen and John K. Seaberg

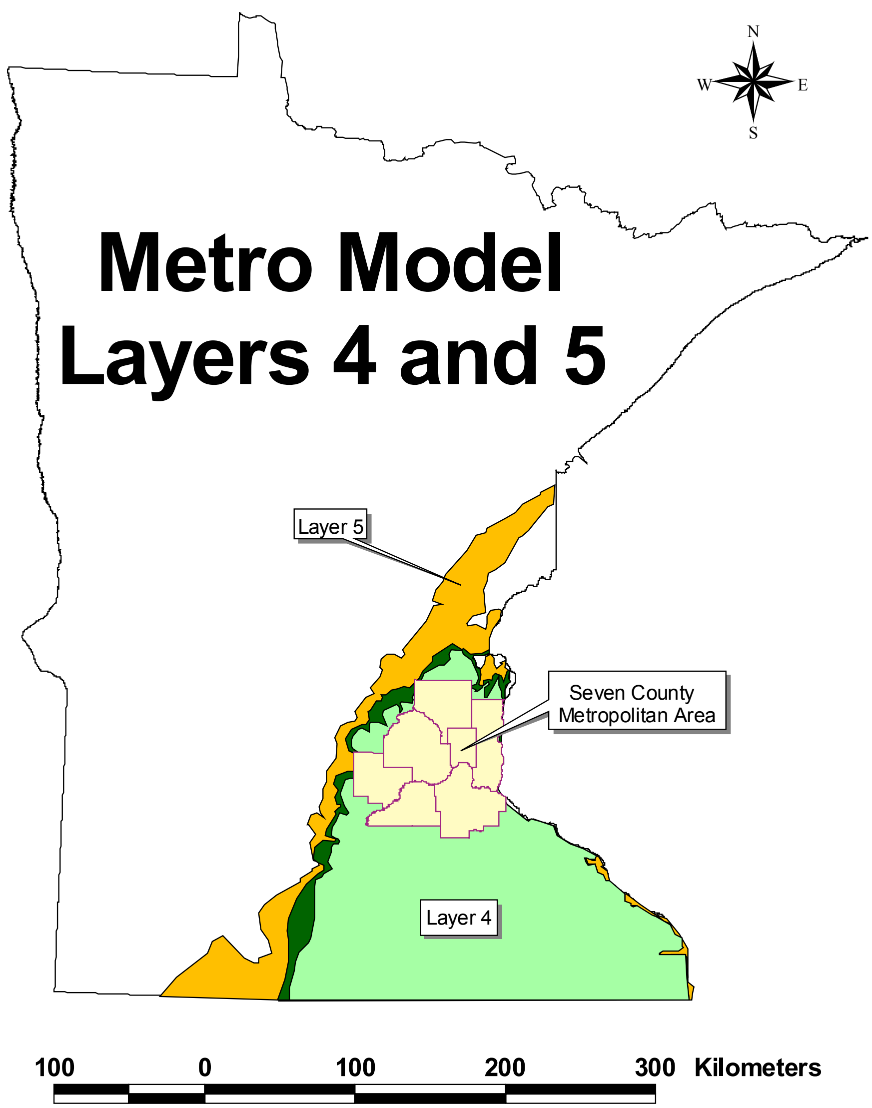

Table of Contents

Figures

Figures Continued

Tables

Metropolitan Area Groundwater Model
Project Summary

Lower Aquifers Model
Layers 4 and 5

Version 1.00, November 2000

Introduction

This document summarizes the development and construction of a module of the Metropolitan Area Groundwater Model (Metro Model) that represents two lower aquifers, and provides a new look at their flow systems and water budgets. The Metro Model is actually comprised of four different steady-state regional groundwater flow models for the seven-county Twin Cities metropolitan area (Figure 1).

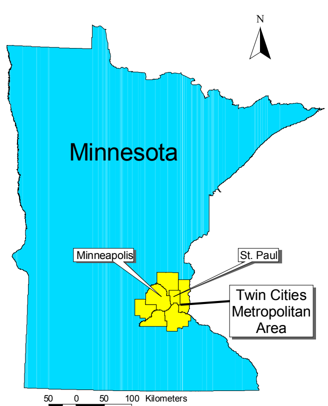

Figure 1 – Metro Model Index Map

Three of the models are for Layers 1 (Glacial Drift Aquifer), 2 (St. Peter Sandstone Aquifer), and 3 (Prairie du Chien/Jordan Aquifer), each model covering a separate hydrologic province as defined by major river valleys (Figure 2).

The fourth model is for the lower portion of the aquifer system representing the Franconia-Ironton-Galesville Aquifer (Layer 4), and the Mt. Simon-Hinckley Aquifer (Layer 5), and encompasses the entire metropolitan area (Figure 3).

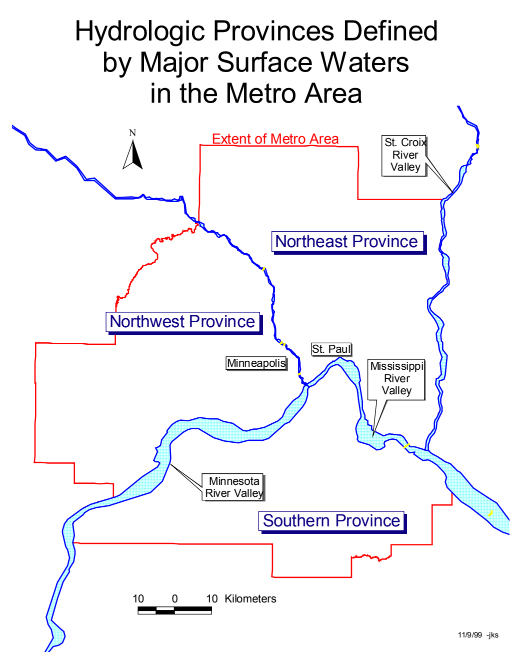

Figure 2 – Hydrologic Provinces

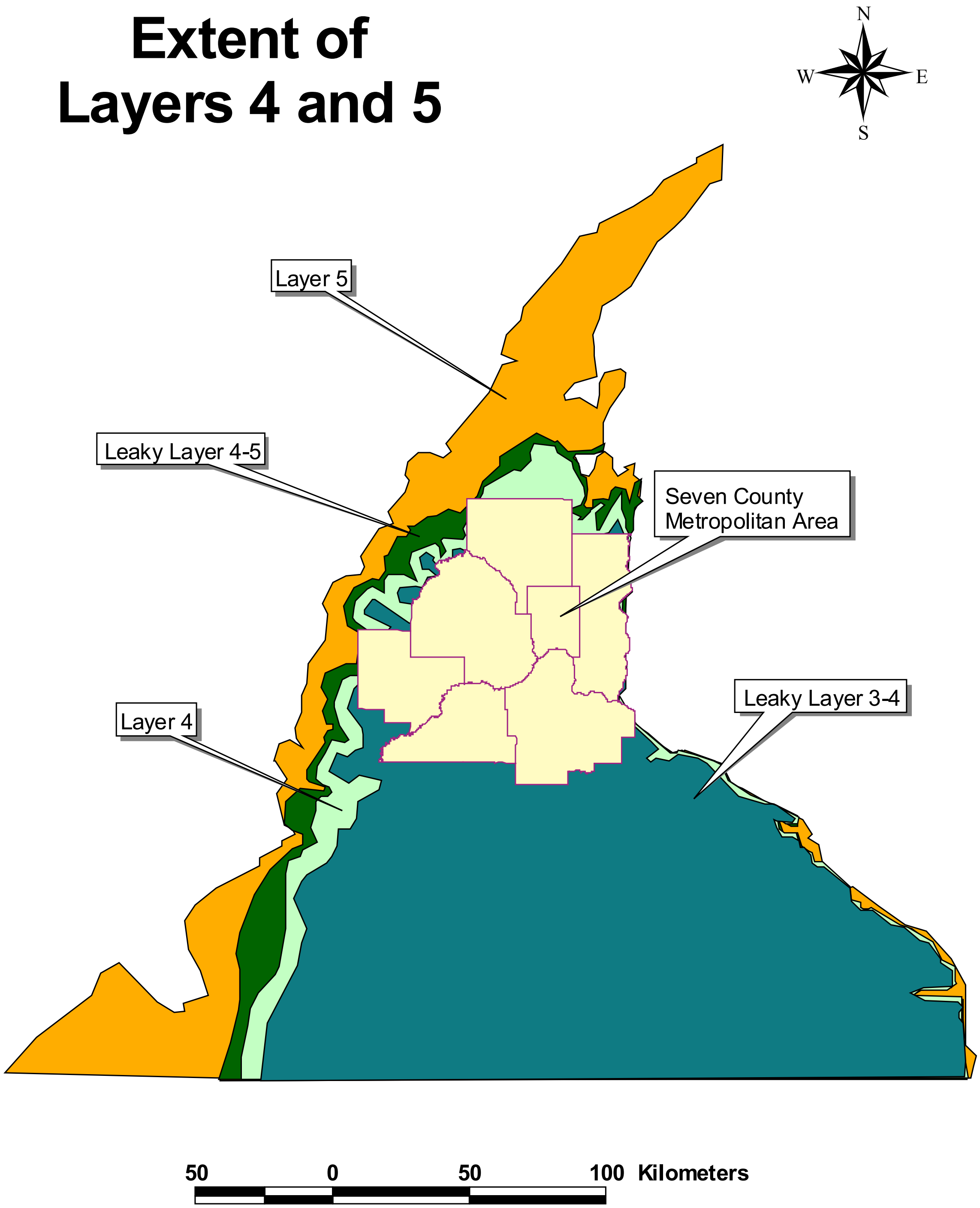

Figure 3 – Extent of Layers 4 and 5 in Minnesota

This report summarizes the development and construction of a steady-state model for Layers 4 and 5, and their connection to the three provinces of Layer 3. The extent of these lower aquifers reaches far beyond the seven-county Twin Cities metropolitan area. Due to their depth and the separating confining layers, they are assumed to be controlled by different boundary conditions than the upper three aquifers. In general, the modeled area encompasses most of the central to southeastern portion of Minnesota. Layers 1, 2, and 3 are absent in this model, but may be linked to the top of Layer 4 for each province on an as-needed basis.

Layer 4 represents the Franconia-Ironton-Galesville Aquifer, which is separated from the Jordan Sandstone above by the St. Lawrence Formation. Layer 5 represents the Mt. Simon-Hinckley Aquifer consisting of sandstone formations. It lies on basement Precambrian rock that is assumed to be impermeable, and is overlain by the Eau Claire Formation, an extensive confining layer comprised of quartzose sandstone with interbedded shales.

This summary has been prepared to provide the user with the basic information required to understand and use the Layers 4 and 5 Model, and to share observations on the flow and water budget of these aquifers derived from the modeling exercise. A full documentation log (over 250 pages) chronicling the construction and development of this module of the Metro Model is contained in four documents that are available on request. Also, more detailed information regarding the overall conceptual model may be found in the general report titled Overview of the Twin Cities Metropolitan Groundwater Model (Seaberg, 2000), which discusses development of the conceptual model and its application to the Multi-Layer Analytic Element Model (MLAEM), the software used for development of the model. Review of and familiarity with this report provides a more complete context in which to read this summary for the Layers 4 and 5 Model. Refer to that document for more complete descriptions of the conceptual model and its implementation in MLAEM.

The development and construction of the Layers 4 and 5 Model are presented in this document, starting with a summary of the lower hydrostratigraphic units, along with global parameters used in the model. This is followed with a discussion regarding the construction of the polygon mesh used to simulate infiltration and leakage and how it is tied in to the hydrogeology. The construction phase of the model is completed with a presentation of how surface waters, buried bedrock valleys, and heterogeneities are represented in the model. A discussion of calibration targets and procedures naturally follows, in which water levels and water budget information were used to tie the model to measured conditions. The final portion of this report presents the actual model datasets that are available for use.

Conceptual Model

Hydrostratigraphy

As stated, the Layers 4 and 5 Model represents the two lowermost aquifers of the five designated aquifers in the Metro Model. Leaky layers representing aquitards separate these layer aquifers. For reasons that will be discussed later, the intrinsic hydraulic properties of the aquitard are not used to determine leaky flow between layers. Instead, the regional Metro Model represents flow between aquifer layers by specifying the actual flux or leakage rates, which are adjusted during calibration procedures. A brief description of the hydrostratigraphy beginning with Layer 3 is provided in this section. Table 1 summarizes the global aquifer parameters used in model construction. The derivation of these parameters is discussed in the Overview of the Twin Cities Metropolitan Groundwater Model (Seaberg, 2000).

Layer 3. Layer 3 represents groundwater flow in the Prairie du Chien Group and the Jordan Sandstone, which together are treated as one aquifer of variable areal extent (Figure 4). Although Layer 3 is absent from the Layers 4 and 5 Model, it is included in the discussion because the geometry of some of the polygons defining leakage to Layer 3 is propagated to some of the leakage polygons of this model. Recharge to Layer 3 occurs as leakage from overlying bedrock units and also from the glacial drift where the formation subcrops beneath it. The geometry of the leakage polygons is a function of major changes in the hydraulic properties within Layer 3 and any aquifer or leaky units overlying it, which will alter the vertical distribution of leakage throughout the aquifer system. Discharge occurs to surface water bodies, primarily the major river systems that physically dissect the aquifer. The assigned global base elevation is 120 meters (m) MSL with a thickness of 60 m. The global value for hydraulic conductivity is 12 meters/day (m/d) and the porosity is 0.090.

Leaky Layer 3-4. This leaky layer represents the St. Lawrence Formation, a regional confining unit that generally allows only negligible leakage to lower aquifers. However, where the Jordan Sandstone is absent, in areas outside its areal extent, or in buried bedrock valleys, the St. Lawrence Formation may be eroded enough to enhance leakage between the Glacial Drift and the Layer 4 aquifers. In addition, erosion of bedrock sequences raised by normal faults along the western portion of the seven-county area may also allow greater leakage between aquifers. This requires the model to take into account leakage through the bottom of Layer 3.

Layer 4. Layer 4 represents groundwater flow in the Franconia, Ironton, and Galesville Formations, and treats them as one hydrostratigraphic unit (Franconia-Ironton-Galesville Aquifer) that extends beyond the seven-county area. Figure 5 shows the extent of these units in Minnesota, but combines the Franconia and St. Lawrence Formations as a confining unit. The decision to consider the Franconia Formation as an aquifer results from its use as the primary aquifer in areas where it is the first bedrock. Recharge to this aquifer occurs as leakage from overlying bedrock units and also from the glacial drift where it overlies the subcrop zone. Water is discharged to major rivers occurring above the erosional subcrop zones of the Franconia-Ironton-Galesville Aquifer and along the St. Croix and Mississippi Rivers, where the formations either subcrop or occur as outcrops. Layer 4 has been assigned a global base elevation of 52 m MSL, a thickness of 60 m, a hydraulic conductivity of 1.7 m/d, and a porosity of 0.28.

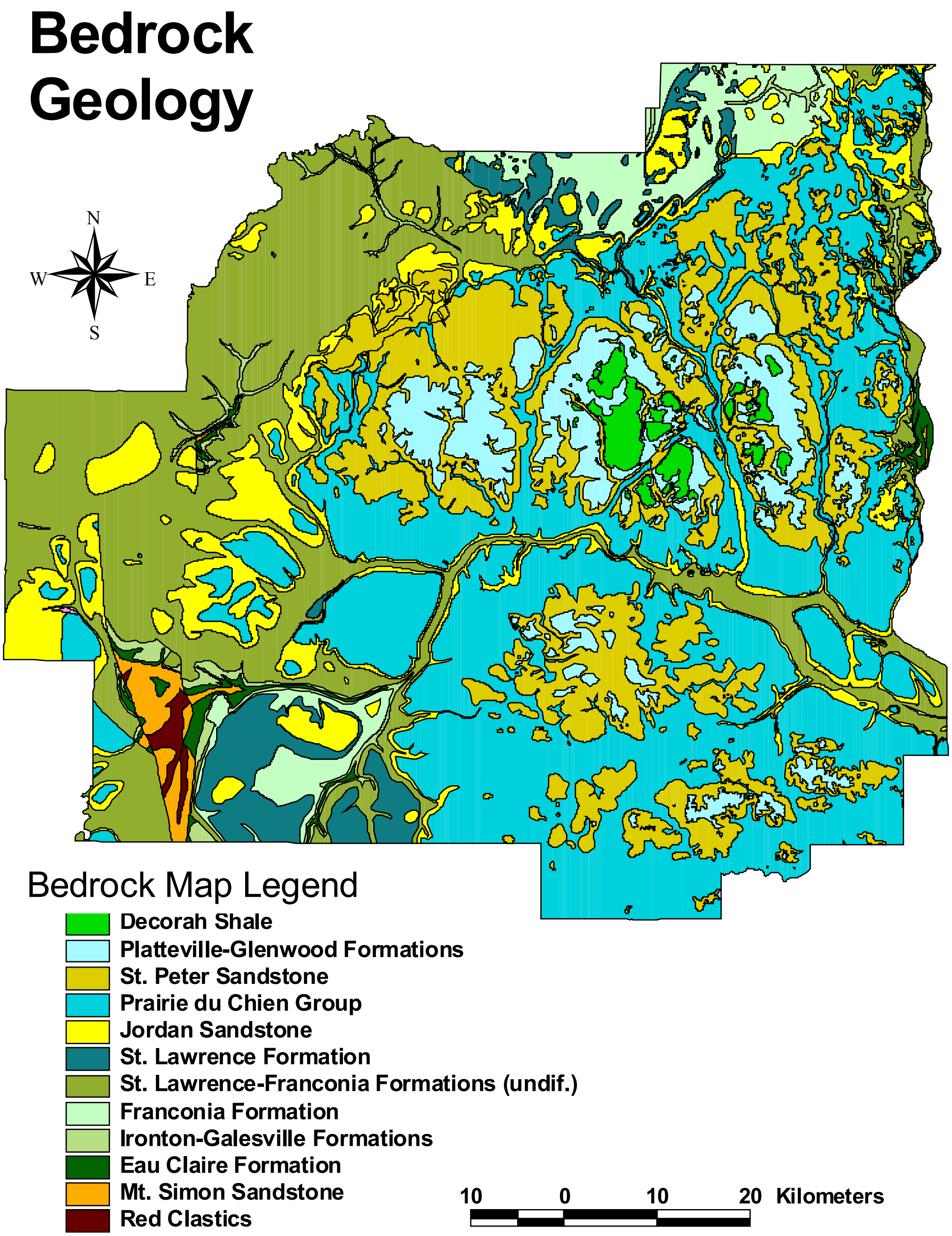

After Mossler and Tipping (2000)

Figure 4 – Bedrock Geology of the Metropolitan Area

Leaky Layer 4-5. This leaky layer represents the Eau Claire Formation, a regional confining unit that generally allows only negligible leakage to the lower aquifer. This aquitard is assumed to occur continuously throughout the modeled area except in two areas: 1) southwestern Scott and southern Carver Counties, and 2) western Hennepin County (Figure 4). Block uplift due to normal faulting and subsequent erosion has exposed lower bedrock aquifers, creating apertures through which inter-aquifer flow is likely enhanced. Leakage may also be enhanced in areas where the Eau Claire Formation occurs as the first bedrock, especially if much of its thickness has been significantly eroded. This is assumed to be the case in the narrow subcrop zone at the outer extent of the formation to the west and north of the metropolitan area, where the unit occurs as the first bedrock beneath glacial drift material (Figure 5).

Layer 5. Layer 5 represents groundwater flow in the Mt. Simon and Hinckley Sandstone Formations, and treats the two formations as one hydrostratigraphic unit extending beyond the seven-county area (Figure 5). Recharge to this aquifer occurs as leakage from overlying bedrock units and also from the glacial drift where the formations subcrop beneath it. Discharge occurs to major rivers below which the Mt. Simon-Hinckley Aquifer is the first bedrock and along the St. Croix and Mississippi Rivers, where the formations either subcrop or occur as outcrops. The assigned global base elevation is -38 m MSL with a thickness of 60 m. The global value for hydraulic conductivity is 4.2m/d and the porosity is 0.22. Precambrian bedrock underlies this aquifer and is assumed to provide an impermeable base to Layer 5 in this model.

Table 1

Global Aquifer Parameters, Layers 4 and 5 Model
Version 1.00

Model Layer	Aquifer	Base Elevation (m MSL)	Thickness (m)	Hydraulic Conductivity (m/day)	Porosity
Layer 4	Franconia-Ironton-Galesville	52	60	1.7	0.28
Layer 5	Mt. Simon-Hinckley	-38	60	4.2	0.22

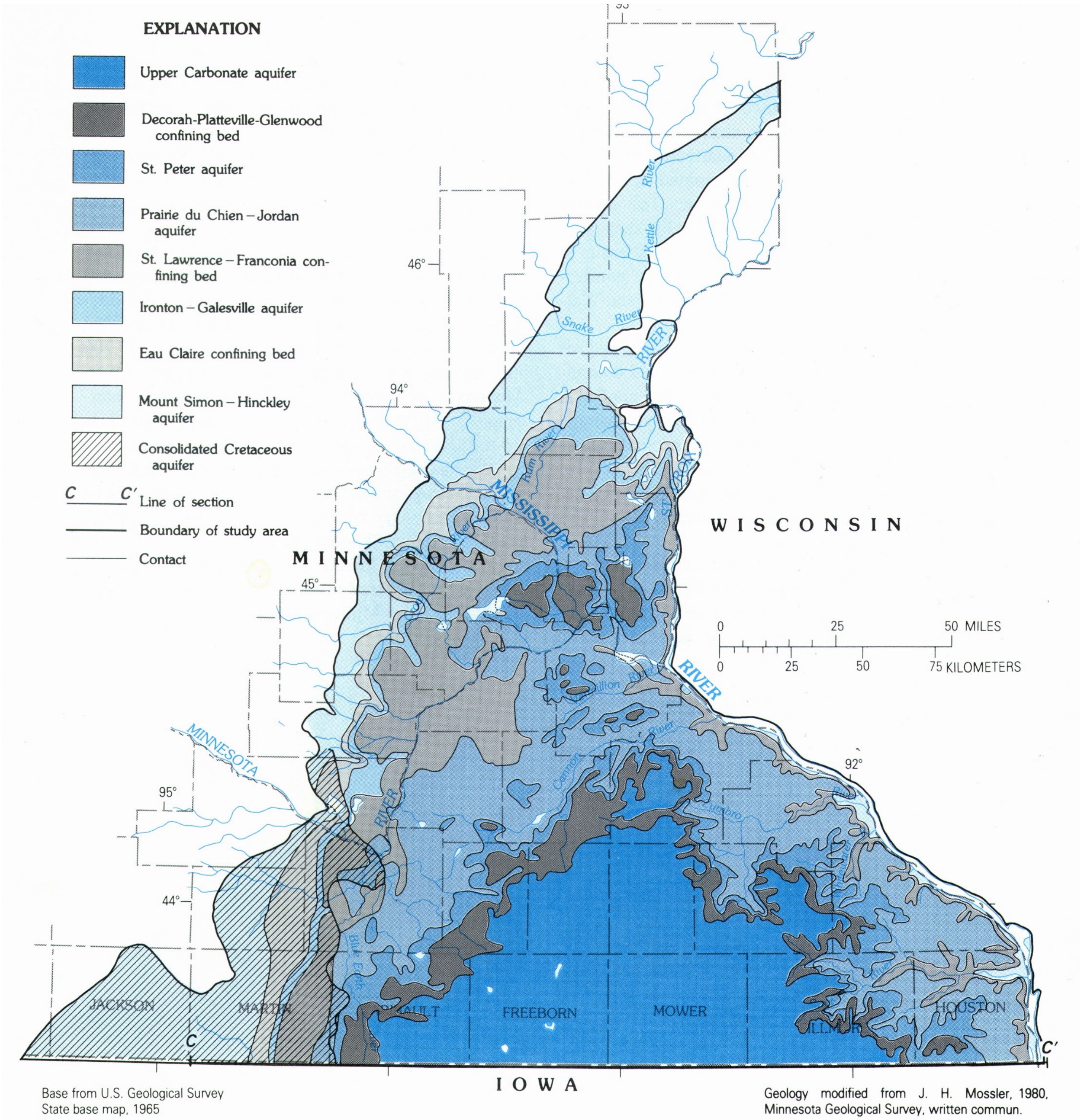

After Figure 2.4-1 of Delin and Woodward (1984)

Figure 5 – Extent of Hollandale Embayment in Minnesota

Implementation. Aquifers constructed using MLAEM are treated as extending infinitely, when in reality they are of very limited extent. However, boundaries are imposed on Layers 4 and 5 by representing the major rivers with hydraulic connections to the aquifers, recharge zones, and general inter-aquifer leakage, which act as hydrologic boundaries to the system. Since the actual bedrock layers have variable limited extents, there are areas in the model where the aquifer is erroneously represented as present within a layer. Depending on the location and on the application of the model, this either may be of no consequence, or may require site-specific customization to model the system and to ensure a proper water balance.

Layers 4 and 5 do not use the same hydrologic boundaries used in Layers 1, 2, and 3. Instead they extend west and north to their respective subcrop zones, where it is assumed both receive most of their recharge. The aquifers continue to the south and east out of the modeled region. Here, large area elements are used to produce leakage over a large area, which, in essence, serves as a hydrologic boundary. In general, the St. Croix River and Mississippi River downstream of the two rivers' juncture act as a near-field hydrologic boundary for the eastern side of the model.

The three province models use only groundwater recharge and leakage rates to maintain the water balance for inter-aquifer flow. The Layer 4 and 5 Model is also calibrated by adjusting recharge and leakage rates, but includes high-capacity pumping in the central portion of the metropolitan area in both layers. This was found to be a necessary part of the water balance in Layer 5. The reason for using pumping wells in Layer 5 stems from previous modeling work and observation well data showing the presence of a regional-scale, or at least province-scale, cone of depression beneath the central metropolitan area. The inclusion of pumping wells helps to simulate this depression cone, which is believed to be changing through time, indicating that this steady state model can provide only a snapshot of changing conditions. This topic will be discussed in greater detail later in this report.

Recharge and Discharge Zones

Groundwater recharge to Layers 4 and 5 is assumed to occur largely throughout the modeled area, including areas where confining units have an estimated resistance to vertical flow (resistivity) that is several magnitudes greater than in upper confining units. Figure 3 shows the extent of the modeled aquifers and confining units, and shows that the lower aquifers have relatively narrow subcrop zones, where the units are free of overlying bedrock confining units. In areas where the overlying confining unit is not covered by other bedrock units, we assume that the effects of lithostatic unloading and weathering decrease the resistivity and allow greater leakage to occur. Therefore, the modeled subcrop zones in both layers include the exposed aquifer unit as well as the exposed overlying confining unit. Although these areas are considered to be major recharge zones for the aquifers, recharge may be enhanced in other areas due to erosion of overlying bedrock.

In the three province models the bottom of Layer 3 is considered to have negligible leakage to lower layers throughout most of the metropolitan area. The geologic unit that corresponds with this negligible leakage boundary is the St. Lawrence Formation. It is generally considered to occur continuously, where it is overlain by the Jordan Sandstone, but as Figure 4 shows a bifurcating buried bedrock valley has eroded to, and in some areas, through the St. Lawrence Formation within the metropolitan area. These erosional zones may represent areas of enhanced inter-aquifer leakage in Leaky Layer 3-4 relative to the adjacent areas where the St. Lawrence Formation is intact.

The condition of the St. Lawrence Formation is not known in the area west and north of the metropolitan area between the subcrop zones of the Jordan and Franconia Formations. Fracturing due to lithostatic unloading, and weathering due to pre-glacial exposure allow us to assume there is increased leakage through the St. Lawrence Formation subcrop zone in comparison to the area directly to the east and south, where it is covered with the Jordan Sandstone. Additionally, leakage through the St. Lawrence Formation in this zone is likely to be enhanced by increased primary hydraulic conductivity effected by a high-energy depositional environment in the northern part of the Hollandale Embayment.

Also, uplift and erosion of bedrock in southwestern Scott, southern Carver, and western Hennepin Counties expose lower aquifers. These erosional apertures may enhance either recharge to or discharge from Layers 4 and 5.

Discharge of groundwater from Layer 4 is assumed to occur via leakage to over- or underlying units and discharge to the Mississippi, Minnesota and St. Croix River valleys. Additionally, there is a net loss of groundwater owing to extraction from pumping wells. High capacity pumping wells are included in this model, but multi-aquifer wells are not explicitly included in this regional scale model. It is assumed their combined discharge effect is reflected in the leakage rates, which were calibrated to measured head data of the County Well Index (CWI).

Discharge of groundwater from Layer 5 is assumed to occur to the major river systems. The greatest influence of the Minnesota River on Layer 5 discharge is assumed to be in southwestern Scott and southern Carver counties. Here, structural activity has elevated the Mt. Simon and Hinckley Sandstone units closer to the surface. In addition, areas where the Mt. Simon-Hinckley Aquifer subcrops along the St. Croix and lower Mississippi River valleys as shown in Figure 5, likely serve as discharge zones for Layer 5.

The Layer 4 and 5 aquifers are both in an ever-changing state that can be attributable, at least in part if not mostly, to changes in storage in aquifers and aquitards effected by pumping regimes that vary over time. Nowhere is this transient nature more apparent than in the Layer 5 aquifer. A groundwater model of the metropolitan area developed by the United States Geological Survey (USGS) (Schoenberg, 1990) and current observation well data from the Minnesota Department of Natural Resources (MNDR) (MDNR, 2000a) indicate that a cone of depression exists in the Mt. Simon-Hinckley aquifer in the metropolitan area. Moreover, analysis of the data from MDNR indicates that the shape, size, and position of the drawdown cone changes over time. The morphology of this drawdown cone reflects both past and present pumping conditions within the Mt. Simon-Hinckley Aquifers and does not represent a steady-state condition. For this reason pumping wells from MDNR's State Water Use Data System (SWUDS) database (MNDNR, 2000b) have been included in Layer 5 to create this existing condition. High-capacity pumping data were derived from SWUDS for the year 1995 and entered into the Layer 4 and 5 model. Currently, we assume that no regional inhomogeneities exist in the Mt. Simon-Hinckley Aquifer or the overlying Eau Claire Formation without the data and information to indicate otherwise.

Initial calibration attempts showed poor agreement between the modeled heads of Layer 5 and the observation well data for the Mt. Simon-Hinckley Aquifer (MDNR, 2000a), which were determined by taking the mean of March data from 1993 through 1998. Although the spatial distribution of the observation well data is quite sparse and varies with time, it is of very high quality. The initial poor calibration could be attributed to any of the following: 1) inhomogeneities in the aquifer and/or aquitard not accounted for by the model, 2) a calibration data set of "observed" heads that does not reflect the 1995 high-capacity pumping conditions derived from the SWUDS database, 3) inaccurate reporting of high-capacity well discharges in SWUDS, or 4) transient effects of a complicated pumping regime over time. Although the degree to which the first three potential causes might impact the results is unknown, observation well data (MDNR, 2000a) clearly show that the piezometric surface of the Mt. Simon-Hinckley Aquifer changes with time within the broader context of a major cone of depression in the metropolitan area. Therefore, in the absence of data or information indicating other causes, the differences between the "observed" and modeled results are attributed primarily to transient conditions within the Layer 5 aquifer. Because the transient history of the aquifer is very complicated and our knowledge likely very incomplete, calibrating the model to transient conditions is not possible with currently available resources. We assumed that changes in the piezometric surface of the Mt. Simon-Hinckley Aquifer are largely a function of changes to its pumping regime, and that matching the "observed" conditions is most appropriately accomplished by adjusting the discharges of the pumping wells since there is uncertainty associated with the congruency of well extraction rates and "observed" heads. Despite the fact that the system is undoubtedly transient, this steady-state model is presented as a first approximation for the regional flow system of the Mt. Simon-Hinckley Aquifer. When and if a true transient model of the Mt. Simon-Hinckley Aquifer is constructed, it will be necessary to account for changes in storage in the aquifer as well as within the leaky Eau Claire Formation.

A discussion on the SWUDS well locations, 1995 pumping rates, and changes to these rates to create the depression cone appears later in the model calibration and results sections.

Model Development and Construction

Polygon Development

Polygons are used to represent infiltration rates and inter-aquifer leakage in MLAEM. There are three different types of variable strength areal elements (VARELs) in MLAEM; each associated with different types of input parameters:

1) **Given-strength** elements are constructed by specifying the actual infiltration or leakage rate for the specified polygon;

2) **Leaky** elements, that separate aquifers specify only the hydraulic resistance (aquitard thickness divided by its vertical hydraulic conductivity); and
3) **Resistance** elements, which have head value (e.g., a surface water elevation), as well as a hydraulic resistance (e.g., of a lakebed) specified.

We have chosen to use given-strength VARELs to simulate inter-aquifer flow since it provides the most computationally expedient means to simulate water throughput on a regional basis. In order to build local models that can effectively simulate inter-aquifer responses to stresses placed on the system, given-strength VARELs in the area of interest must be replaced with Leaky or Resistance VARELs.

Development of the polygon mesh for the lower layers will be described very briefly here. In the three province models polygon construction was based largely on the theory that infiltration to the top of a layered aquifer system will be distributed to the various layers proportional to their transmissivity values in steady-state conditions. This means that any change in hydraulic properties, such as transmissivity or hydraulic resistance, in any of the layers will result in changes in the leakage distribution to all the layers of the system. The polygon mesh that is used to represent various leakage rates must be used to represent all the separating layers between aquifers and all the changes to parameters. This results in the use of a cookie-cutter approach to propagate the mesh throughout all the aquifer separating layers.

The detail of each province model polygon mesh was the result of the heterogeneity of the three uppermost-modeled aquifers. The lower two aquifers occur more or less continuously over large regions and, to the best of our present knowledge, do not exhibit significant spatial variability in hydraulic properties. Therefore fewer polygons are required in the polygon mesh used to model leakage in the lower two aquifers. However, the development of the polygon mesh for this model was influenced by each province polygon mesh in order to provide a means of easily adding upper layers should the need arise. To that end, this model's polygon shapes take into account province polygon shapes as well as the recharge, discharge and far-field zones, and heterogeneities of these layers.

In general the polygons used in this model are large, covering tens to hundreds of square kilometers, with a few far-field elements that are even larger. In some cases, province model polygons are used, and in other cases the province model polygons are subdivided further. Although the polygon mesh for the top of Layer 4 (Leaky Layer 3-4) has several polygons in common with that for the top of Layer 5 (Leaky Layer 4-5), two aspects in the hydrogeology have resulted in a distinctively different polygon mesh for each separating layer. First, the stratigraphically younger position of the formations comprising Layer 4 puts them in closer proximity to surficial processes and features than the Layer 5 formations. Hence, Leaky Layer 3-4 contains more finely subdivided polygons than Leaky Layer 4-5, representing inter-aquifer apertures created by buried bedrock valleys and hydraulic connection to surface water bodies. Note, in particular, the buried bedrock valley in Figure 4 that cuts completely through upper bedrock units and into Leaky Layer 3-4 through the central portion of the seven county metropolitan area. This feature occurs as a series of continuous polygons in Layer 4 (Figure 6) but is not included in Layer 5 (Figure

7). The second difference is that the outer subcrop zone for the Mt. Simon-Hinckley Aquifer (Layer 5) extends farther to the north and west than that for Layer 4. Therefore,

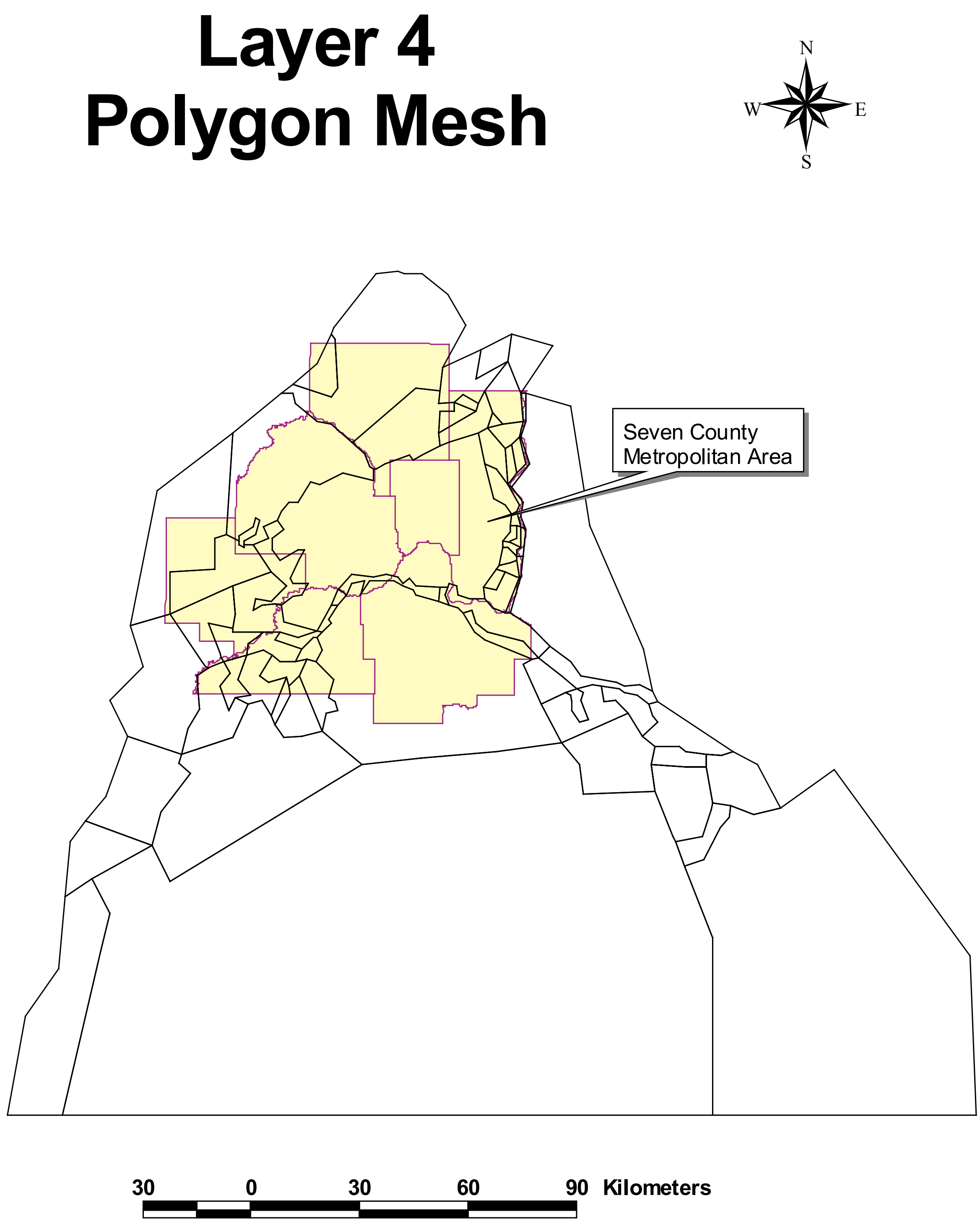

Figure 6 – Layer 4 Polygon Layout

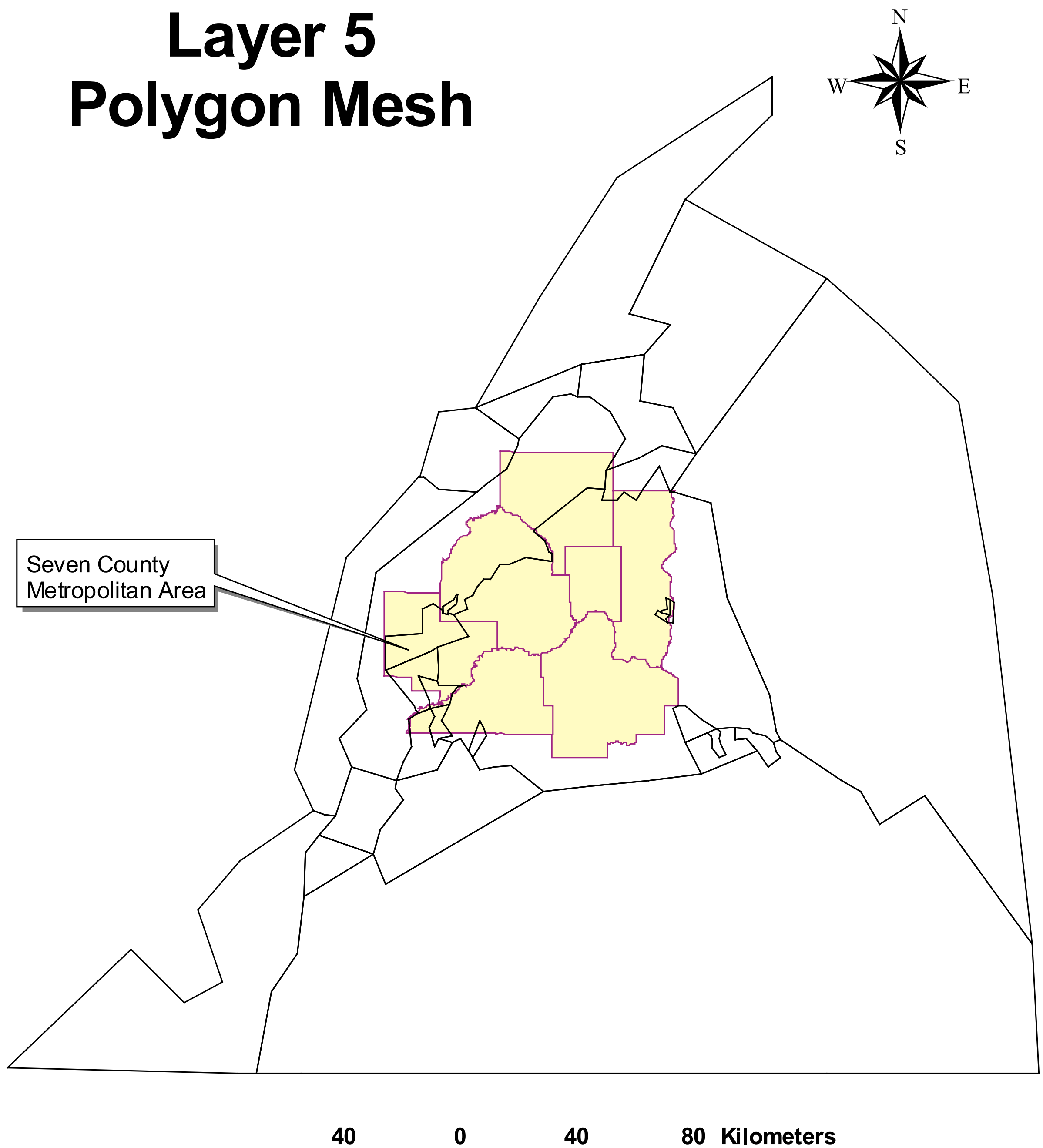

Figure 7 – Layer 5 Polygon Layout

polygons in Leaky Layer 4-5, representing recharge to Layer 5 in its subcrop zone, have been placed to adjoin the west and north edges of the Leaky Layer 3-4 mesh. The polygon mesh on top of Layer 4 is shown in Figure 6 and the one on top of Layer 5 is depicted in Figure 7.

Also note that since the St. Lawrence Formation is likely more permeable in its own subcrop zone as a result of weathering and fracturing, its subcrop expression is also included in the outer recharge zone for the Layer 4 aquifer. This effect is further enhanced in the northern reaches of the Hollandale embayment, where deposition occurred in a near-shore high-energy environment, resulting in a higher primary porosity. Similarly, the outer subcrop zone for the Eau Claire Formation was included as part of the Layer 5 subcrop recharge zone.

Polygon Designation

In order to distinguish between the polygons that comprise the mesh as presented in the preceding pages, the individual polygons must be given unique designations. Since some of the province model polygons are used in this model, the names remain the same to provide consistency between models. The polygon naming convention, therefore, reflects the use of these polygons. In areas over which we have no data indicating variability in the hydraulic properties of the leaky layers, some polygons are grouped together into larger polygons with new names. This is based on the assumption, however, that the hydrogeologic system down to the Prairie du Chien-Jordan Aquifer is largely isolated from the lower aquifers. Outside the hydrologic provinces, polygons used to represent leakage to Layers 4 and 5 have names that reflect whether they represent recharge, discharge, or far-field conditions. There are also a few instances where polygons were required to accommodate geologic structure, which has exposed the lower layers.

The general naming convention for standard infiltration and leakage polygons uses the following format:

[field 1][field 2]-[number]

Where: field 1 — Is a single letter that represents which hydrologic province the model lies in. Because this document is describing the Layers 4 and 5 model, which has incorporated polygons from all the provinces, each of these designations appear in the polygon mesh. The letter prefixes are assigned as follows:

E	Northeast Province
S	South Province
W	Northwest Province

In some instances large leakage polygons are used in this model, to represent areas within an aquitard that have not indicated variability in hydraulic characteristics. These polygons encompass most of the standard infiltration and leakage polygons of the three province models. A different designator is used in field 1, which pertains to a specific layer. The prefixes assigned in this case are:

L4	Layer 4
L5	Layer 5

field 2 Is generally represented by the first letter of the county name in which the polygon predominantly lays. One or more of the following may be found:

A	Anoka County
C	Carver County
D	Dakota County
H	Hennepin County
R	Ramsey County
S	Scott County
W	Washington County
LS	Le Sueur County
RI	Rice County
G	Goodhue County

Where large leakage polygons extend over more than one county, field 2 is represented simply by:

LKG	Leakage

Number This is the sequential number assigned to the polygons within each county. These numbers are generally assigned by starting in the northernmost part of the county and working southward.

Polygons not falling under the general category include those defined by buried bedrock valleys, recharge, subcrop, and far-field zones. These are covered in the following paragraphs:

Buried Bedrock Valleys: A continuous buried bedrock valley reaching from southwestern Scott County, into southeastern Hennepin County, and eastern Dakota County is shown in Figure 4. Province model polygon names are used where individual polygons occur, but through the central portion of Layer 4 the polygons were lumped into one, as well as in the lower Mississippi River valley within the metropolitan area. Here, an L4 prefix is used to indicate that the polygon represents a connection to Layer 4. The polygon names are listed below in order from west to east as they are used in this model.

SS-BV_5	Southern portion of the eastern fork of the Scott County buried bedrock valley
SS-BV_4	Middle portion of the eastern fork of the Scott County buried bedrock valley
SS-BV_3	Northern portion of the eastern fork of the Scott County buried bedrock valley
SS-BV_2	Western fork of the Scott County buried bedrock valley
SS-BV_1	Northern portion of the Scott County buried bedrock valley
MNR_BV_2	Minnesota River intersection with buried bedrock valley at Scott County
L4-BV_1	All of the buried bedrock valley in Hennepin County and the northern portion of the Dakota County buried bedrock valley
SD-BV_2	Northern portion of the Dakota County buried bedrock valley that is directly west of Spring Lake on the Mississippi River
L4-BV_2	The portion of the buried bedrock valley underlying Spring Lake and the Mississippi River in eastern Dakota County.
L4-BV_3	Portion of the Dakota County buried bedrock valley that is directly south of Spring Lake on the Mississippi River
L4-BV_4	The portion of the buried bedrock valley underlying the Mississippi River south from near Red Wing, MN.

Layer 5 Recharge Zones: These zones refer to areas where the aquifer unit is exposed beneath drift material and where the overlying Eau Claire Formation is presumed to have undergone some erosion, resulting in reduced resistance to vertical flow compared to the areas where the overlying bedrock aquifers are still intact. Polygons representing these zones have the following designators:

[field 1][field 2]-[number]

Where:	field 1	Layer designation.
	field 2	Is "RE", indicating "recharge".
	Number	Is the sequential number assigned to each of these polygons.

Subcrop Zones: In Layer 5 these zones lie between the recharge zones and the areas where upper bedrock aquifers of the province models exist. They also represent areas of Layer 4, where the aquifer unit is exposed beneath drift material and where the overlying aquitard is presumed to have undergone some erosion and therefore its resistance to vertical flow is less significant than in areas where there are overlying bedrock aquifers. Polygons representing these zones have the following designators:

[field 1][field 2]-[number]

Where:	field 1	Layer designation.
	field 2	Is “SC”, indicating “subcrop”.
	Number	Is the sequential number assigned to each of these polygons.

In some cases subcrop zones may be represented by province polygons, where the areas are the same.

Far-Field Features: These polygons generally represent areas down-gradient from the area of concern, but which affect flow to hydrologic boundaries. Polygons representing these zones have the following designators:

[field 1][field 2]-[number]

Where:	field 1	Designates the layer —“L4” is used for Layer 4, “L5” for Layer 5.
	field 2	Is “FF”, indicating “far-field”.
	Number	Is the sequential number assigned to each of these polygons.

The geometry of these polygons is determined in part by the areal extent of lower hydrostratigraphic units, which will help facilitate linking the upper layers with the lower layers, should the need arise.

The polygon mesh with labels for Layer 4 is presented in Figures 8 and 9 below. Figure 8 emphasizes the regional layout, and Figure 9 focuses on the metropolitan area. The polygon mesh with labels for Layer 5 is presented in Figure 10.

Layer 4 Regional Polygon Mesh with Labels

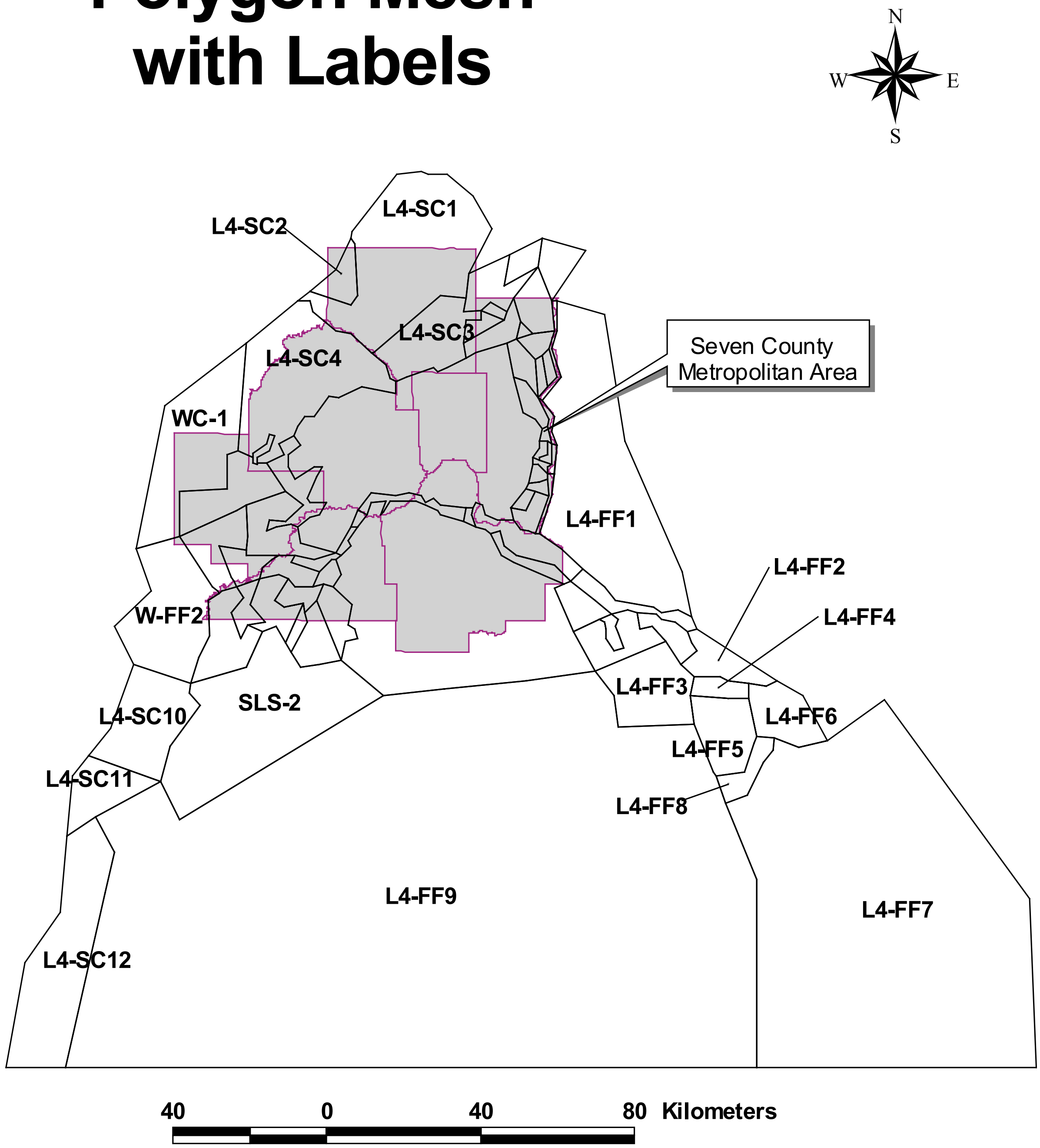

Figure 8 – Layer 4 Regional Polygon Mesh with Labels

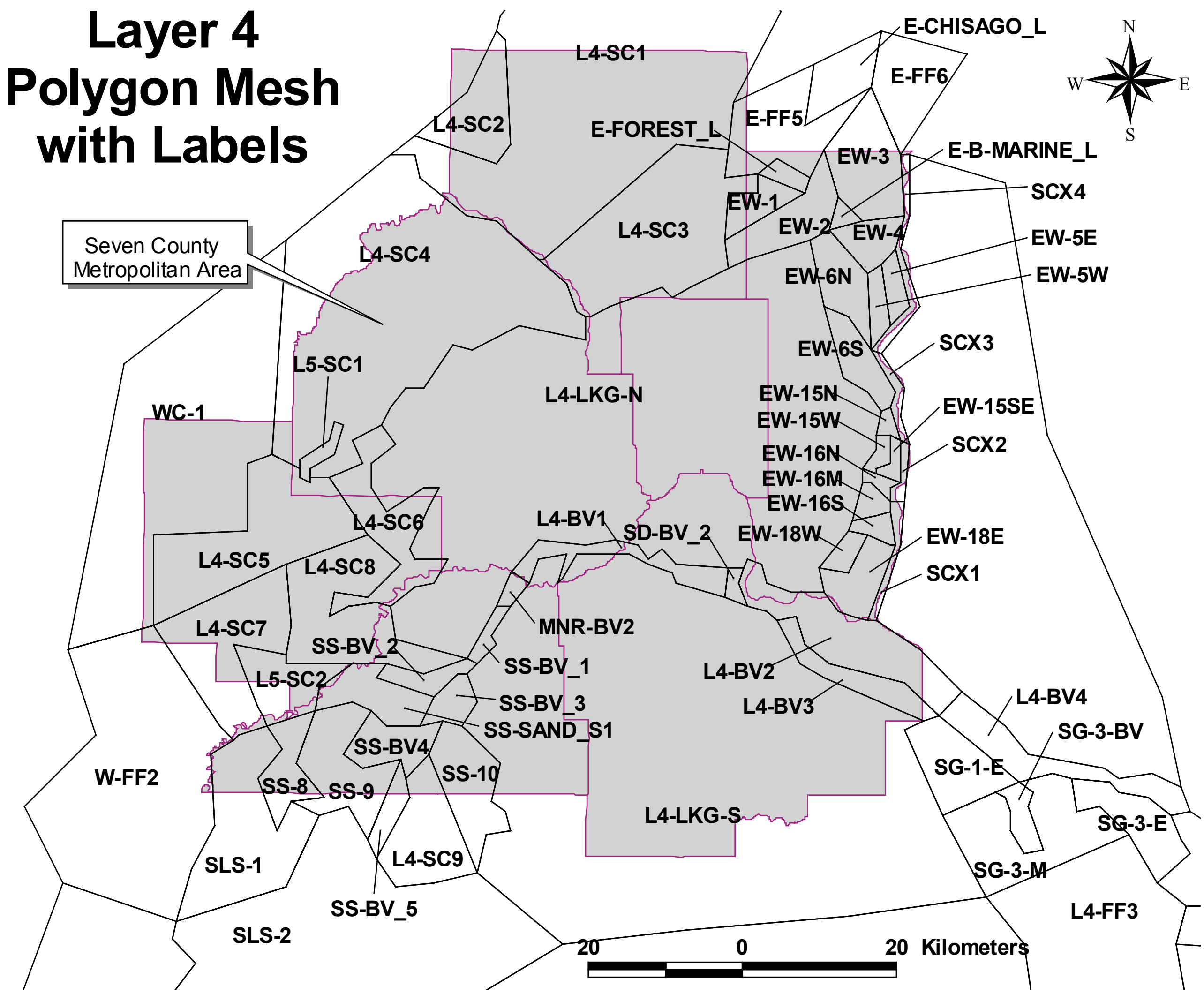

Figure 9 – Layer 4 Polygon Mesh with Labels, Metro Area

The polygon mesh provides the framework for modeling infiltration and leakage values, which are entered in the model as given-strength rates. Assignment of the leakage values to individual polygons for each layer will be discussed below in the section labeled **Modeling of Leakage**.

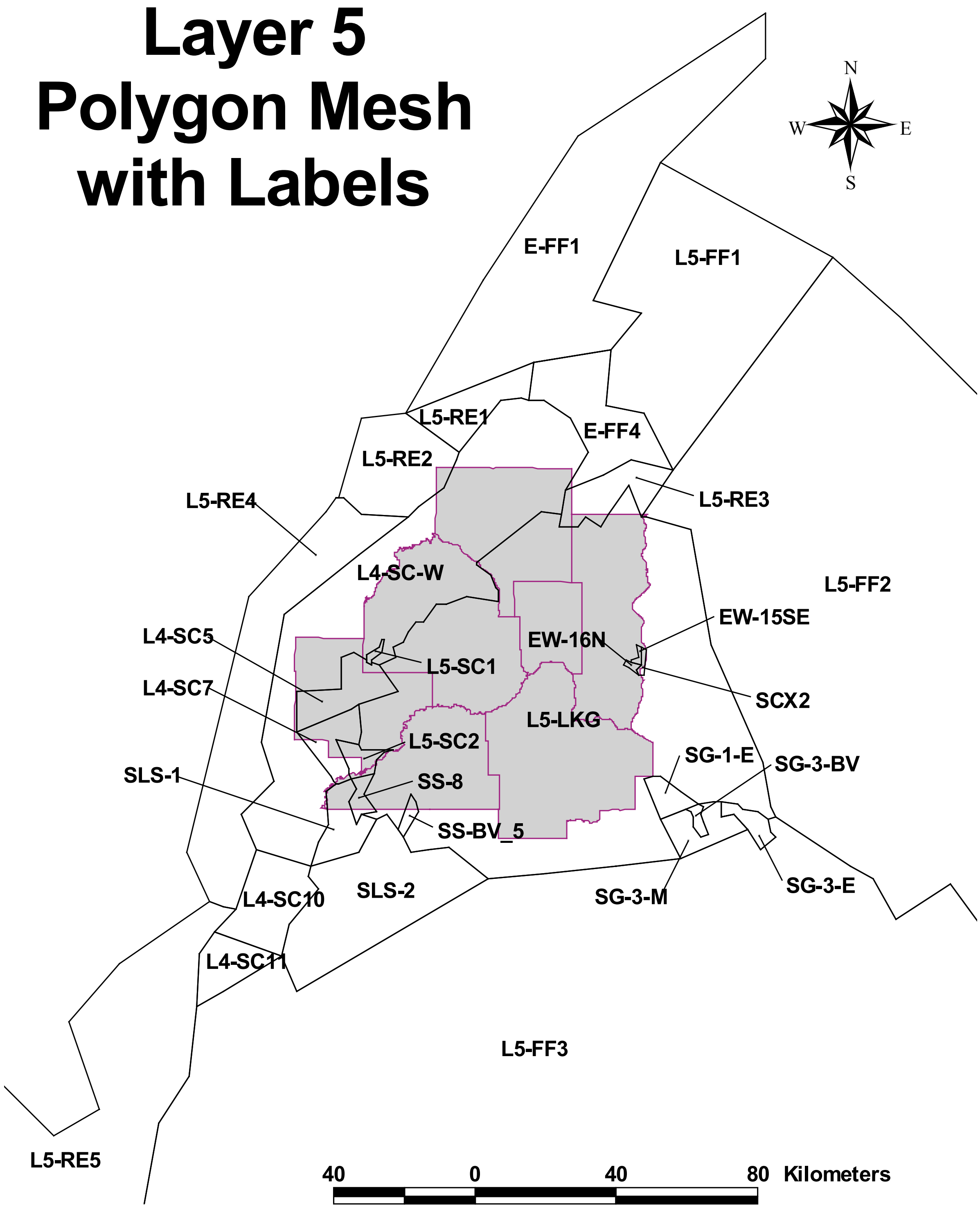

Figure 10 – Layer 5 Polygon Mesh with Labels

Curvilinear Line-sink Construction

Head-specified curvilinear line-sinks were used to represent hydrologic boundaries in both layers. Experimentation was conducted using different types of elements to represent the surface waters: head-specified line-sinks, resistance line-sinks; head- and resistance-specified (resistance) variable strength areal elements (VARELs), and resistance-specified (leaky) VARELs to vertically transmit flow between aquifers to the modeled boundary. We found that the head-specified line-sink was the most computationally efficient and also provided a good approximation of the boundary conditions for the regional models. This was true even if they represented surface water bodies that are not in direct hydraulic communication with the aquifer.

Order and overspecification values for curvilinear line-sinks control model accuracy and optimization of the solution in a least squares sense in the vicinity of the element. In this model, the order of the curvilinear elements generally is set at 4, with an overspecification of 1.5 to 2. These values provide sufficient accuracy for the regional extent of this model. However, a lower value was used for the continuation of the Mississippi River into southeastern Minnesota, where less accuracy is sufficient for the far-field condition. Site-specific applications will necessitate increasing order and overspecification values on curvilinear elements in the area of interest—the respective default values of 6 and 4 assigned by MLAEM provide a good starting point for this type of detailed work.

Head-specified curvilinear line-sinks are used in this model to represent rivers, either as hydrologic boundaries, or as features lying in the interior of the province, where they are considered to have a hydrologic connection to the aquifer. Some of the line-sinks also represent seepage faces of the aquifer that may daylight near the river valley.

Impermeable curvilinear line-sinks are used to simulate linear no-flow zones for two special situations. The first situation regards the physical areal extent of the aquifers. The model extends to the western and northern subcrop zones of Layers 4 and 5, beyond which the aquifers do not exist. Impermeable boundaries were placed immediately outside the subcrop zone for each layer to impose a no flow boundary that prevents the simulation of recharge that is not actually occurring.

The second situation involves a normal fault in southeastern Washington County in Layer 4. An impermeable line-sink simulates the hydraulic obstacle imposed by a portion of the fault along the eastern side of an anticline in that area. Although this is certainly not the only fault occurring within the metropolitan area, it has been included in this regional model because of its impact on calibration. The fault is referred to as the Hastings Fault on Plate 1 of the MGS map M-55 (MGS, 1986) and is shown in Figure 11.

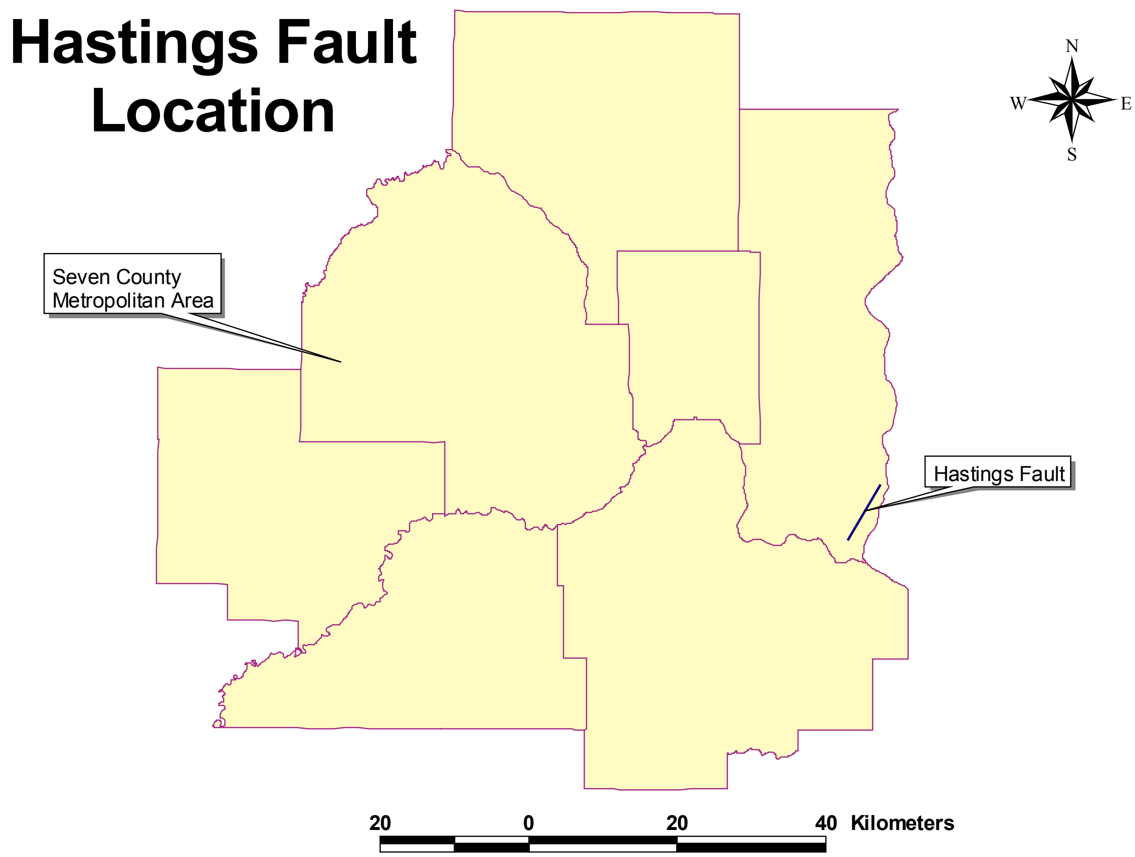

Figure 11: Modeled Hastings Fault

Use of curvilinear line-sinks in each aquifer layer are presented and illustrated in the following paragraphs.

Layer 4 Curvilinear Line-sinks

Figure 12 illustrates the placement of the curvilinear line-sinks in Layer 4 to represent significant regional river features assumed to be in hydraulic connection with the aquifer. The choice of river features to include in the model was also dependent upon available calibration data, which provided insight into hydraulic connection between the aquifer and surface features. Refer to the section on calibration data sets for locations of calibration data points. A comparison of the hydrography with the curvilinear line-sinks illustrates that the model is a simplification of reality. Clearly, site-specific modeling will require detailed work to include features representing flow on a local basis.

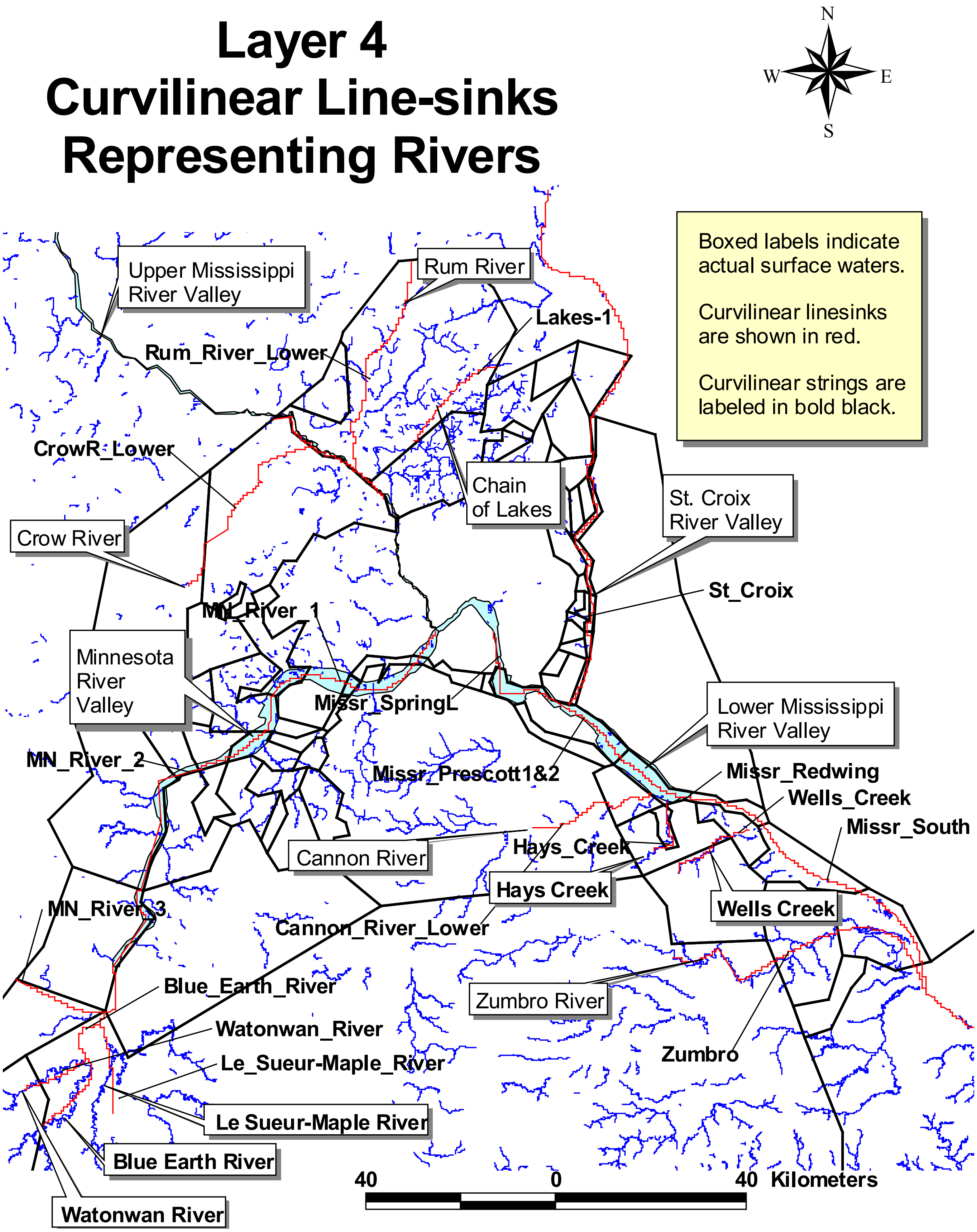

Figure 12 – Layer 4 Curvilinear Line-sinks

In addition to the line-sinks shown above, Layer 4 contains impermeable line-sinks to represent a no flow boundary along the west and north and the Hastings Fault as shown in Figure 13.

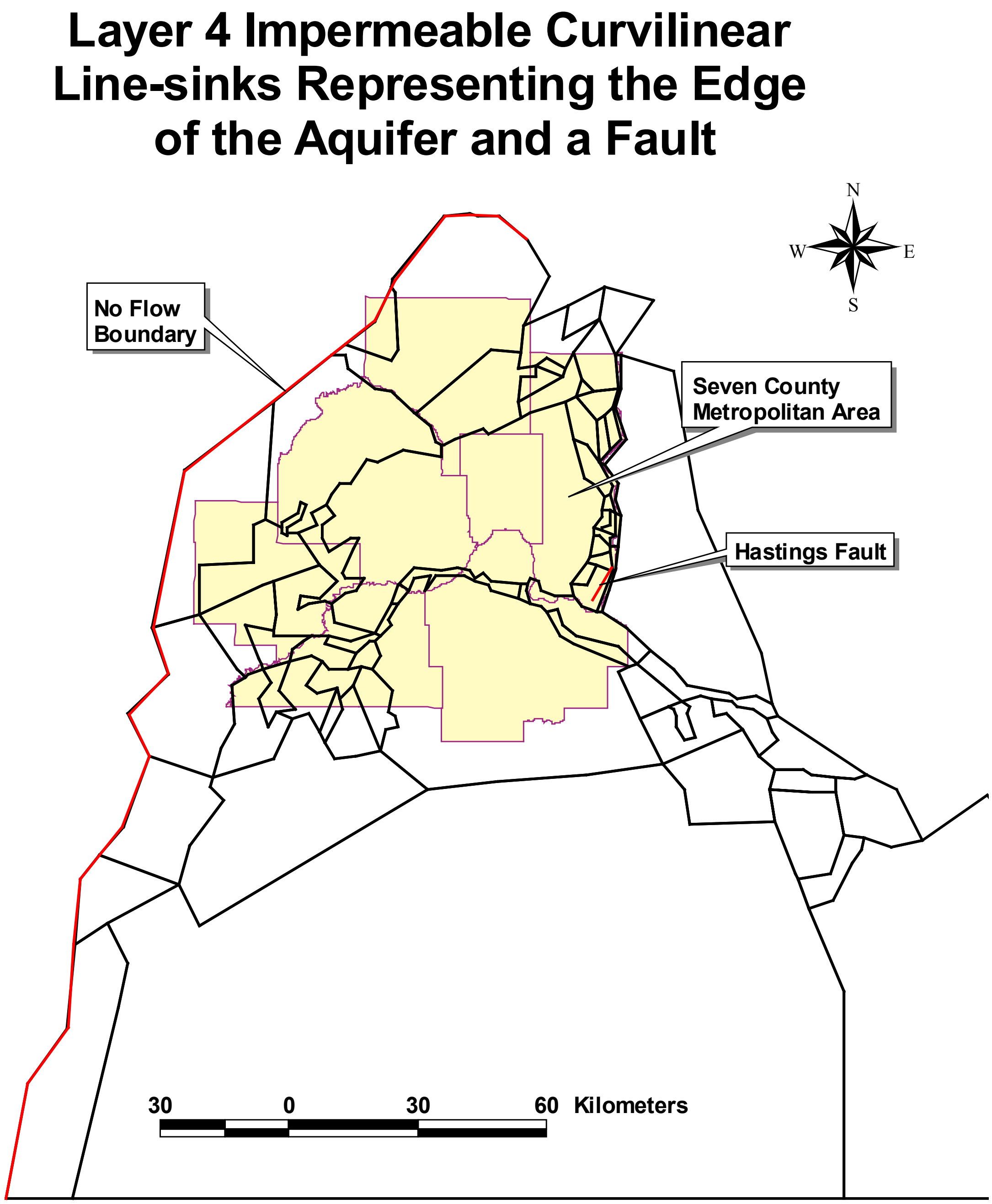

Figure 13 – Layer 4 Impermeable Line-sinks

Layer 5 Curvilinear Line-sinks

A connection between the Mt. Simon-Hinckley aquifer and surface water features is assumed to occur where the aquifer is the first bedrock beneath the feature or there is sufficient erosion of overlying bedrock units to permit interaction. Figure 14 illustrates the placement of the curvilinear line-sinks in Layer 5 to model river elements. Again, a comparison of the hydrography with the curvilinear line-sinks illustrates that the model is a simplification of reality and site-specific modeling will necessarily require detailed work to include features impacting flow on a local basis.

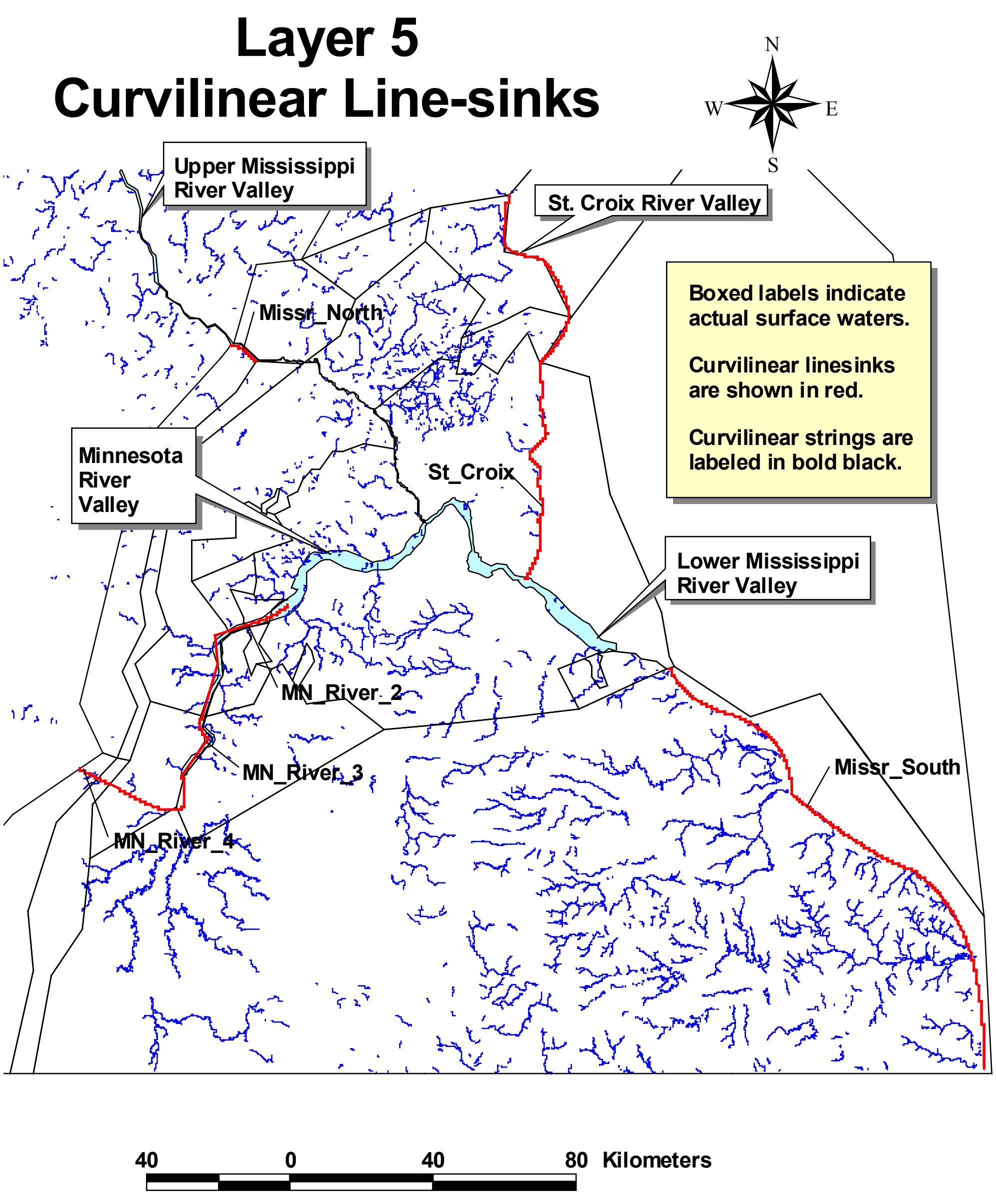

Figure 14 – Layer 5 Curvilinear Line-sinks

In addition to the line-sinks shown above, Layer 5 contains an impermeable line-sink to represent a no flow boundary along the west and north. It is shown in Figure 15.

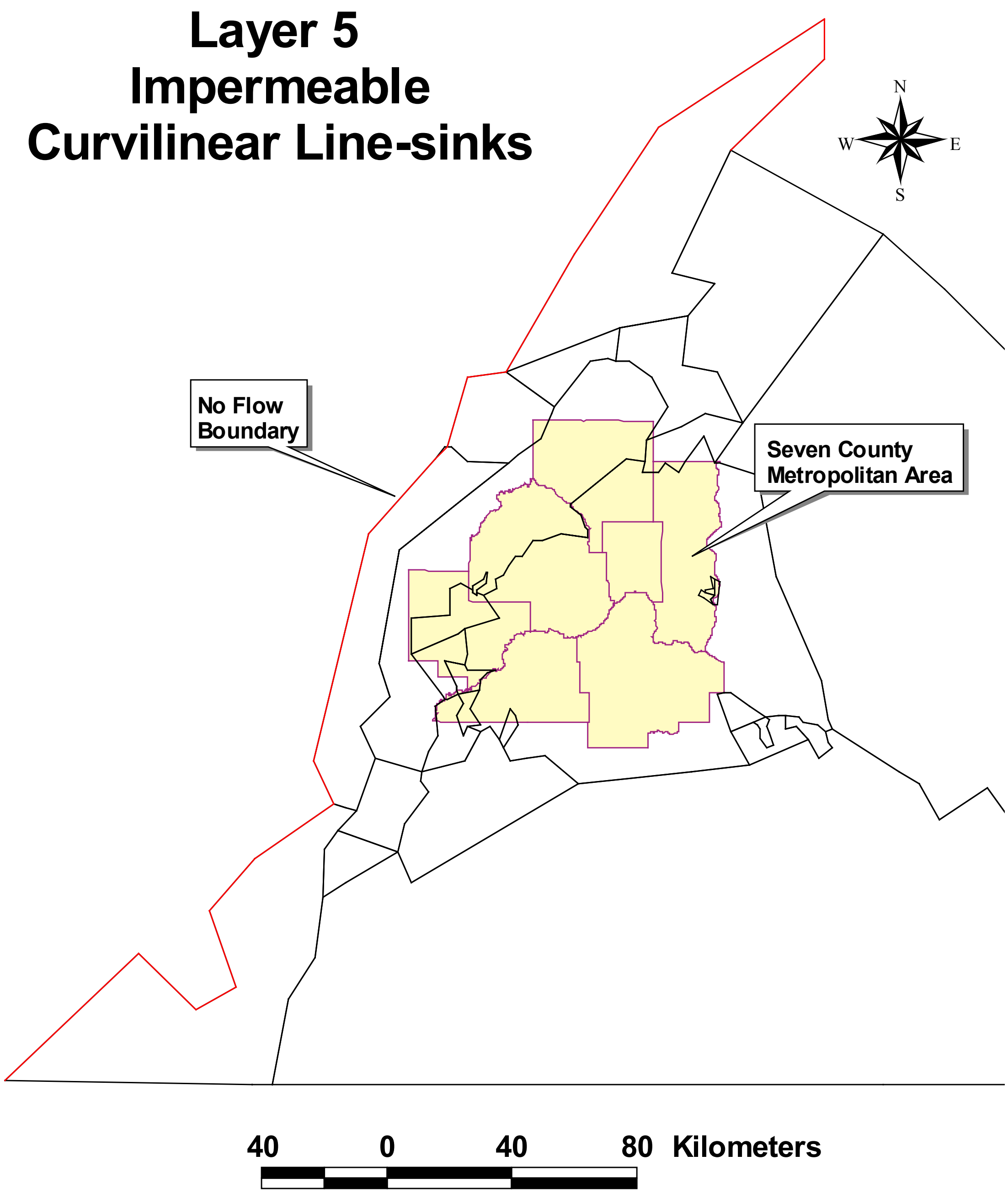

Figure 15 – Layer 5 Impermeable Line-sink

Model Adjustment and Calibration

Layers 4 and 5 were calibrated by manually adjusting the infiltration and leakage rates of the polygons. Additionally, the input elevations of the northern portion of the St. Croix curvilinear line-sink were modified during the calibration procedures.

After input heads were assigned to the curvilinear line-sinks, high capacity pumping wells were added to the model in both Layers 4 and 5. The discharge rates for the wells were taken from the SWUDS database. Well locations for Layers 4 and 5 are shown in Figures 16 and 17 respectively, and average daily discharge rates, in cubic meters per day (cmd), are given in Tables 2 and 3 respectively. These average daily discharge rates are based upon the reported annual total pumping in 1995. However, pumping rate adjustments were made to certain wells in Layer 5 during the calibration process. The assigned discharge rates are the result of the model calibration process and reflect the current state of the cone of depression with respect to the calibration data set. Initial and final pumping rates for these wells are shown in Table 3.

Multi-aquifer wells that are open to both Layers 4 and 5 for which pumping data was available from 1995 were tested, but are not included in the final model. It was hoped the addition of these wells would provide the required draw down in Layer 5 without adjusting pumping rates in certain Layer 5 wells. The distribution of the multi-aquifer wells was such that the regional piezometric head in Layer 4 was lowered, requiring additional leakage to be added, which in turn was transported to Layer 5 via the multi-aquifer wells. The result was a higher piezometric surface in Layer 5 and a lower one in Layer 4, the opposite of the desired result.

Since the amount of water drawn from each aquifer by these multi-aquifer wells is unknown and the exercise above resulted in adding more water to Layer 5, the multi-aquifer wells were not included in the model. It is assumed the calibration data sets for each layer reflect the use and effects of multi-aquifer wells.

NOTE: For users of this model who are uncomfortable with the adjustments made to pumping rates, subsequent work with well data prior to the release of this model version is included in Appendix A. New average daily discharge rates for Layer 5 were calculated from average annual total pumping for the years 1995 through 1998 as reported in the SWUDS database. Multi-aquifer wells that are open to both Layers 4 and 5 for which pumping data was available from 1995 were also included. Keep in mind that the use of multi-aquifer wells does not allow each layer to be modeled independently of the other. This work points out that pumping plays a critical role in the hydrogeology of the lower layers and this model’s interpretation of the system is by no means the final word.

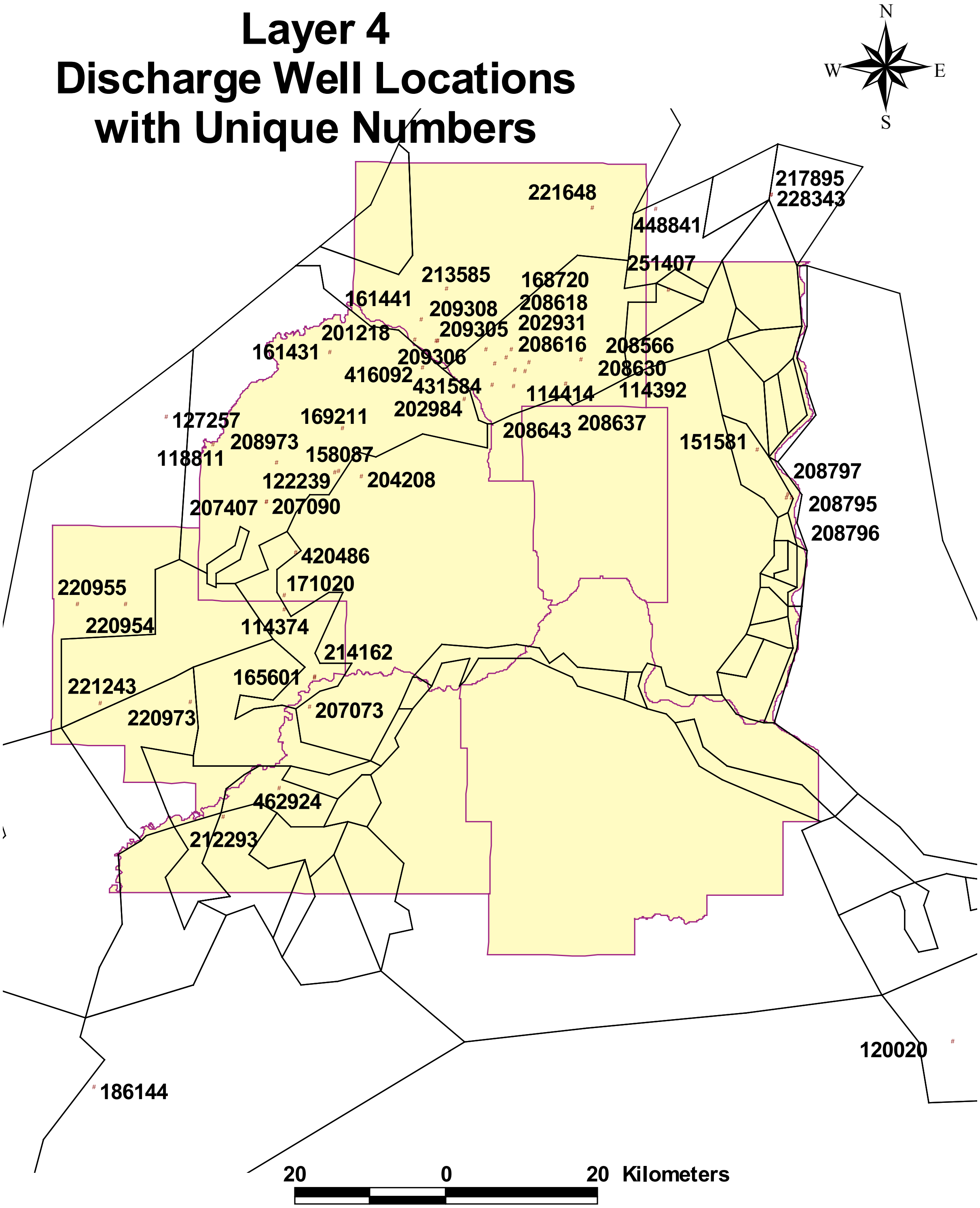

Figure 16 – Pumping Wells in the Franconia-Ironton-Galesville Aquifer

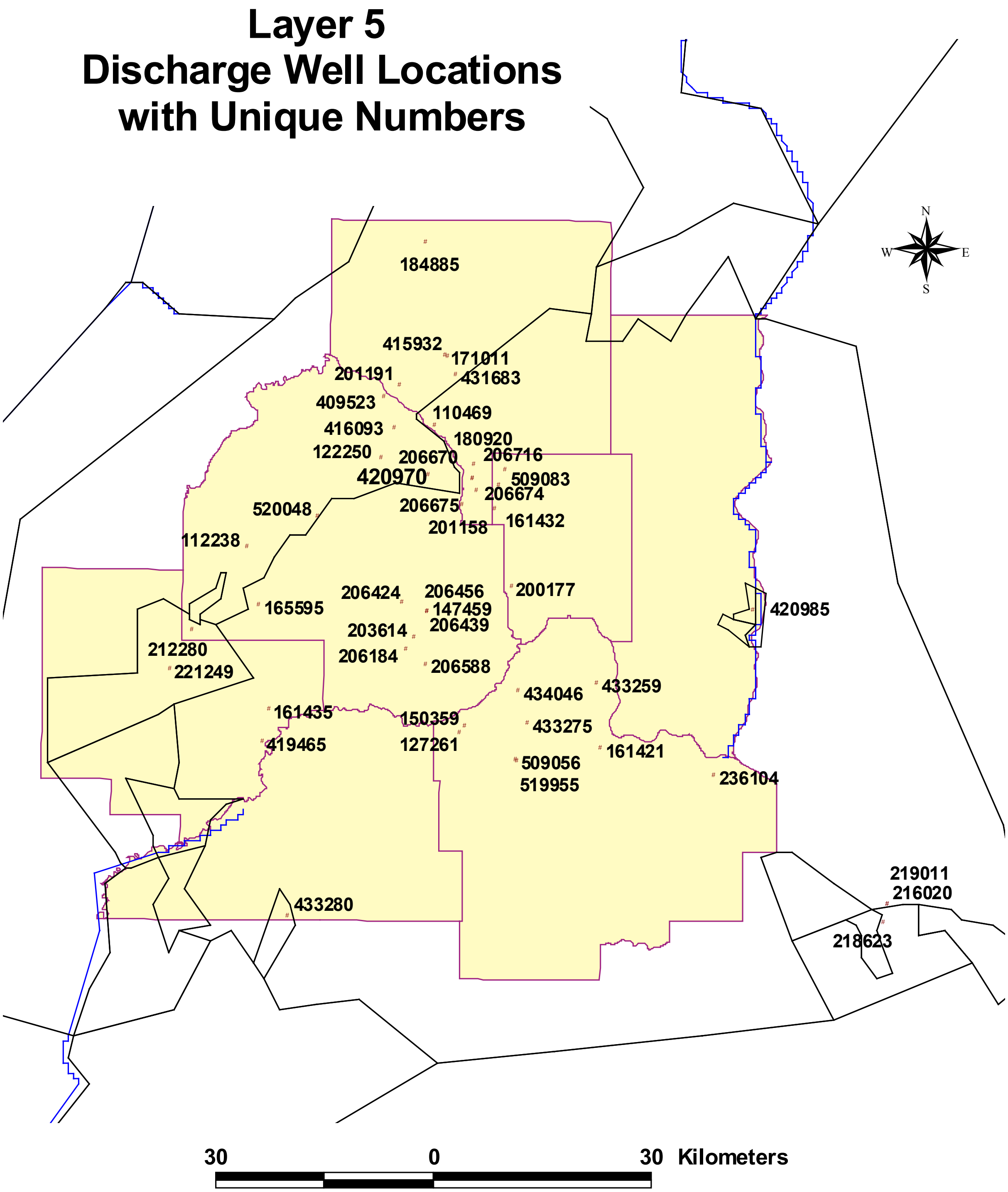

Figure 17 – Pumping Wells in the Mt. Simon-Hinckley Aquifer

Table 2: Layer 4 Discharge Wells

UTM_E	UTM_N	Unique Number	Discharge (cmd)
450801	4970091	114374	96.74
483006	5002703	114392	20.74
482538	5001454	114414	9.33
441399	4991766	118811	50.25
538887	4912946	120020	30.98
457377	4988054	122239	76.97
435190	4995439	127257	60.32
513242	4991073	151581	30.02
457965	4988256	158087	102.72
456703	5003987	161431	904.69
468782	5008315	161441	1184.37
454673	4960985	165601	187.84
477386	5004347	168720	143.14
458401	4993923	169211	57.54
450758	4971805	171020	185.28
425588	4906866	186144	28.71
468048	5005617	201218	1162.45
478587	5002538	202931	672.03
474496	4997799	202984	0.54
460949	4987618	204208	65.10
454068	4957159	207073	138.98
448375	4984155	207090	3.17
448375	4984155	207407	718.91
489840	5002936	208566	280.13
480024	5003362	208616	493.83
480640	5004374	208618	276.79
481217	5001560	208630	1187.53
487816	4999727	208637	789.65
480984	4999542	208643	511.28
516957	4984700	208795	313.72
517255	4985204	208796	258.59
517661	4984804	208797	187.88
449713	4989388	208973	185.39
470944	5005422	209305	114.95
470743	5005529	209306	39.98
470944	5005422	209308	594.43
442734	4942489	212293	10.89
472096	5012307	213585	45.07
454675	4961181	214162	604.85
514949	5024790	217895	69.90
429855	4970617	220954	161.08
423542	4970664	220955	144.50
438345	4957729	220973	5.51
426507	4957654	221243	256.16
491486	5023133	221648	95.84
514949	5024790	228343	75.80
501400	5012263	251407	55.94
468923	5002013	416092	184.51
452232	4977582	420486	45.84
478183	4999678	431584	53.14
499823	5022851	448841	7.66
450070	4946450	462924	673.27

Table 3: Layer 5 Discharge Wells

UTM_E	UTM_N	Unique Number	Modeled Discharge (cmd)	Reported Discharge (cmd)
472910	5026061	184885	665.14	665.14
479594	4995372	180920	1043.78	1043.78
475687	5010465	171011	729.38	729.38
475884	5010258	415932	101.89	101.89
477061	5007816	431683	720.37	720.37
477966	4989842	201158	3197.29	3197.29
479333	4993405	206670	389.70	389.70
479947	4991793	206674	2249.19	2249.19
479333	4993405	206675	1860.09	1860.09
469273	5006417	201191	1696.51	1696.51
474094	5000807	110469	215.58	215.58
450441	4957213	419465	198.37	198.37
437670	4967221	221249	22.86	22.86
451349	4961675	161435	3665.75	1835.71
512542	4952604	236104	183.77	251.22
496422	4965225	433259	2396.32	2396.32
477500	4958550	127261	3976.84	799.03
478215	4959451	150359	3976.84	2020.76
486901	4959756	433275	4508.73	96.07
485683	4964181	434046	2710.00	677.23
485296	4954702	509056	2415.66	143.08
485496	4954500	519955	4831.32	231.23
497002	4956269	161421	10560.91	10560.91
536420	4934734	216020	422.51	422.51
535824	4932338	218623	747.84	747.84
536420	4934734	219011	780.60	780.60
440858	4972581	212280	346.90	346.90
450035	4976036	165595	378.45	378.45
457965	4988256	520048	288.10	288.10
448375	4984155	112238	12.04	12.04
467122	5004833	409523	2105.29	2105.29
468533	5000417	416093	1368.74	1368.74
473251	4994003	420970	38.83	38.83
471309	4971574	203614	1056.60	1056.60
470249	4969920	206184	3088.47	3088.47
472962	4967878	206588	1684.30	1684.30
473123	4975193	147459	1675.09	0.00
473123	4975193	206439	1719.96	1719.96
473123	4975193	206456	3671.91	3671.91
466900	4996262	122250	1746.77	32.17
483772	4994764	206716	47.53	47.53
482459	4989279	161432	246.95	246.95
482939	4992641	509083	57.79	57.79
484718	4978538	200177	1400.00	25.39
453896	4933119	433280	488.70	488.70
517932	4975399	420985	550.67	550.67
469655	4976502	206424	4472.99	4472.99

Modeling of Leakage

The final infiltration rates used in the model are presented in Tables 4 and 5 below (Layers 4 and 5 Leakage Inputs, Version 1.00). Note that the negative values refer to downward leakage, and that a negative net value indicates a gain of water, while a positive value indicates a net loss of water within the aquifer from that polygon, following MLAEM's convention of data input. This is seen both in Table 4 and in the figures that plot the net leakage rates for each polygon. However, this convention is dropped in the discussions of infiltration and leakage presented here, so that leakage and infiltration rates will not be referred to as negative. These values were determined through manual adjustment and calibration procedures, in conjunction with manually adjusting the input heads on the curvilinear line-sinks. An automated optimization program could be used to attempt to improve the fit to measured heads by adjusting the leakage values. However, the current leakage rates should suffice until we learn more about the hydrogeology of the lower aquifers or until more detailed modeling is conducted. Modifications to the regional model or site-specific applications could entail changes to hydraulic properties, boundary heads, and high-capacity pumping rates. Further adjustments to leakage would be most beneficial after the other input parameters have been better defined.

Total system infiltration rates (inches/year) are plotted for each polygon on Figure 18, where both layers exist. Net leakage rates for each aquifer layer will be presented in a similar fashion later as part of this discussion. The most notable value perhaps is that for polygon L5-SC1 (Figure 10), which at 19 inches/year, is apportioned primarily (18.68 inches) to Layer 5. Figure 19 shows this polygon coinciding with a zone where the Mt. Simon-Hinckley aquifer is exposed beneath drift material in western Hennepin County.

The overlying drift material was geostatistically analyzed by MPCA staff for sand content percentage. An explanation of this analysis can be found in the report entitled, "Preparation of Supporting Databases for the Metropolitan Groundwater Model" (Streitz, 2000). These sand content analyses show a high percentage of sand (40 to 90 percent) in the lower 40 meters of the 80 meters of analyzed thickness over the area of the Mt. Simon-Hinckley exposure. Figure 20 shows the different sand content intervals overlying the subcropping aquifer.

The high leakage rate to Layer 5 in polygon L5-SC1 is also influenced by the presence of nearby calibration wells. Their locations with respect to this subcrop zone are shown on Figure 19. Matching model heads to the average head assigned to these wells required the leakage rate of 19 inches/year.

Table 4
Layer 4 Leakage Inputs
Version 1.00

POLYGON	Layer 4 Top (Total Infiltration) (m/day)	Layer 4 Top (Total Infiltration) (in/year)	Layer 4 Bottom (m/day)	Layer 4 Net (Top - Bottom) (m/day)	Layer 4 Net (Top - Bottom) (in/year)	Corresponding Layer 5 POLYGON
L4-SC1	-2.51E-05	-0.36	-3.10E-06	-2.20E-05	-0.316	L4-SC-W
L4-SC2	-5.51E-05	-0.79	-3.10E-06	-5.20E-05	-0.747	L4-SC-W
L4-SC3	-1.02E-05	-0.15	-1.00E-07	-1.01E-05	-0.145	L5-LKG
L4-SC4	-2.82E-05	-0.41	-3.10E-06	-2.51E-05	-0.361	L4-SC-W
L4-SC5	-3.10E-06	-0.04	-1.10E-06	-2.00E-06	-0.029	L4-SC5
L4-SC6	-6.02E-05	-0.86	-1.00E-07	-6.01E-05	-0.863	L5-LKG
L4-SC7	-5.61E-05	-0.81	-1.10E-06	-5.50E-05	-0.790	L4-SC7
L4-SC8	-1.40E-07	0.00	-1.00E-07	-4.00E-08	-0.001	L5-LKG
L4-SC9	-4.13E-05	-0.59	-1.00E-07	-4.12E-05	-0.593	L5-LKG
L4-SC10	-3.13E-05	-0.45	-1.10E-06	-3.02E-05	-0.435	L4-SC10
L4-SC11	-5.70E-05	-0.82	-1.10E-06	-5.59E-05	-0.803	L4-SC11
L4-SC12	-1.40E-05	-0.20	-2.50E-06	-1.15E-05	-0.165	L5-FF3
L5-SC1	-1.32E-03	-18.97	-1.30E-03	-2.00E-05	-0.287	L5-SC1
L5-SC2	-1.59E-04	-2.28	-2.09E-04	5.00E-05	0.718	L5-SC2
WC-1	-1.11E-05	-0.16	-3.10E-06	-8.00E-06	-0.115	L4-SC-W
W-FF2	-1.81E-05	-0.26	-3.10E-06	-1.50E-05	-0.216	L4-SC-W
SLS-1	-2.61E-05	-0.38	-4.87E-05	2.26E-05	0.324	SLS-1
SLS-2	-2.10E-06	-0.03	-1.00E-07	-2.00E-06	-0.029	SLS-2
SS-8	-8.01E-04	-11.50	-8.70E-04	6.95E-05	0.999	SS-8
SS-9	-1.39E-04	-2.00	-1.00E-07	-1.39E-04	-1.997	L5-LKG
SS-10	-8.01E-05	-1.15	-1.00E-07	-8.00E-05	-1.150	L5-LKG
SS_SAND_S1	-3.01E-05	-0.43	-1.00E-07	-3.00E-05	-0.431	L5-LKG
SS-BV_1	-2.00E-04	-2.88	-1.00E-07	-2.00E-04	-2.874	L5-LKG
SS-BV_2	-1.00E-07	0.00	-1.00E-07	0.00E+00	0.000	L5-LKG
SS-BV_3	-3.01E-05	-0.43	-1.00E-07	-3.00E-05	-0.431	L5-LKG
SS-BV_4	-6.10E-06	-0.09	-1.00E-07	-6.00E-06	-0.086	L5-LKG
SS-BV_5	1.17E-04	1.69	-1.50E-04	2.67E-04	3.843	SS-BV_5
MNR_BV_2	-5.00E-04	-7.19	-1.00E-07	-5.00E-04	-7.185	L5-LKG
SD-BV_2	-4.00E-04	-5.75	-1.00E-07	-4.00E-04	-5.748	L5-LKG
L4-BV1	-2.00E-04	-2.88	-1.00E-07	-2.00E-04	-2.874	L5-LKG
L4-BV2	-2.00E-07	0.00	-1.00E-07	-1.00E-07	-0.001	L5-LKG
L4-BV3	-1.10E-06	-0.02	-1.00E-07	-1.00E-06	-0.014	L5-LKG
L4-BV4	-3.00E-07	0.00	-1.00E-07	-2.00E-07	-0.003	L5-LKG
L4-LKG-S	-5.20E-06	-0.07	-1.00E-07	-5.10E-06	-0.073	L5-LKG
L4-LKG-N	-4.10E-06	-0.06	-1.00E-07	-4.00E-06	-0.057	L5-LKG
L4-FF1	-5.20E-06	-0.07	-1.00E-07	-5.10E-06	-0.073	L5-LKG
L4-FF2	4.84E-04	6.96	-2.50E-06	4.87E-04	6.993	L5-FF3
L4-FF3	-8.65E-05	-1.24	-2.50E-06	-8.40E-05	-1.207	L5-FF3
L4-FF4	-4.90E-04	-7.04	-2.50E-06	-4.88E-04	-7.005	L5-FF3
L4-FF5	-2.00E-05	-0.29	-2.50E-06	-1.75E-05	-0.251	L5-FF3
L4-FF6	-1.40E-04	-2.01	-2.50E-06	-1.38E-04	-1.976	L5-FF3
L4-FF7	-7.50E-06	-0.11	-2.50E-06	-5.00E-06	-0.072	L5-FF3
L4-FF8	-1.77E-04	-2.54	-2.50E-06	-1.75E-04	-2.508	L5-FF3
L4-FF9	-5.00E-06	-0.07	-2.50E-06	-2.50E-06	-0.036	L5-FF3
SG-1-E	-1.86E-04	-2.68	-1.40E-06	-1.85E-04	-2.658	SG-1-E
SG-3-M	-3.48E-04	-5.01	-5.00E-07	-3.48E-04	-4.999	SG-3-M
SG-3-E	-1.53E-05	-0.22	-1.40E-06	-1.39E-05	-0.200	SG-3-E
SG-3-BV	-1.83E-04	-2.63	-5.57E-04	3.74E-04	5.374	SG-3-BV
E-FF5	-8.50E-06	-0.12	-7.00E-06	-1.50E-06	-0.022	L5-RE3
E-FF6	-6.20E-05	-0.89	-7.00E-06	-5.50E-05	-0.790	L5-RE3
E-CHISAGO_L	-3.70E-05	-0.53	-7.00E-06	-3.00E-05	-0.431	L5-RE3
E-B-MARINE_L	-7.01E-05	-1.01	-1.00E-07	-7.00E-05	-1.006	L5-LKG
E-FOREST_L	-1.21E-05	-0.17	-1.00E-07	-1.20E-05	-0.172	L5-LKG
EW-1	-6.10E-06	-0.09	-1.00E-07	-6.00E-06	-0.086	L5-LKG
EW-2	-3.30E-06	-0.05	-1.00E-07	-3.20E-06	-0.046	L5-LKG
EW-3	-9.51E-05	-1.37	-1.00E-07	-9.50E-05	-1.365	L5-LKG
EW-4	-4.00E-04	-5.75	-1.00E-07	-4.00E-04	-5.748	L5-LKG
EW-5-E	-5.50E-04	-7.90	-1.00E-07	-5.50E-04	-7.904	L5-LKG
EW-5-W	9.99E-05	1.44	-1.00E-07	1.00E-04	1.437	L5-LKG
EW-6N	-1.00E-04	-1.44	-1.00E-07	-1.00E-04	-1.437	L5-LKG
EW-6S	-4.00E-04	-5.75	-1.00E-07	-4.00E-04	-5.748	L5-LKG
EW-15W	-5.57E-04	-8.01	-1.00E-07	-5.57E-04	-8.004	L5-LKG
EW-15N	-1.39E-04	-2.00	-1.00E-07	-1.39E-04	-2.000	L5-LKG

Table 5

Layer 5 Leakage Inputs

Version 1.00

POLYGON	Layer 5 Top (m/day)	Layer 5 Top (in/year)
E-FF1	-1.00E-07	-0.001
E-FF4	-1.20E-04	-1.724
L5-RE1	-1.00E-05	-0.144
L5-RE2	-2.50E-05	-0.359
L5-RE3	-7.00E-06	-0.101
L5-RE4	-2.55E-05	-0.366
L5-RE5	-1.50E-05	-0.216
L5-SC1	-1.30E-03	-18.681
L5-SC2	-2.09E-04	-3.000
L5-LKG	-1.00E-07	-0.001
L4-SC-W	-3.10E-06	-0.045
L5-FF1	-1.00E-07	-0.001
L5-FF2	-5.00E-08	-0.001
L5-FF3	-2.50E-06	-0.036
L4-SC5	-1.10E-06	-0.016
L4-SC7	-1.10E-06	-0.016
L4-SC10	-1.10E-06	-0.016
L4-SC11	-1.10E-06	-0.016
SLS-1	-4.87E-05	-0.700
SLS-2	-1.00E-07	-0.001
EW-15SE	-2.09E-04	-3.003
EW-16N	-5.57E-04	-8.004
SCX2	-5.57E-04	-8.004
SS-8	-8.70E-04	-12.502
SS-BV_5	-1.50E-04	-2.156
SG-1-E	-1.40E-06	-0.020
SG-3-M	-5.00E-07	-0.007
SG-3-E	-1.40E-06	-0.020
SG-3-BV	-5.57E-04	-8.004

Note that some polygons have positive total infiltration values in Table 4 and Figure 18. This indicates upward leakage following MLAEM's convention of data input, but does not necessarily mean that water is actually exiting at the surface in the real world. Instead it may point to areas where local models should consider the loss of water to additional wells not included in this model or to upper aquifers. The total system infiltration rates for polygons within the metropolitan area range from 1e-7 m/day to 1.3e-3 m/day (0.001 inches/year to 19 inches/year). In general, the subcrop zones of Layers 4 and 5 to the west and north have greater leakage rates than areas where they are overlain with bedrock units. Areas exposed by structural activity and erosion offer an exception to this generalization. Leakage rates are highly variable over these smaller areas, and can be greater than an order of magnitude different from the values for the subcrop zones.

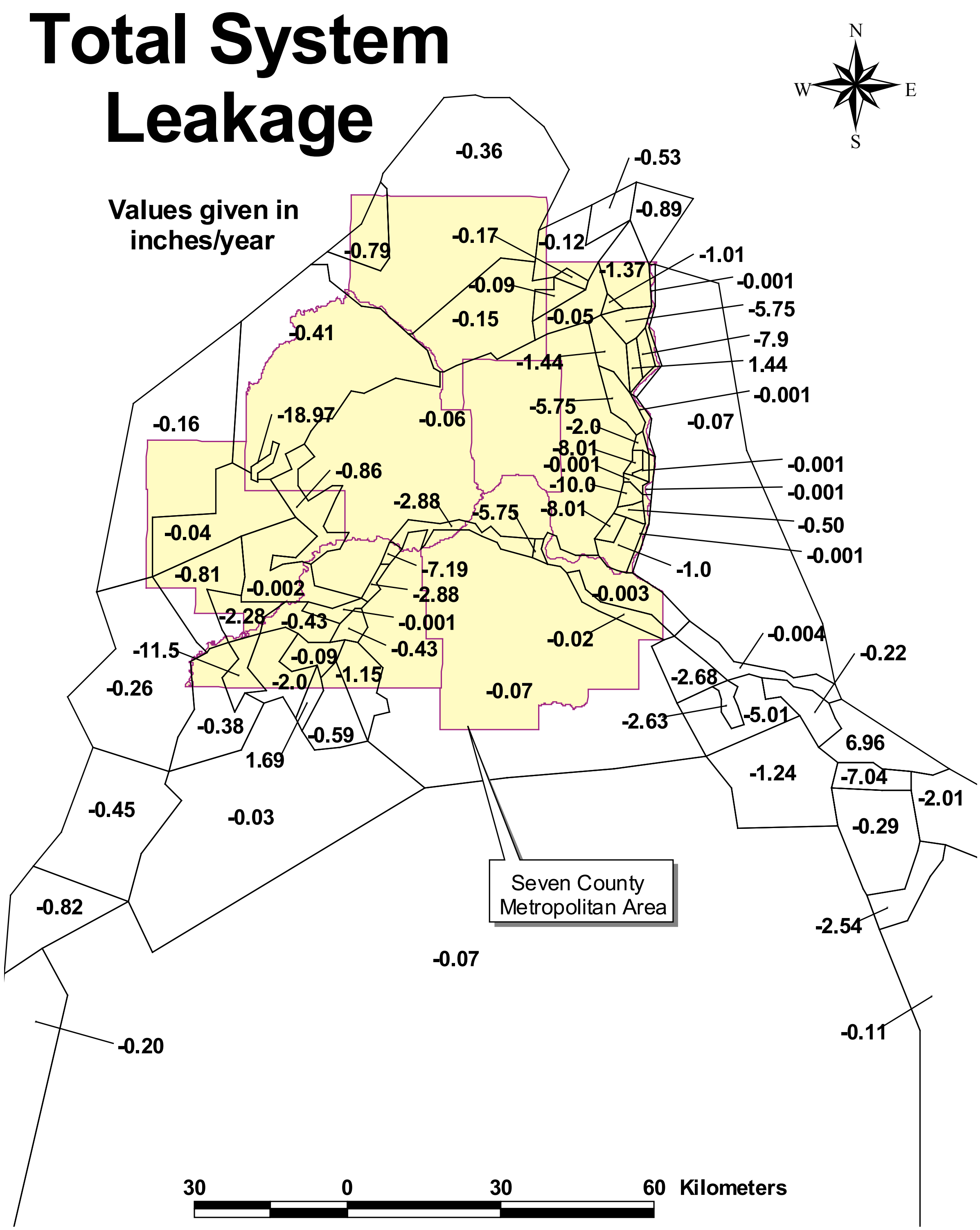

Figure 18 – Total System Leakage Rates

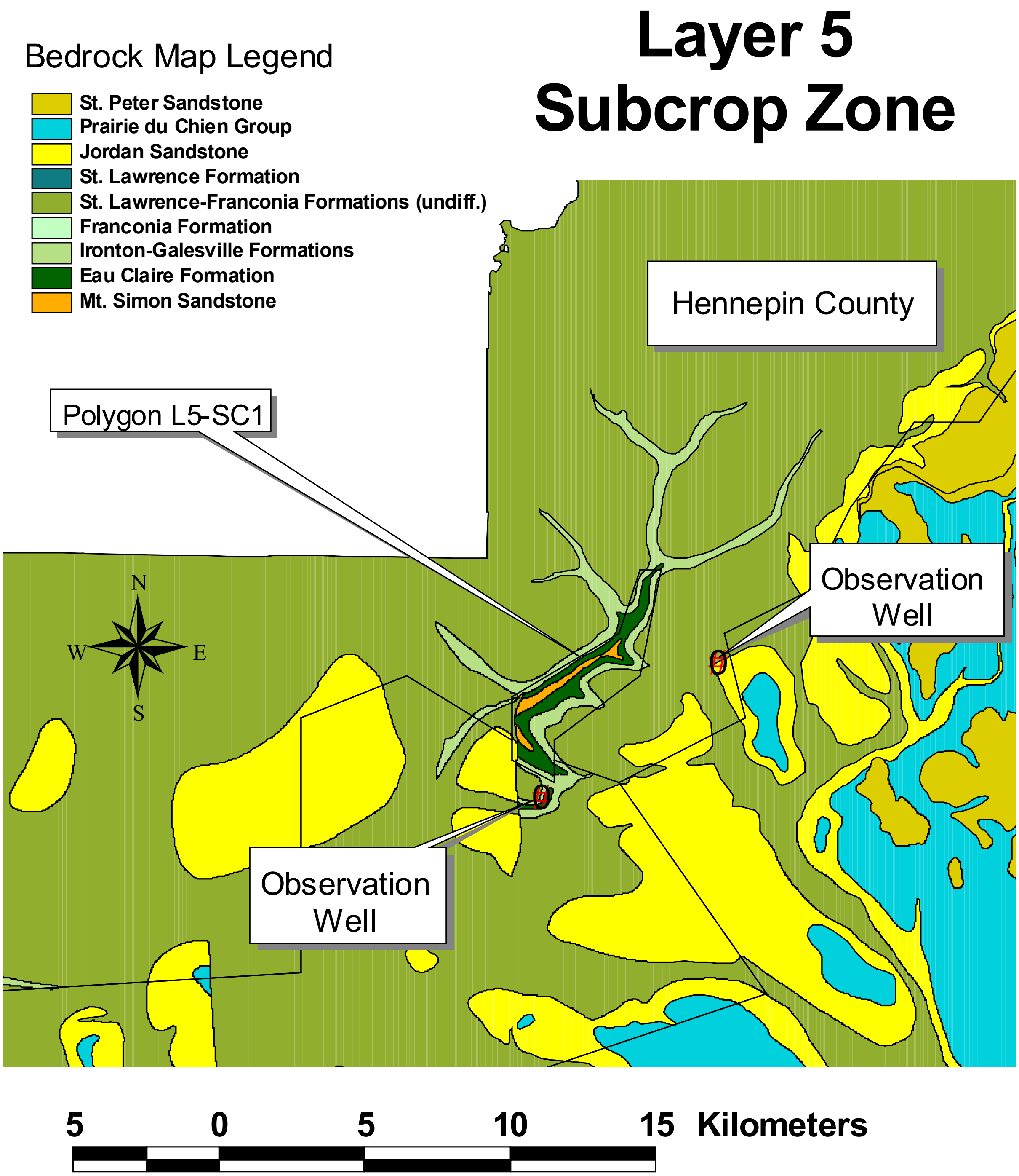

Figure 19 – Layer 5 Subcrop Zone in Western Hennepin County

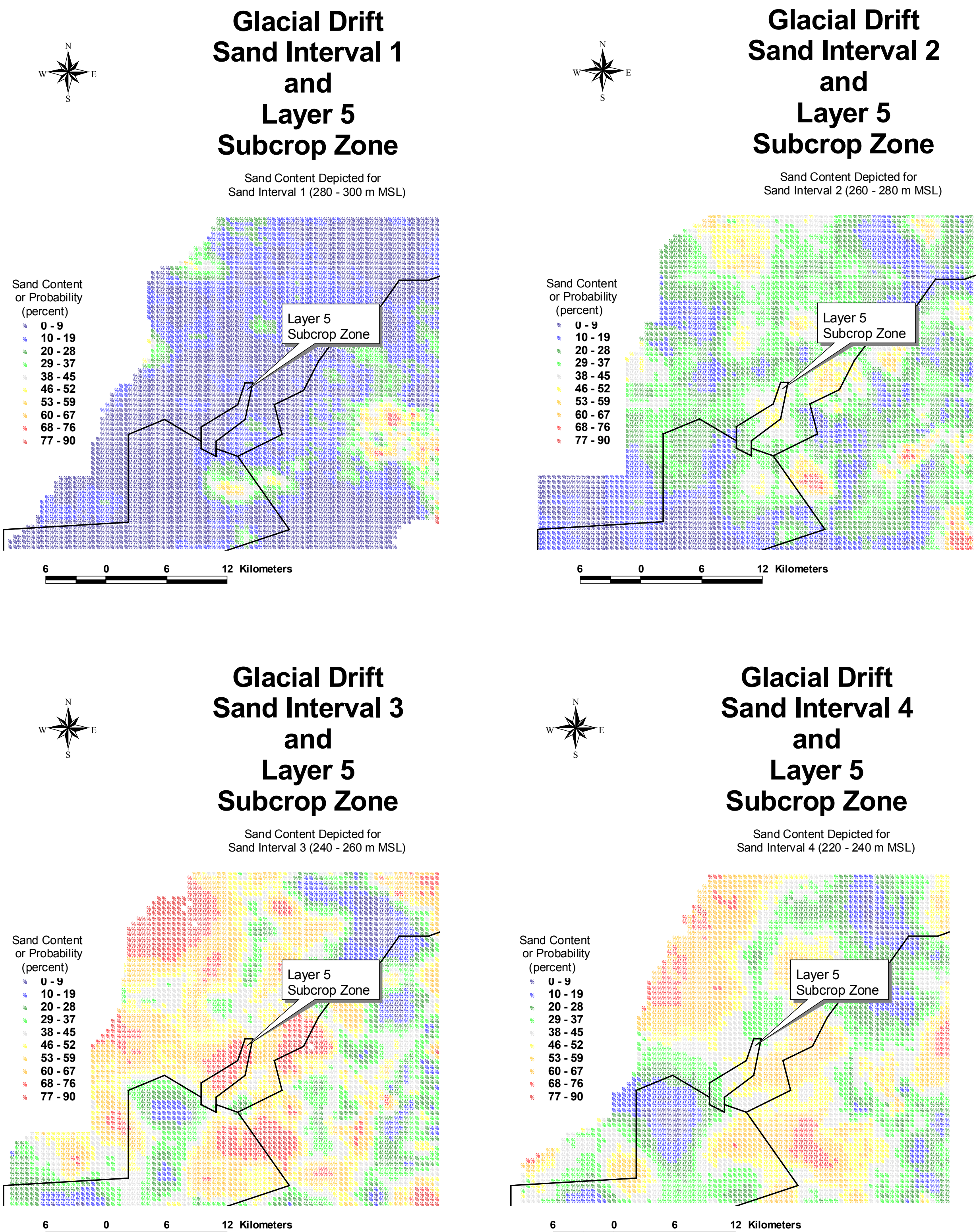

Figure 20 – Sand Content and Layer 5 Subcrop Zone
Western Hennepin County

Another area with large leakage rates, 8 to 10 inches per year, is along the St. Croix River in southeastern Washington County, where erosion has exposed both Layers 4 and 5 beneath drift material and river sediments. Various scenarios were tested in the model to reduce these leakage rates, but each did not produce the lower leakage rates found elsewhere in the system. The most difficult leakage area to characterize lies in and around the city of Afton, Minnesota, where calibration head data varies from below river level to about 60 meters above the river level (Figure 21).

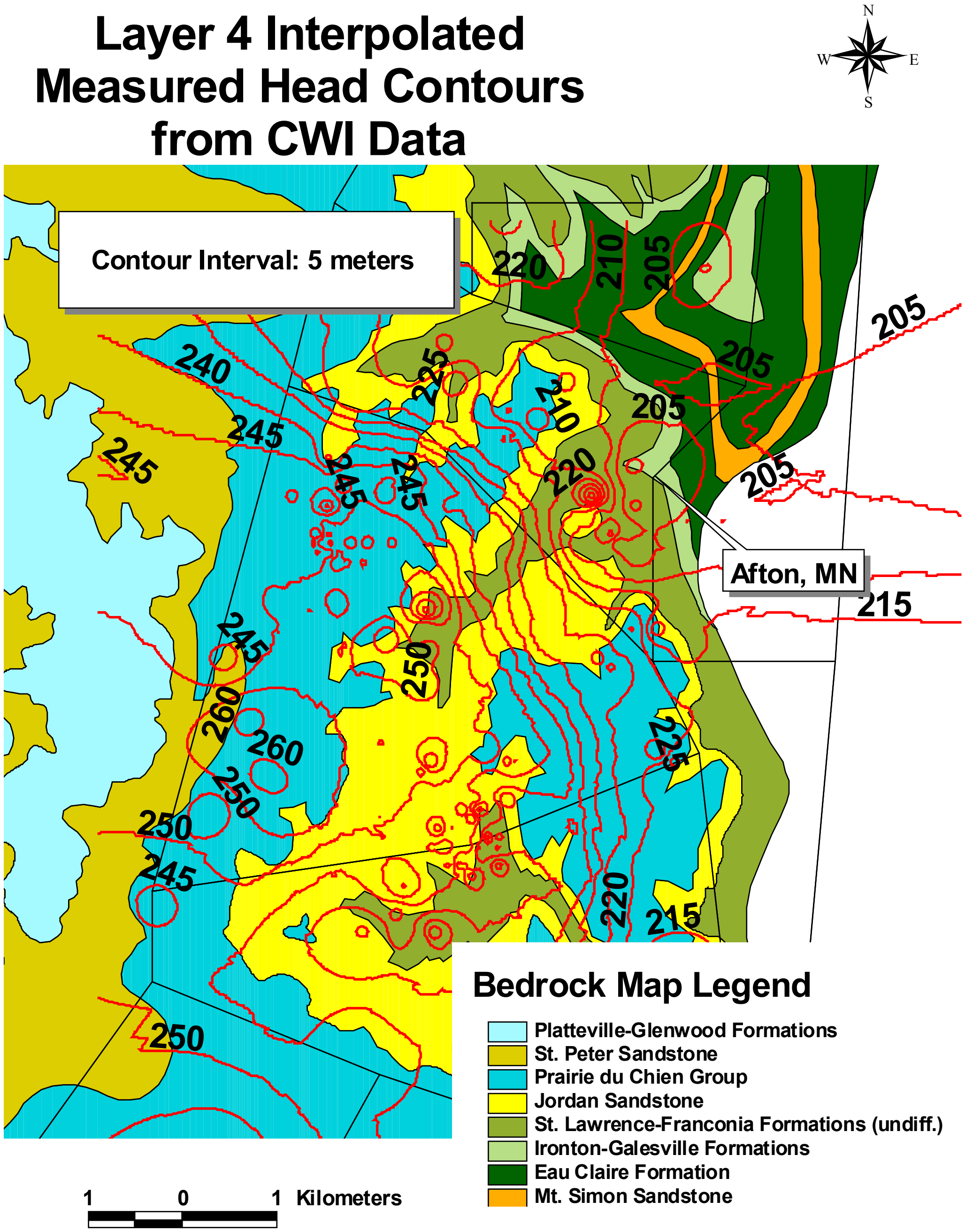

Figure 21 – Layer 4 Interpolated Head Contours Near Afton, MN.

The elevation on the St. Croix River curvilinear element was raised in both Layers 4 and 5 in the first attempt to lower leakage rates. Improvement was seen in Layer 5, but not in Layer 4 where the area west and north of Afton received too much water requiring higher leakage rates to remove water from the aquifer.

An alternative to raising river elevations was an investigation of the structural geology in the area. The exposed portion of Layers 4 and 5 coincides with the higher end of a southwest-plunging anticline. This anticline has also undergone uplift as a horst type structure, as evidenced by two normal faults, the Hastings and Cottage Grove faults, that flank each limb. The Hastings Fault to the east appears to isolate the lower aquifers from the St. Croix River. The presence, extent, and location of the Cottage Grove fault on the western flank are not as clear, nor is its effect on the hydrogeology (Figure 22).

A scenario was tested, where it was assumed a hydraulic connection existed between the aquifer units of Layers 3 and 4 along the Cottage Grove Fault thereby increasing the head in the lower aquifer. The effect of this interconnection was also assumed to be muted east of the crest of the anticline in Layer 4, where either the Hastings Fault or farther north, the St. Croix River impose more dominant constraints. Two head-specified curvilinear elements were added representing the Cottage Grove Fault and the crest of the anticline. The heads assigned to the Cottage Grove element represent heads found in Layer 3 in the area and the element provides water to Layer 4 that is assumed to come from Layer 3. The crest curvilinear element represents a localized boundary condition, an assumed “dam” caused by the underlying aquitard along the spine of the anticline, where Layer 4 becomes unsaturated to the east of its position.

The result of this scenario was a reduction in leakage rates from 8 to 10 inches/year to around 6 inches/year. Although these leakage rates were more palatable, the existence and location of the geologic entities used to create the scenario have no clear basis and are presented here as a hypothetical possibility for further study.

A second alternative is that the aquifers within the anticline possibly represent a subsystem that is largely isolated from the aquifers on the outside of the anticline, due to the discontinuity imposed by the presence of the faults. Difficulties in calibrating the Layer 4 model to heads in this area lead us to postulate that the Layer 4 aquifer within the anticline, isolated on either side by the faults, is recharged primarily through the eroded area where the lower aquifers are exposed at the upper end of the anticline. As additional information is obtained, this area will require new characterization.

The distribution of net leakage to Layer 4 on a polygon-by-polygon basis is presented in Figure 23. Most of the total leakage throughout the seven-county metropolitan area is retained in Layer 4 without passing on to Layer 5 except in southwestern Scott, southern Carver, and western Hennepin counties, where Layer 5 has been exposed through the upper bedrock units.

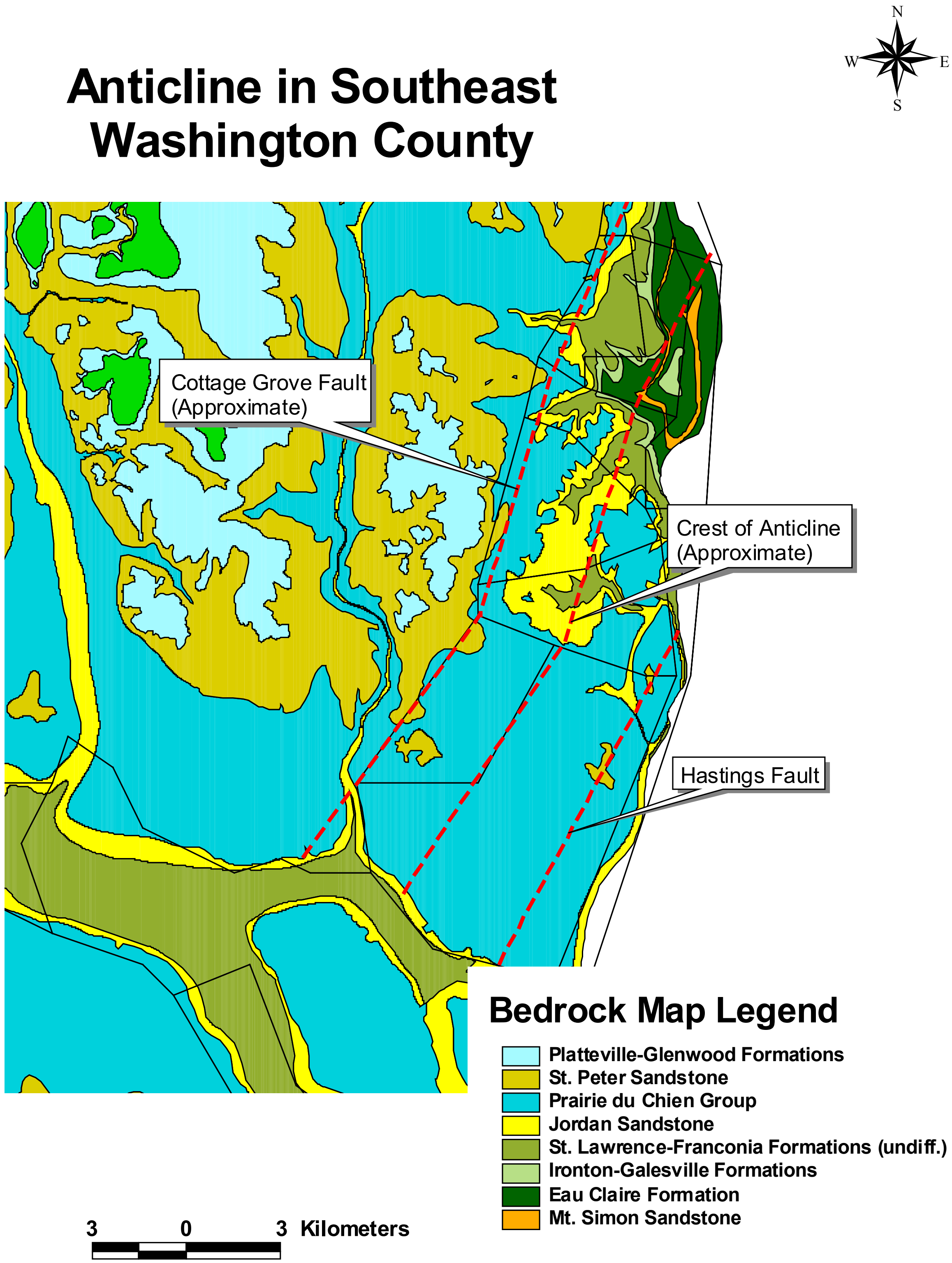

Figure 22 – Anticline in Southeast Washington County

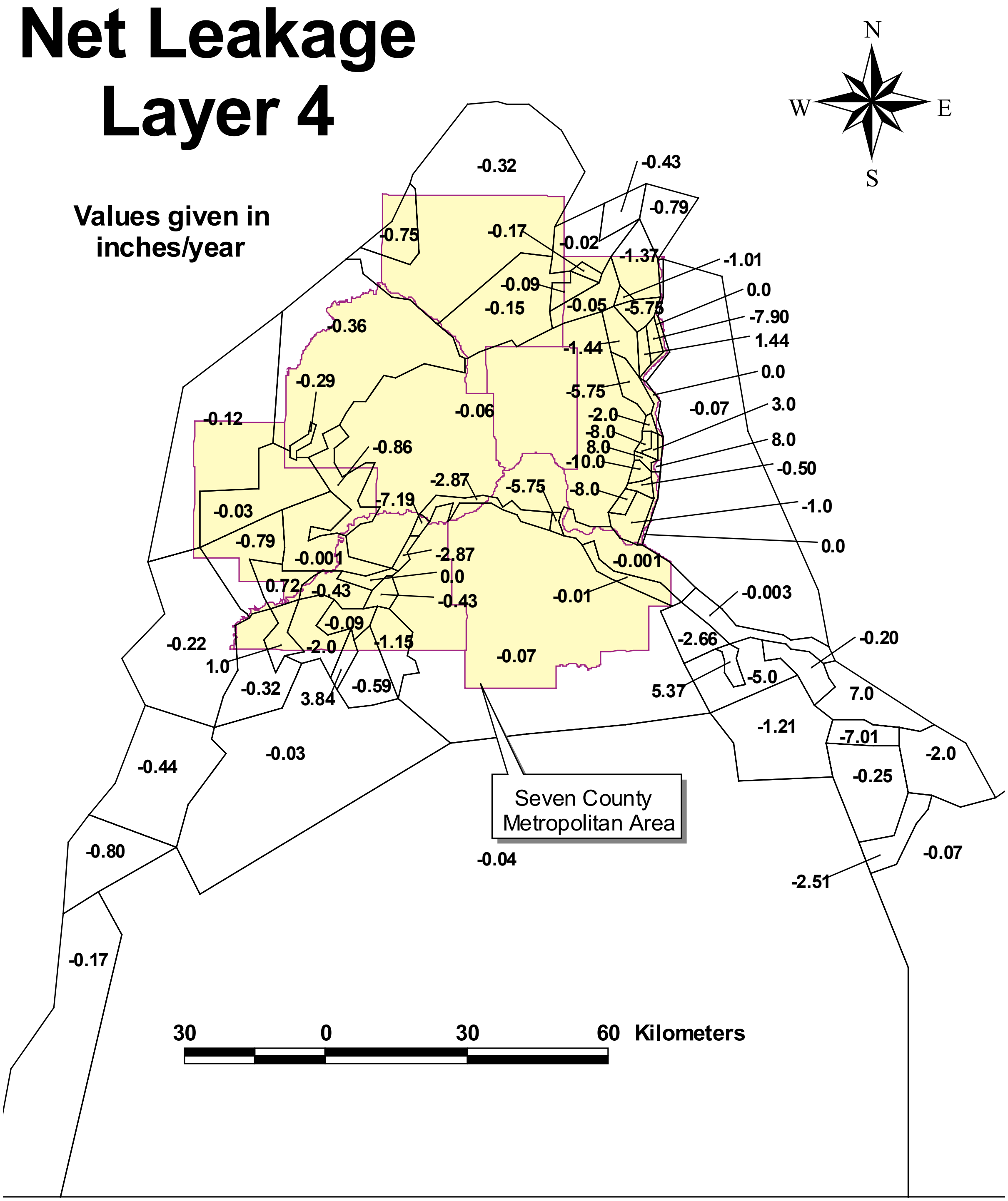

Figure 23 – Net Leakage to Layer 4

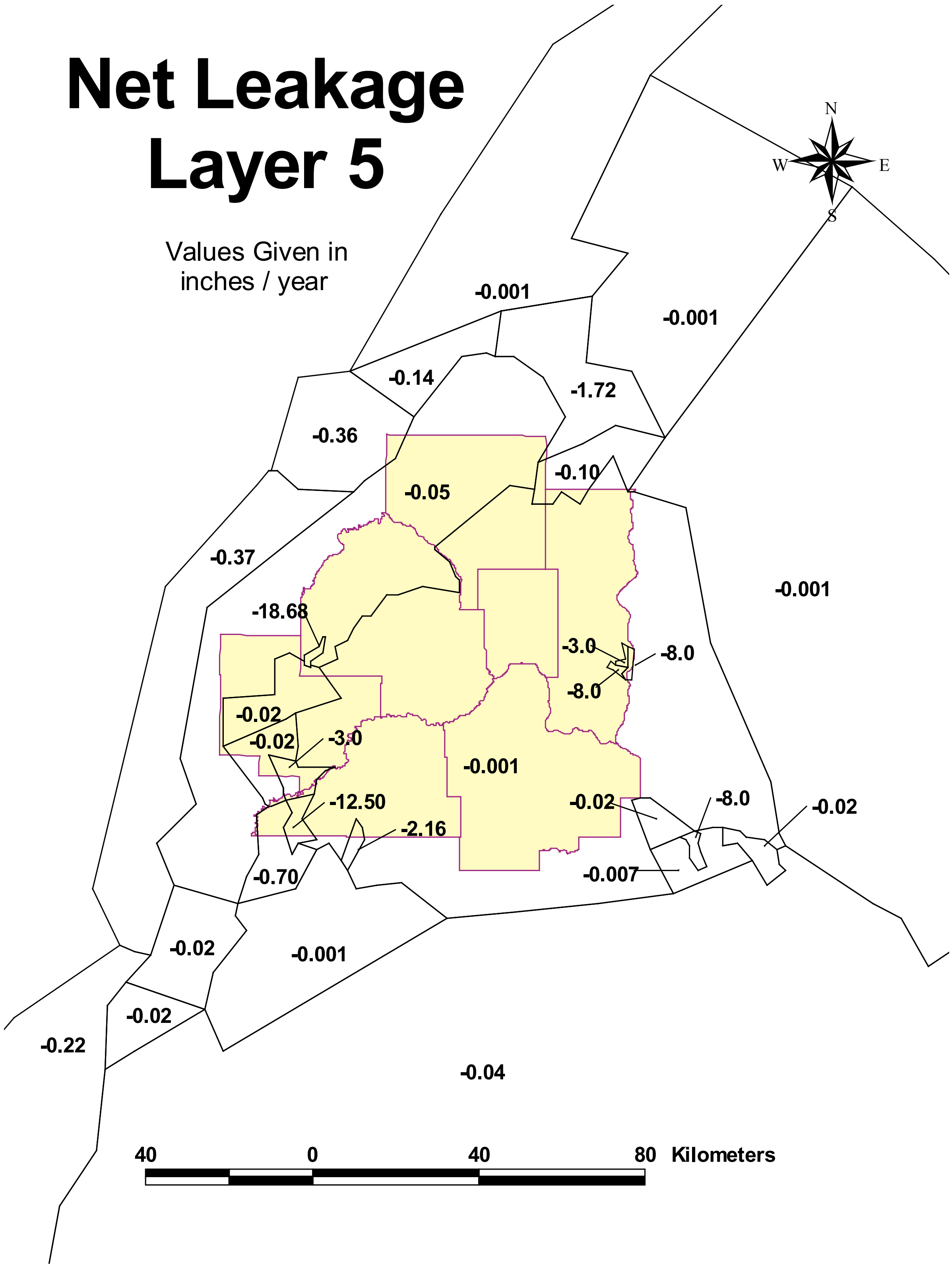

Figure 24 – Net Leakage to Layer 5

Net infiltration rates to Layer 5, the Mt. Simon-Hinckley aquifer, are presented in Figure 24. As might be suspected, the leakage to Layer 5, where the overlying aquitard is intact can be considered insignificant. This aquifer is primarily recharged to the west and north of the metropolitan area where it subcrops beneath the glacial drift, and also in zones where it has been exposed through erosion. The model shows significant local recharge in the western metropolitan area through a buried bedrock valley that has eroded down to the Layer 5 aquifer, as represented by polygon L5-SC1 (Figure 19).

As additional work is conducted on the model and as new information and data are gathered, these leakage rates will be re-evaluated to determine how well they represent natural conditions. Changes to the conceptual model and to the leakage values will undoubtedly change, as more information becomes available.

Calibration Data Sets

Layer 4

A brief discussion is provided here on the development and use of a calibration data set for Layer 4. A detailed explanation and description of this process can be found in the report entitled "Preparation of Supporting Databases for the Metropolitan Area Groundwater Model" (Streitz, 2000). Wells screened in the geologic units that comprise the Franconia-Ironton-Galesville Aquifer generally lie beyond the areal extent of the Prairie du Chien-Jordan Aquifer in the metropolitan area. Geostatistical analysis cannot readily be applied to this distribution of points because the area in the central metropolitan region is essentially void of wells.

To overcome this problem, the wells found in CWI that correspond to Layer 4 were grouped into "zones". Each zone was separately subjected to geostatistical analysis. The current calibration data set for Layer 4 contains 3450 wells taken from the seven zones shown in Figure 25.

Layer 5

Originally, a calibration data set for Layer 5 was prepared from CWI containing 77 wells screened in the Mt. Simon-Hinckley aquifer. No geostatistical filtering could be performed on this set, because the wells occur too far apart to exhibit spatial correlation. This data set was abandoned in favor of more reliable and current data available from MDNR's observation well network (MDNR, 2000a). Although this data-set produced only 19 observation points for use as head calibration targets for Layer 5, it is very high quality data.

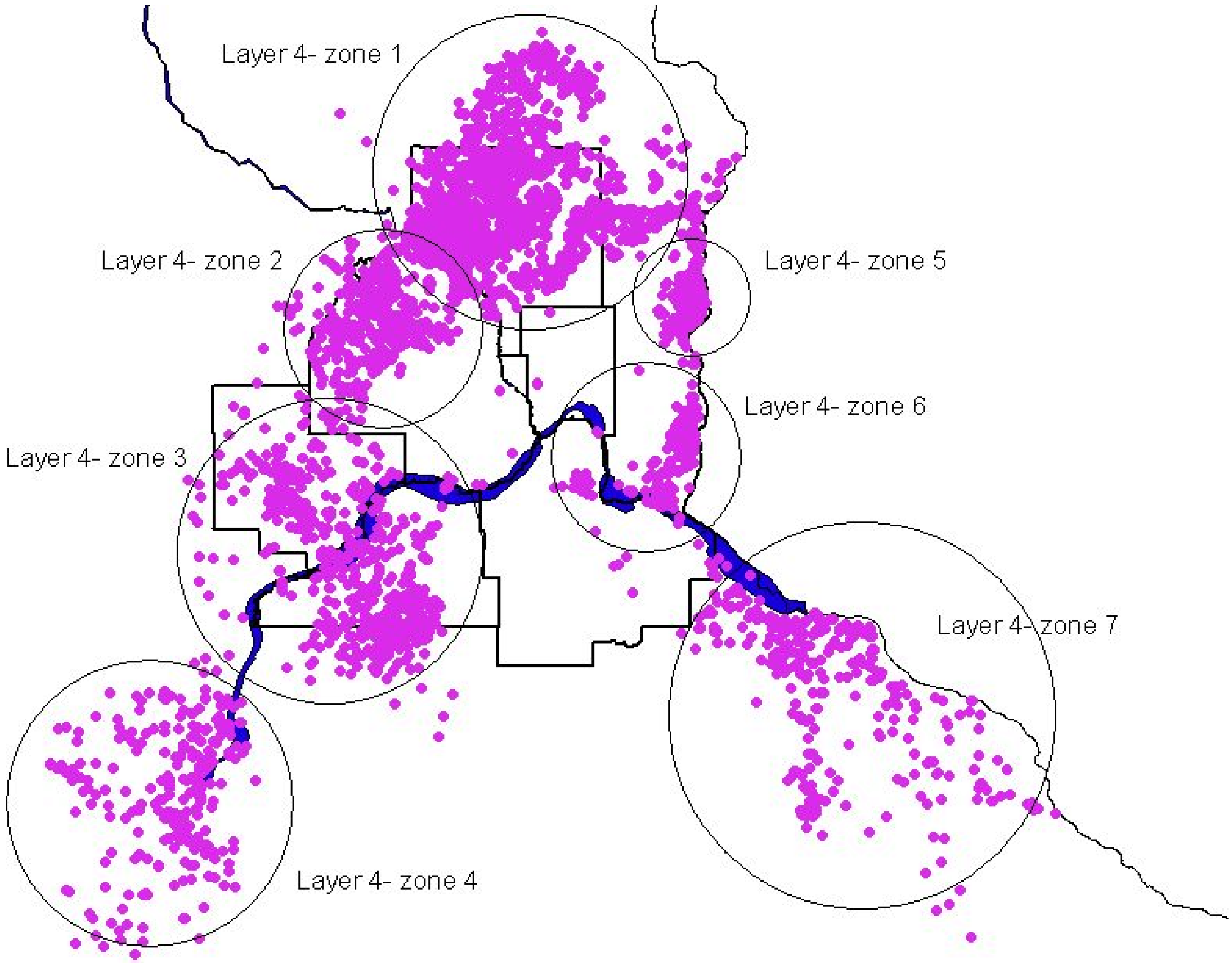

Figure 25 – Layer 4 Calibration Wells

Model Results

Comparison to Measured Heads

This section presents the most current calibration results and modeled head contours of the Layers 4 and 5 model. The descriptive statistics of the mean absolute difference (of computed minus measured heads) are presented in Table 6. The calibration and head contour plots for Layers 4 and 5 are presented on the pages following the statistics of mean absolute differences in Figures 26 and 27.

Table 6
Descriptive Statistics for Mean Absolute Difference Values

	Layer 4	Layer 5
Mean	4.06	3.10
Standard Error	0.07	0.63
Median	2.93	2.09
Mode	1.37	#N/A
Standard Deviation	4.01	2.65
Sample Variance	16.08	7.05
Kurtosis	6.26	-0.14
Skewness	2.14	1.04
Range	31.26	8.41
Minimum	0.002	0.023
Maximum	31.26	8.43
Sum	13969.86	55.73
Count	3450	18

In general the mean absolute difference between modeled and measured heads in Layer 4 is comparable to those for the province models. As can be seen in Figure 26, the model is calibrated better in the western portion of the model than on the east side.

In the east, Zone 5 (Figure 24) corresponds to an area where erosion has exposed the aquifer beneath drift material and alluvial sands. In addition, this aquifer, which is locally dipping in a southerly direction, begins to crop out along the river moving northward, increasing the possibility that a seepage face above the river exists. At present this model provides some detail in the area by using more given-strength polygons to model leakage. As more information becomes available, this model will be adjusted to provide a better fit to measured head data.

Directly south of Zone 5 lies Zone 6, and although greater model detail has improved the calibration here, the model would still benefit from additional information. This zone corresponds with an anticline that trends to the south-southwest along the west side of the St. Croix River valley (Figure 22).

The modeled head contours shown in Figure 27 are presented in English units of feet above Mean Sea Level (MSL). These contours show recharge for the aquifer in the metropolitan area occurring to the north and west, and discharge zones along the Minnesota, Mississippi and St. Croix River valleys, with lesser discharge to secondary rivers.

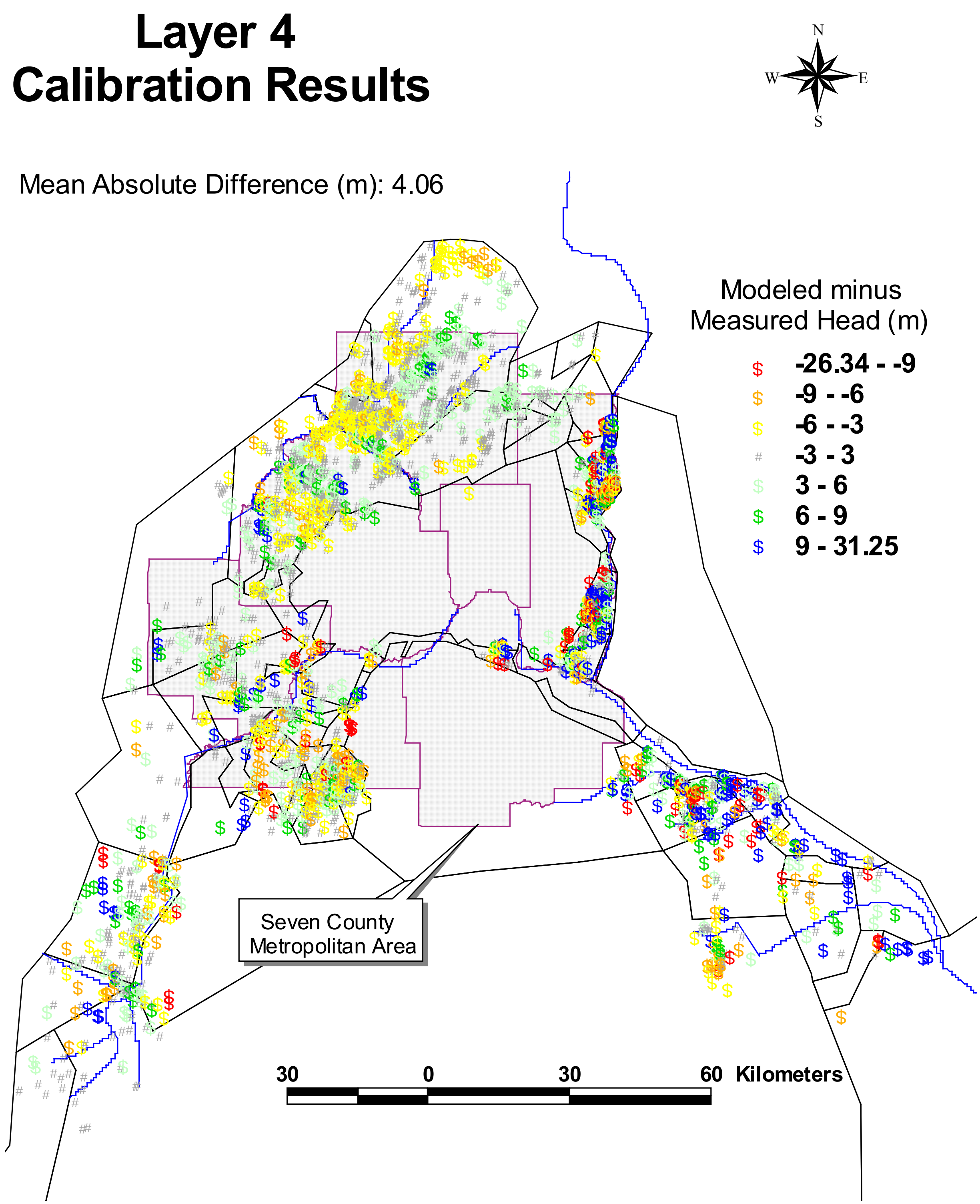

Figure 26 – Layer 4 Calibration Plot

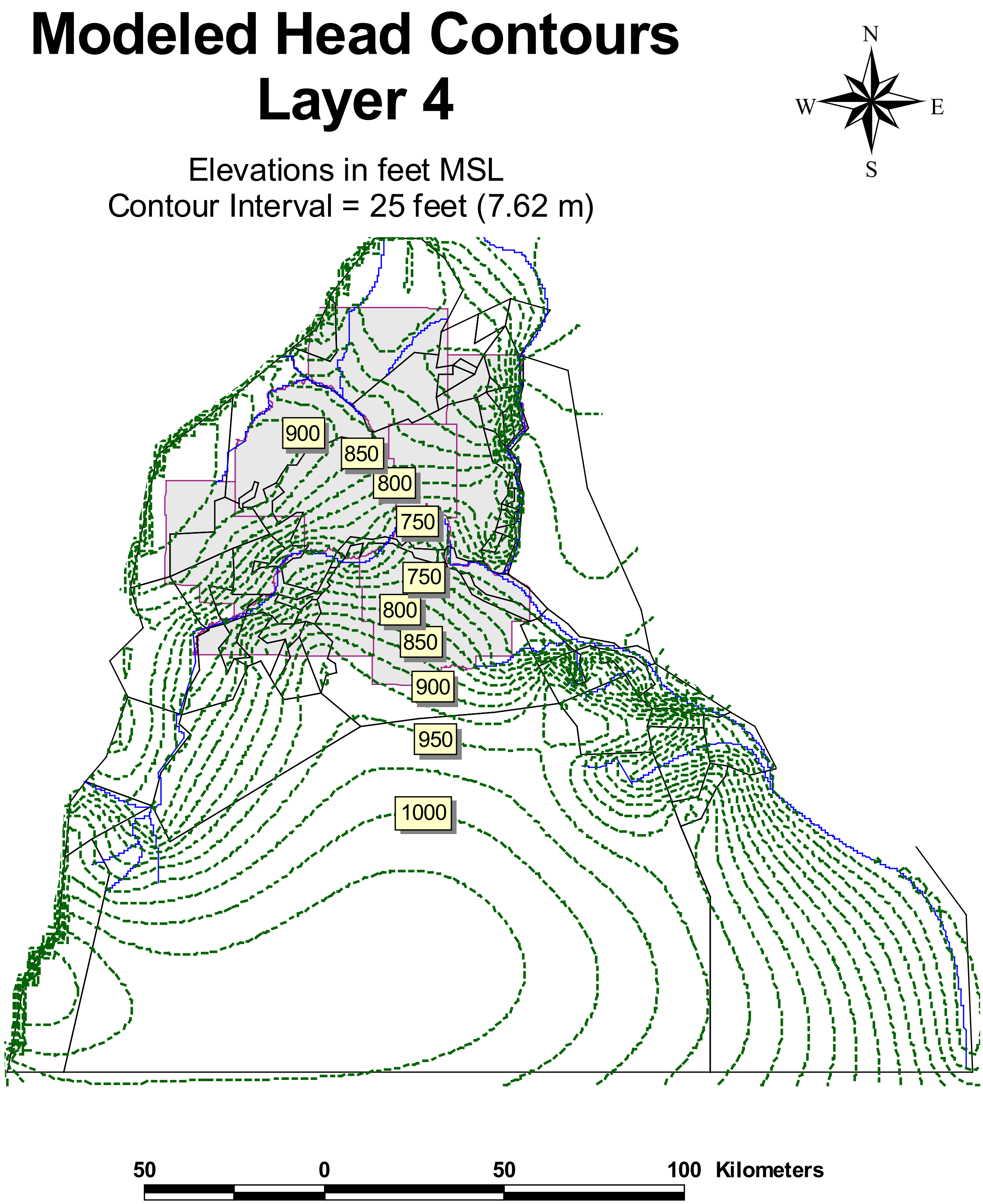

Figure 27 – Layer 4 Piezometric Contours

The latest calibration and modeled head contour plots for Layer 5 are presented in Figures 28 and 29. The mean absolute difference of modeled minus measured heads for Layer 5 was 3.10 m (Table 6). Despite the relatively small number of head calibration sites for an area covering thousands of square kilometers, their areal distribution, coupled with the associated high quality of head measurements provide us with confidence in the regional head distribution and flow regime. The targeted ± 3 meters difference between modeled and measured heads is well distributed among the wells.

The modeled head contours shown in Figure 29 show the depression cone that resulted from the inclusion of steady-state extraction wells. Discharge rates initially assigned to the pumping wells were based on 1995 extraction data from the SWUDS database (MDNR, 2000b). These rates were then manually adjusted along with the leakage rates to match the head calibration targets derived from the mean of March values from 1993 through 1998 (MDNR, 2000a) in order to simulate an averaged condition. Both initial and final pumping discharge rates are presented in Table 3. This procedure was used to approximate the head distribution of a transient system that will continue to change with a steady-state model.

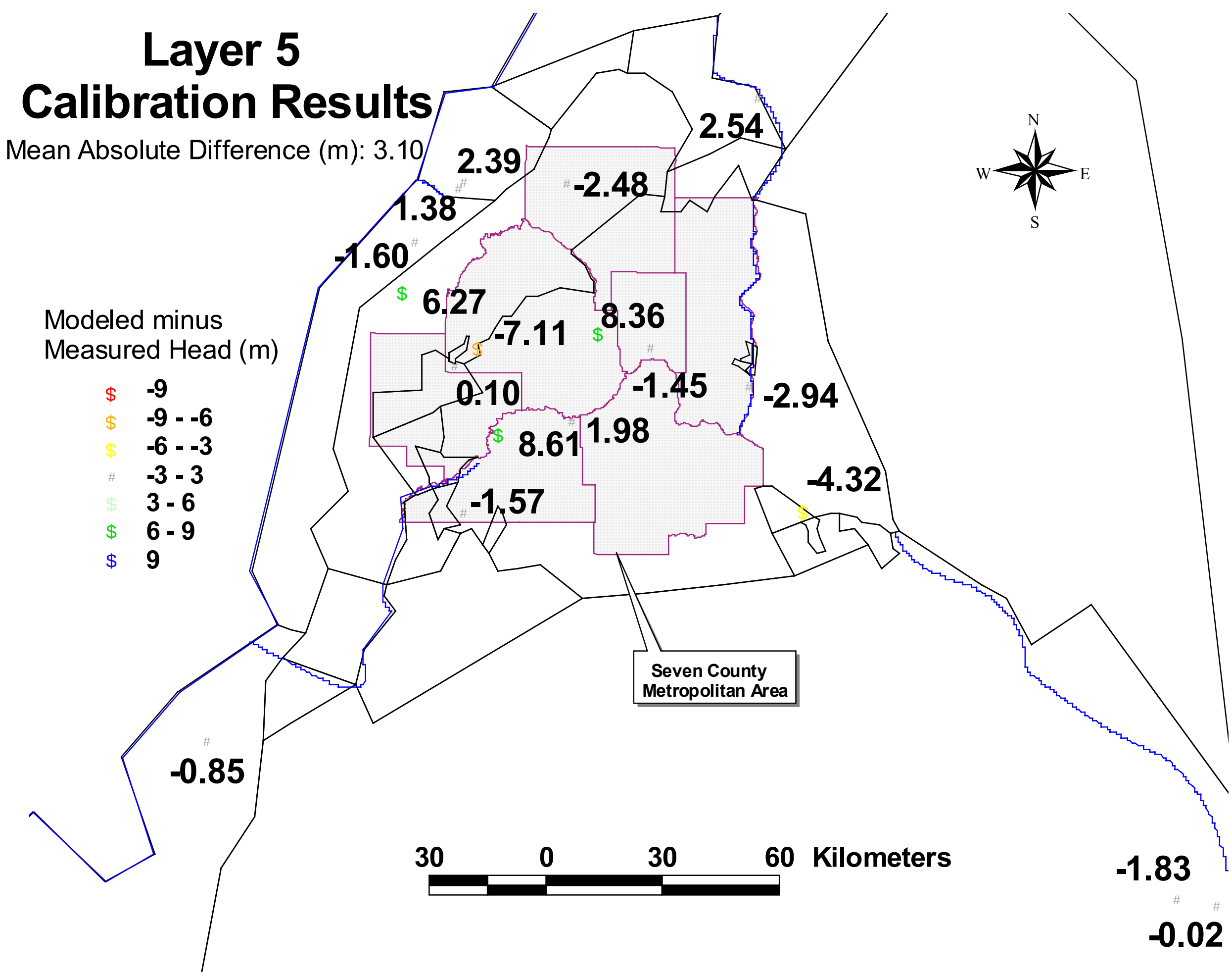

Figure 28 – Layer 5 Calibration Plot

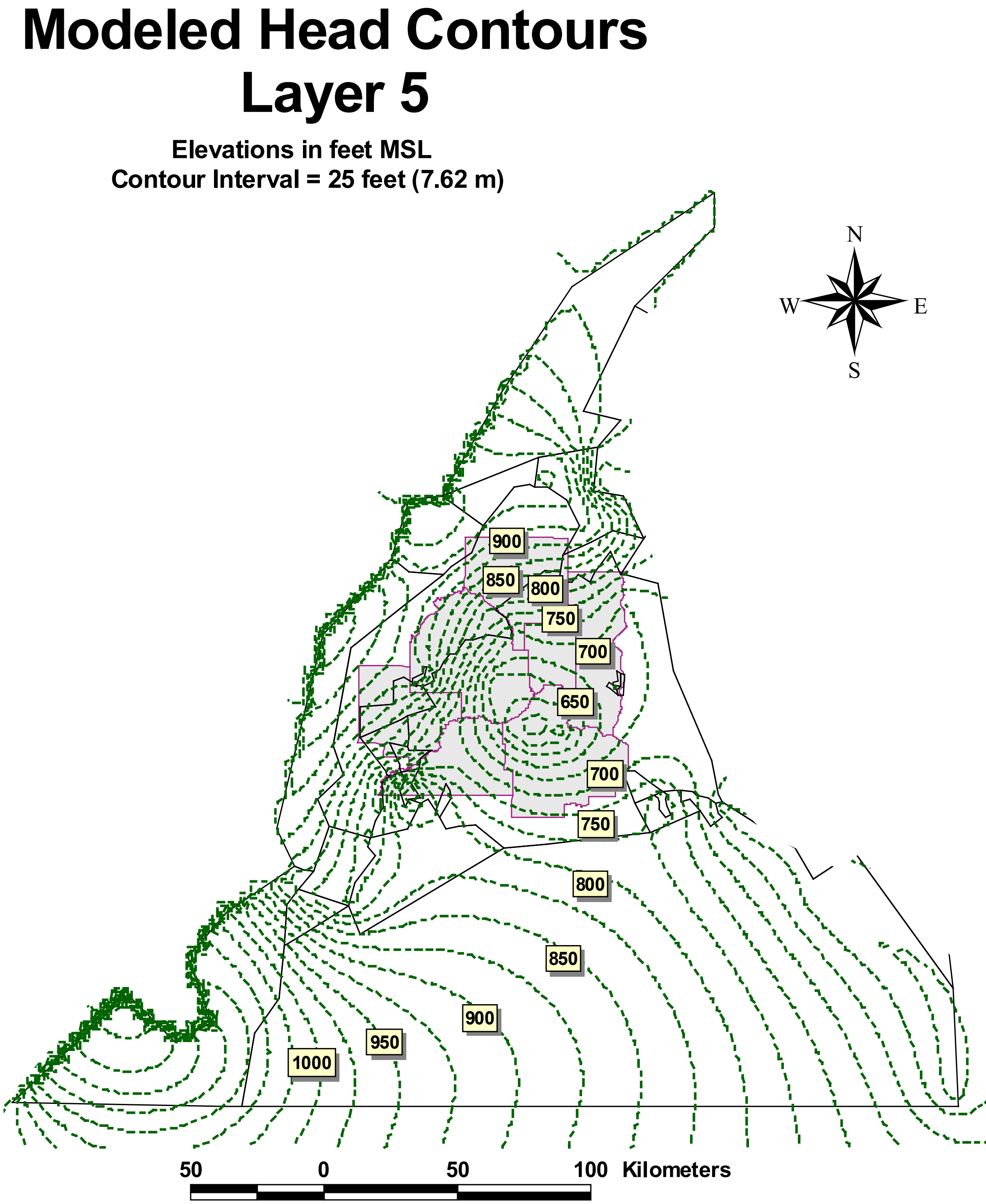

Figure 29 – Layer 5 Piezometric Contours

Comparison to Discharge Estimates

Efforts to fit the model to measured heads are a necessary part of the calibration process, but it does not, however, ensure the water balance is correct. In addition to calibration to head values, it is important that the water throughput in the model compares favorably with that of the actual system, where measured. Presently, we do not have much data on aquifer discharge rates to surface water bodies. Further complicating this issue are the structural geology constraints placed on the system, that render simple flat-lying layer-cake stratigraphy models of the aquifer system to be of little use. The geometry of the seepage faces that serve as discharge zones is likely quite complicated, and does not lend itself well to measuring the actual discharge of groundwater. Although more stream discharge data are becoming available, the only information we had to work with at the time of this analysis were discharge data for tributary streams and rivers to the Minnesota, Mississippi, and St. Croix Rivers.

The Cannon, Rum, Crow, Zumbro, Blue Earth, and Le Sueur Rivers are tributaries to the Minnesota and Mississippi Rivers for which we have obtained stream flow data. A summary of our analysis of the discharge data is presented in Table 7. This data provides the model with groundwater discharge estimates to the rivers setting a maximum cap for curvilinear string discharges representing those rivers from all aquifers. The tributary discharge estimates are also used for maximum capacities for the larger rivers, since stream flow data on the Minnesota, Mississippi, and St. Croix Rivers is assumed to contain a higher percentage of error than the groundwater contribution to their flow between gauging stations.

The surface water features included in this model are assumed to have some hydraulic connection to Layers 4 and 5. In most cases only the portion of a river separated by drift material from the aquifer represented by Layer 4 is used. River interaction with Layer 5 was only considered along the major rivers, and includes some areas where Layer 4 is present. Included river sections are presented in Table 8 along with the modeled groundwater discharge.

Stream flow data for the rivers included in Table 7 were obtained from the historical flow data records of the United States Geological Survey (USGS). Average flow measurements were determined from 7-day monthly minimum values for the month of November in the years 1975 to 1979 for the Zumbro River. The minimum flows for February in the years 1992 to 1997 were used for the Cannon River and for February in the years 1989 to 1997 for the Rum and Crow Rivers. The Blue Earth and Le Sueur Rivers minimum flows were obtained from stream flow data for February in the years 1950 to 1999. Estimates of groundwater discharge per meter of stream length were made from this data and are presented below in Table 7.

The modeled discharges are presented in Table 8 for each individual line-sink in both aquifer layers. The computed discharge values for each string are presented in the first two columns. String lengths are in the next column. The next two columns provide the discharge per unit length for each string, and the sum total discharge from both layers is presented in the far-right column.

Table 7
Layers 4 and 5
Groundwater Discharge Estimates for Tributary Systems to the Minnesota, Mississippi, and St. Croix Rivers

Stream Name	Curvilinear String Name	Average Total Discharge (cms)	Average Total Discharge (cmd)	Estimated Stream Length (m)	Discharge per meter Stream Length (cms/m)	Discharge per meter Stream Length (cmd/m)
Crow River	CrowR-Lower	8.11	700445	320060	2.53E-05	2.19
Rum River	Rum_River_Lower	4.60	397440	73200	6.28E-05	5.42
Cannon River	Cannon_River_Lower	2.18	187897	32710	6.65E-05	5.74
Zumbro River	Zumbro	2.96	255980	68720	4.30E-05	3.73
Le Sueur River	Le_Sueur-Maple_River	1.80	155420	107650	1.67E-05	1.45
Blue Earth River	Blue_Earth_River	3.57	308110	138450	2.58E-05	2.23

The simulated discharges presented in Table 8 are less than the estimated groundwater discharge in Table 7 for all six rivers. This is acceptable since there is groundwater discharge to these rivers from upper aquifers as well.

Table 8
Modeled Discharge to Curvilinear Line-sinks
Layers 4 and 5 Model

Curvilinear String	Modeled Discharge to String (cmd)		Approx. String Length (m)	Discharge per Unit Length (cmd/m)		Total Discharge per Length (cmd/m)
	Layer 4	Layer 5		Layer 4	Layer 5	
MN_RIVER_1	51900	NA	56350	0.92	NA	0.92
MN_RIVER_2	284000	104000	46420	0.61	2.25	2.86
MN_RIVER_3	29600	36700	52870	0.56	0.69	1.25
MN_RIVER_4	NA	5850	9290	NA	0.63	0.63
MISSR_NORTH	NA	10100	8550	NA	1.18	1.18
MISSR_ANOKA	9870	NA	31110	0.32	NA	0.32
MISSR_SPRINGL	21500	NA	25120	0.86	NA	0.86
MISSR_PRESCOTT-1	2270	NA	4010	0.57	NA	0.57
MISSR_PRESCOTT-2	8000	NA	23230	0.34	NA	0.34
MISSR_REDWING	16500	NA	27880	0.59	NA	0.59
MISSR_SOUTH	21700	63600	154760	0.14	0.41	0.55
CANNON_RIVER_LOWER	28300	NA	37850	0.75	NA	0.75
RUM_RIVER_LOWER	13800	NA	99080	0.14	NA	0.14
CROWR-LOWER	11900	NA	62570	0.19	NA	0.19
ST_CROIX	87900	93200	127225	0.69	0.73	1.42
LAKES-1	5090	NA	34220	0.15	NA	0.15
ZUMBRO	58700	NA	72410	0.81	NA	0.81
HAYS_CREEK	22400	NA	17800	1.26	NA	1.26
WELLS_CREEK	19200	NA	25500	0.75	NA	0.75
BLUE_EARTH_RIVER	6310	NA	73510	0.09	NA	0.09
WATONWAN_RIVER	2950	NA	24650	0.12	NA	0.12
LE_SUEUR-MAPLE_RIVER	4430	NA	32890	0.13	NA	0.13

NA: Not Applicable

Comparison to Mt. Simon-Hinckley Radiometric Age Data

A substantial volume of groundwater age-dating data for samples collected from the Mt. Simon-Hinckley aquifer makes it possible to compare modeled residence times within the aquifer to the measured ages. A study by the Minnesota Geological Survey (Lively et al., 1992) presents carbon 14 (^{14}C) age data for Mt. Simon-Hinckley groundwater samples collected from various wells in the metropolitan area. These data were correlated with data from the Minnesota Department of Health to pinpoint well locations. All of the wells used are screened solely in the Mt. Simon Sandstone or combined Mt. Simon-Hinckley Formations.

Since groundwater pumping has only been a major influence most recently over a relatively short time period—say, less than a century—we assume that the measured values of groundwater age better reflect pre-development conditions in the aquifer than the current pumping regime. Therefore, our comparisons of measured age data of the Mt. Simon-Hinckley groundwater samples are being made to groundwater residence times determined by a model of the aquifer representing pre-development conditions.

This model of pre-development conditions was constructed by removing all the pumping wells in Layer 5 and reducing leakage in three of the polygons. The reductions were based upon the assumption that the presence of pumping wells in Layer 5 effected increased leakage in nearby areas, where the aquifer is exposed beneath drift material. Leakage rates for the three impacted polygons were reassigned values that reflect those of adjoining polygons. The resulting modeled potentiometric surface is shown for a regional scale in Figure 30, and for the seven-county metropolitan area in Figure 31.

The modeled piezometric surface for the Mt. Simon-Hinckley Aquifer in the metropolitan area shown in Figure 31 was compared to two interpretations for pre-development conditions. The first interpretation, shown in Figure 32 was made by Reeder (1966), and presents a potentiometric surface of the Mt. Simon-Hinckley aquifer in 1885. Since our research of CWI did not produce any wells screened in this aquifer prior to 1900, we consider it a pre-development interpretation. Documentation was not provided for the figure to determine the justification for the interpretation, which clearly is based on the assumption that segments of the Minnesota and Mississippi Rivers in the metropolitan area exert a strong influence on the potentiometric surface.

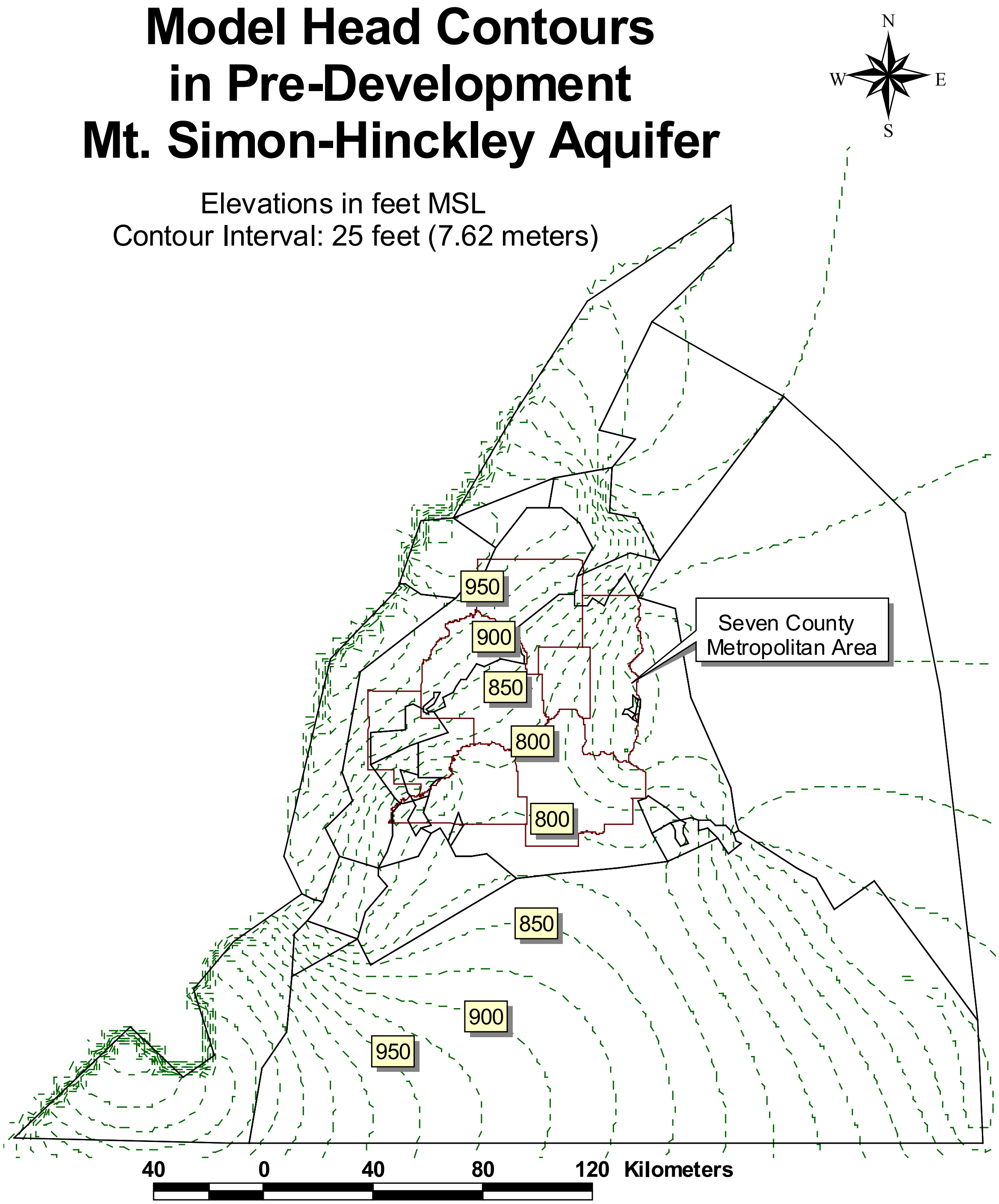

Figure 30 – Modeled Pre-Development Potentiometric Surface of Mt. Simon-Hinckley Aquifer

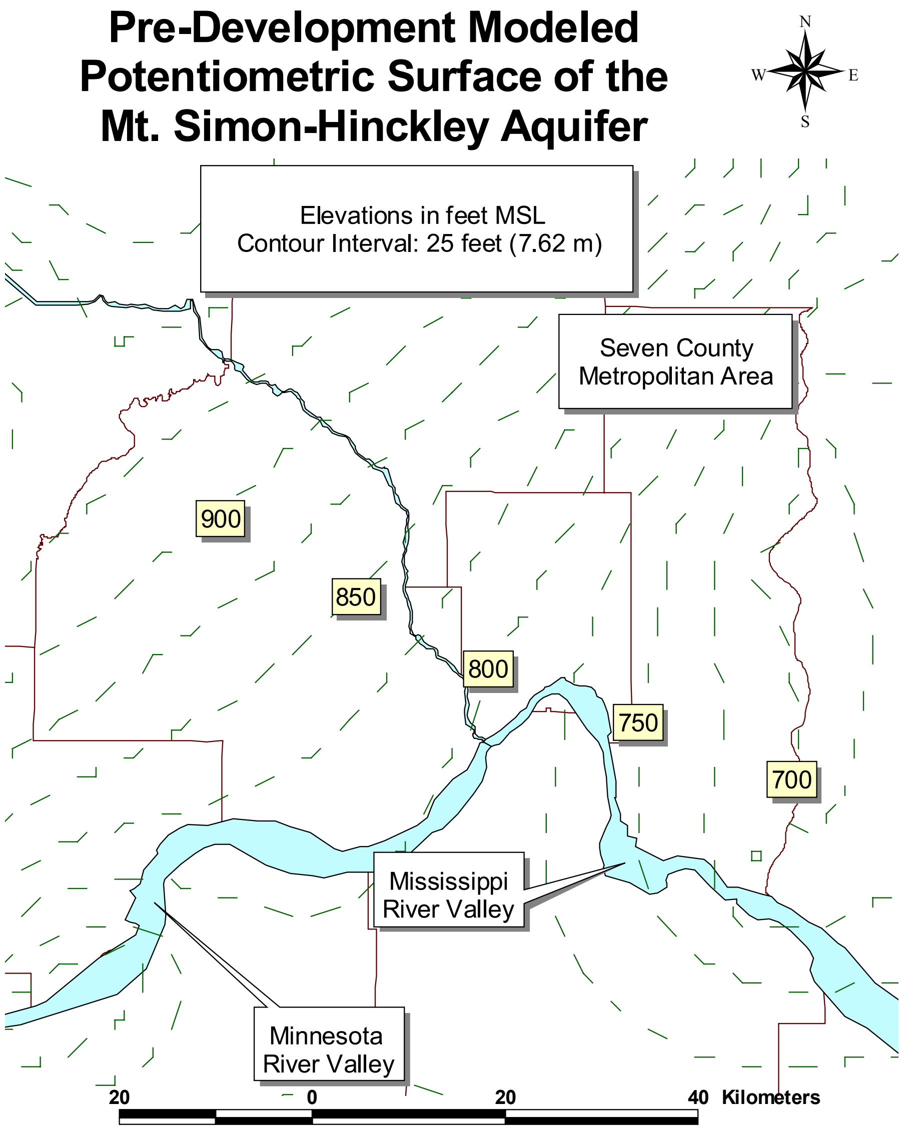

Figure 31 –Modeled Pre-Development Potentiometric Surface of Mt. Simon-Hinckley Aquifer in Seven County Area

Figure 33 illustrates Schoenberg's (1990) modification of this interpretation, and includes wells with associated water level elevations. Information regarding the well data used in Figure 32 could not be found. It is, therefore, difficult to determine the time period over which the wells were drilled and how well the associated static water levels represent the pre-development potentiometric surface. The influence of the Minnesota and Mississippi Rivers is less pronounced in the interpretation in Figure 33 than in Figure 32, which is consistent with our current understanding of the Mt. Simon-Hinckley Aquifer. The modeled piezometric surface of this aquifer compares best to that in Figure 33. The main difference occurs in the western portion of the area where the interpreted contours for elevations 850-ft. MSL and 900-ft. MSL are more heavily oriented in a north-south direction than the modeled contours. The variability in the measured water levels shown in Figure 33 emphasizes the fact that the contours indeed represent an interpretation of the pre-settlement piezometric surface. The depiction of modeled contours in Figure 31 offers an additional interpretation of pre-development conditions in the Mt. Simon-Hinckley Aquifer. Its overall consistency with Schoenberg's (1990) interpretation (Figure 33) lends credibility to it as a plausible representation of pre-development conditions that can be used for determining groundwater residence times to compare to measured groundwater age values.

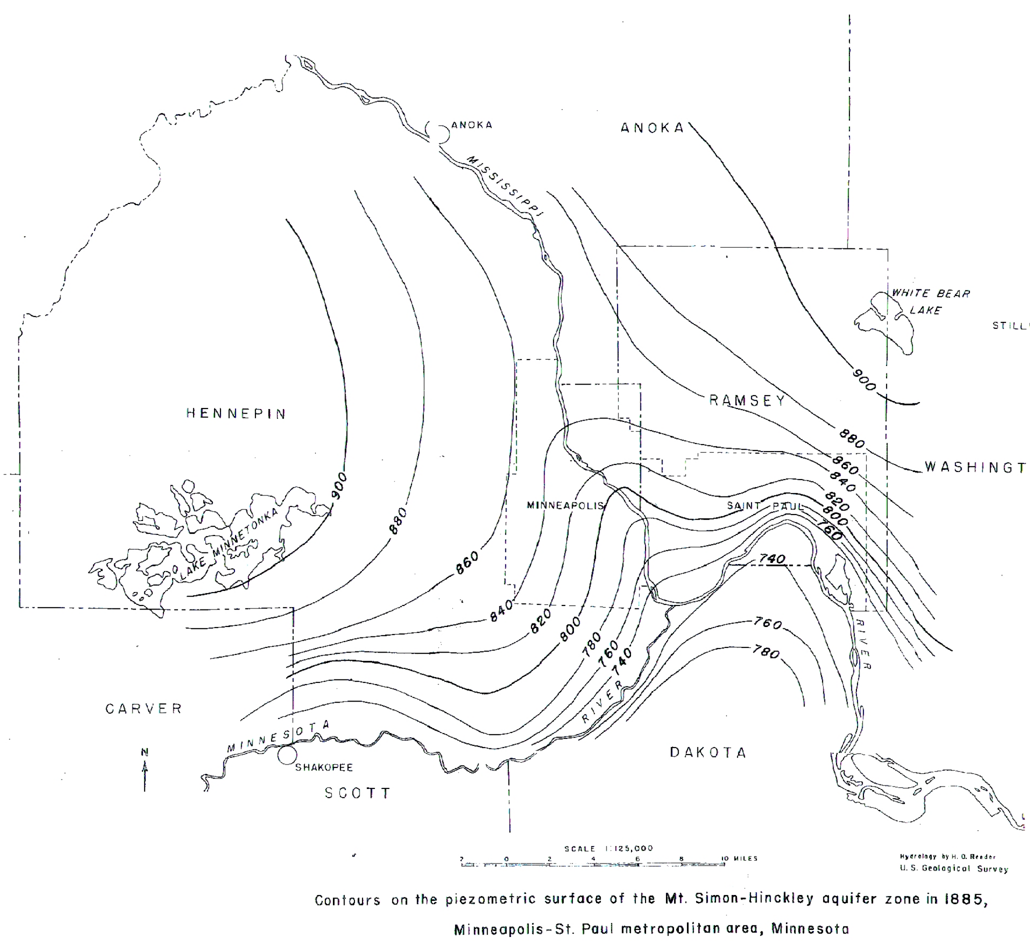

Figure 32 – Pre-Development Piezometric Surface of Mt. Simon-Hinckley Aquifer, after Reeder (1966)

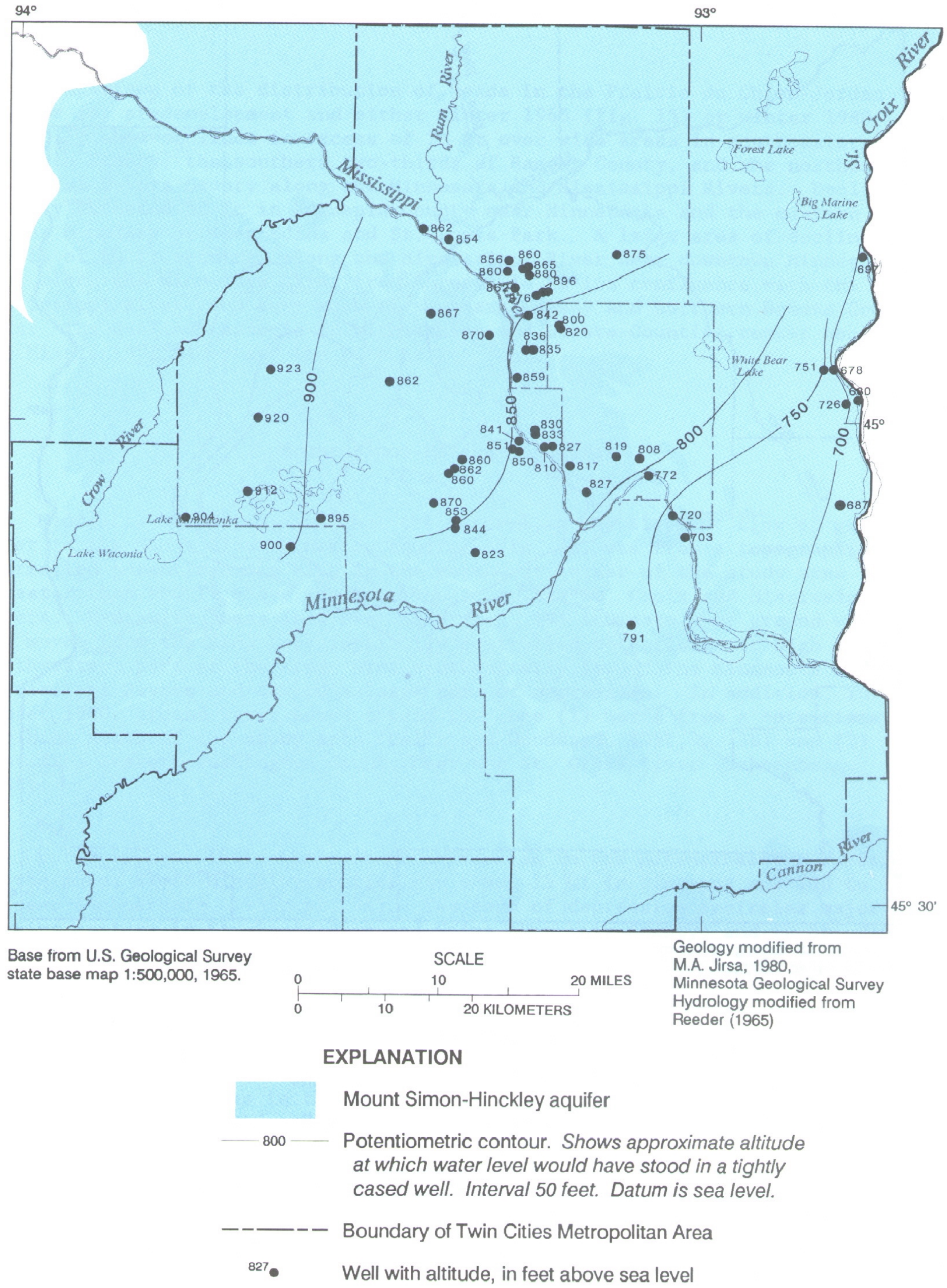

After Figure 18 of Schoenberg (1990)

Figure 33 – Pre-Development Piezometric Surface of Mt. Simon-Hinckley Aquifer, after Schoenberg (1990)

The Layer 5 model of pre-development conditions was used to estimate the residence time of groundwater at the locations of 26 wells screened in the Mt. Simon or Mt. Simon-Hinckley Aquifers, for which groundwater age values were reported in Lively et al. (1992). The modeled residence times were estimated by performing a backward particle trace starting at the base of the aquifer for each well location. These modeled residence times are presented along with the measured age data in Table 9, and are displayed in plan view in Figure 34.

Table 9: Mt. Simon-Hinckley Water Age Dates

Well Description	Unique Number	Approx. Location UTM_E	UTM_N	Age* (years)	Model (years)
Anoka Well #6	224625	470118	5008229	16000	15000
Anoka Well #7	453792	470978	5007226	>35000	16000
Coon Rapids Well #18	110469	476999	5004789	4400	17000
Saint Francis Well #2	184885	472789	5025932	6500	14000
Fridley Well #4	201158	479723	4992030	5200	18000
Andover Well #1	171011	471982	5007369	24000	16000
Andover Well #2	415932	472412	5006652	10100	16000
Andover Well #3	431683	476856	5007513	4100	16000
Chaska Well #6	161435	451052	4961926	23000	11000
Stacy Well #1	217915	501172	5026729	3200	7000
Wyoming Well #2	217901	499896	5019872	2700	6000
Burnsville Well #11	150359	478003	4958485	28000	23000
Eagan Well #11	433275	485744	4963646	16000	24000
Inver Grove Heights Well #6	433259	496352	4965080	>35000	27000
Vermillion Well #1	502689	502373	4946300	>35000	76000
Champlin Well #5	409524	468541	5002208	4600	16000
Champlin Well #7	416093	468971	5002065	3600	19000
Edina Well #9	206588	471408	4971387	23000	18000
Maple Grove Well #5	122250	465101	4991744	5600	17000
Saint Louis Park Well #12	206456	472268	4974398	>35000	20000
Spring Park Well #3	165595	449905	4975831	3300	11000
Mounds View Well #2	206716	483450	4994754	7000	18000
New Brighton Well #11	509083	483880	4989737	9200	16000
Savage Well #2	208816	471552	4957912	>35000	20000
Henderson Well #1	132296	427255	4931105	15000	8000
Minnesota Brewing Company Well #6 (old Schmidt Well #6)	231882	490331	4975115	>35000	21000

*Age dating from Lively, R.S., etal, 1992

A comparison between measured groundwater age and modeled residence time requires that we account for the scale of the time measurements. The radiometric age dates of the groundwater samples vary widely, ranging from 2,700 years to greater than 35,000 years. We compared modeled groundwater travel times to these results to evaluate how well the model simulated groundwater residence times. However, any errors in the modeled travel time will increase and be compounded over time, with the magnitude of the error increasing proportional to the travel time. To illustrate this concept, let's assume that a model is in 10-percent error computing the travel time of a particle. After 1,000 years of

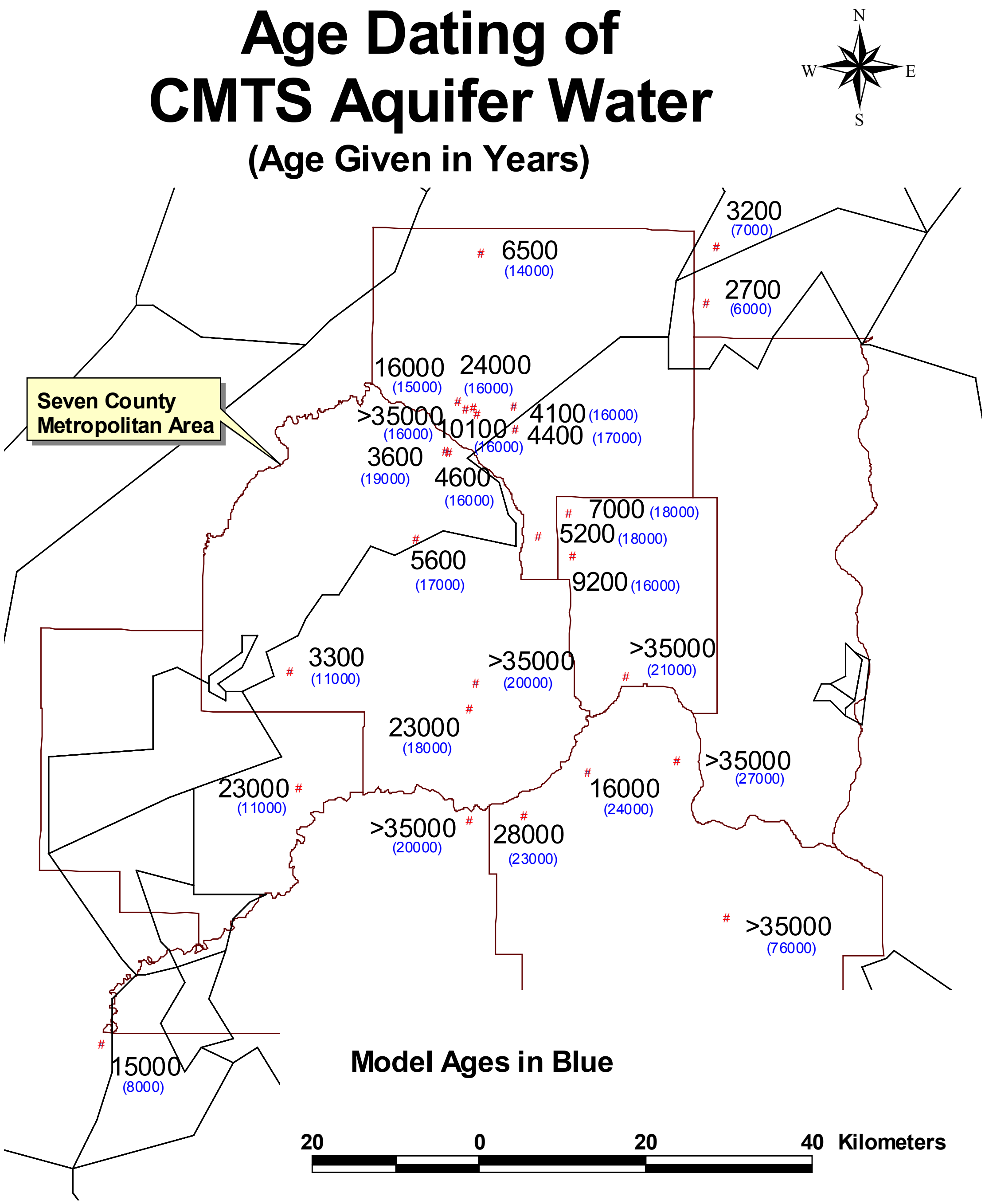

Figure 34 – Age Dates of Mt. Simon-Hinckley Aquifer Water

travel, this error would be 100 years, but after 30,000 years of travel it would be 3,000 years. A common process of calculating residuals utilizes the difference between the observed and modeled value. Typically, it expects well-modeled residuals to be normally and spatially distributed. However, in this case, conventionally derived residuals based on the age of the groundwater would not be distributed normally because the residuals would be increasing in the direction of the discharge point. Therefore, we have chosen to compare relative differences between measured groundwater age and modeled residence times, by expressing the modeled residence time relative to the measured age as a ratio to determine the factor by which the modeled age differs from the measured value for all 26 well locations. Measured values exceeding 35,000 years were set at 35,000 years for this analysis.

Overall, the comparison of the modeled and measured ages for groundwater supports the simulated flow regime. The values of this ratio ranged from 0.5 to 5.3, with a mean value of 1.9. This indicates that all the measured groundwater ages fall easily within an order of magnitude of the modeled residence times. The mean value, within a factor of two of the measured groundwater age, indicates a reasonable comparison between the two values. This is especially true considering that some measured values likely reflect a greater presence of younger water induced by recent human activity affecting the aquifer, as will be discussed further.

In general, Mt. Simon-Hinckley groundwater is assumed to become progressively older moving from the west and north, where major recharge zones occur, to the east and south across the metropolitan area. This is generally corroborated by the ^{14}C data presented in Lively et al. (1992) and our simulation of flow. However, an area that includes Anoka and northern Hennepin Counties provides an exception to this generality as can be seen in Figure 34. Here, the groundwater can be characterized by a mixture of ages within a relatively small area, whereas the model indicates a more consistent increase in age moving to the southeast. Age data indicative of younger water at some of these wells may be a result of mixing recent water with older water in response to human development of the aquifer. Prior to development, the Mt. Simon-Hinckley was likely characterized by confined artesian conditions with a vertical upward gradient over much of the Twin Cities area. Pumping of this aquifer could reduce or even reverse this gradient to induce younger water to flow into the Mt. Simon-Hinckley Aquifer, especially in areas where the overlying Eau Claire Formation has been compromised by erosion and/or past structural geologic activity. Another significant factor potentially affecting the age values is the presence of the numerous multi-aquifer wells in this area (See Figure A-2 in Appendix A). As the head in the Mt. Simon-Hinckley Aquifer is reduced in response to pumping, multi-aquifer wells offer ready conduits for flow from overlying aquifers into the Mt. Simon-Hinckley Aquifer. The exercise conducted for multi-aquifer wells indicates that their presence, under pumping conditions in the Mt. Simon-Hinckley Aquifer, facilitates the transfer of a large amount of water from the Franconia-Ironton-Galesville, into the Mt. Simon-Hinckley Aquifer (see Appendix A). In addition to the anthropogenic influences, apparent anomalies in groundwater age might also be effected by hydrogeologic complexity that we have not accounted for, such as structural controls on the flow system.

A statistical analysis of the modeled and measured water age dates at the wells shown in Figure 34 is presented in Appendix B. Though we assume that human influence has caused the incursion of younger water in parts of the aquifer, resulting in younger measured ^{14}C ages than can be accounted for in the model, an unbiased method of detecting outliers must be employed before we can eliminate affected data points from our statistical analysis, which is based solely on pre-development conditions. One standard deviation was chosen

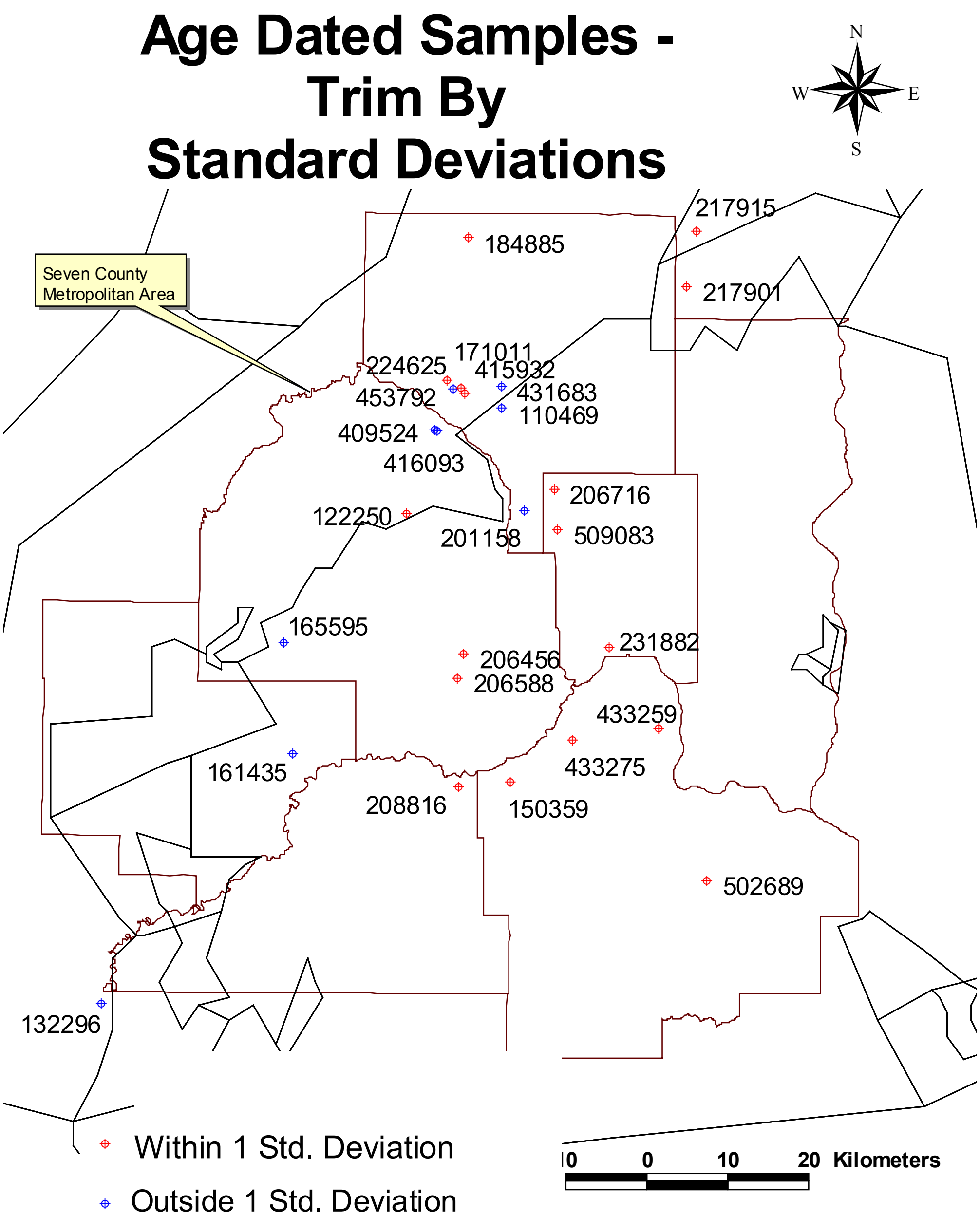

Figure 35 – Age Dating Trim by Standard Deviations

as the cutoff because the wells where mixing is suspected fall outside of this trim and likely do not represent the pre-development scenario. Elimination of these data points left 17 wells and narrowed the range of the ratio of modeled to measured age to 0.5 to 3.0, with a mean value of 1.5, supporting good agreement between the model and the ^{14}C age data. Figure 35 presents the final trim of the analysis showing wells by unique number that fall within and outside one standard deviation of the mean ratio of modeled to measured ages. The modeled simulation of the present day potentiometric surface in Figure 29 indicates a cone of depression centered in northern Dakota County that did not exist in pre-development days. The impact of this cone of depression on well capture zones is shown in

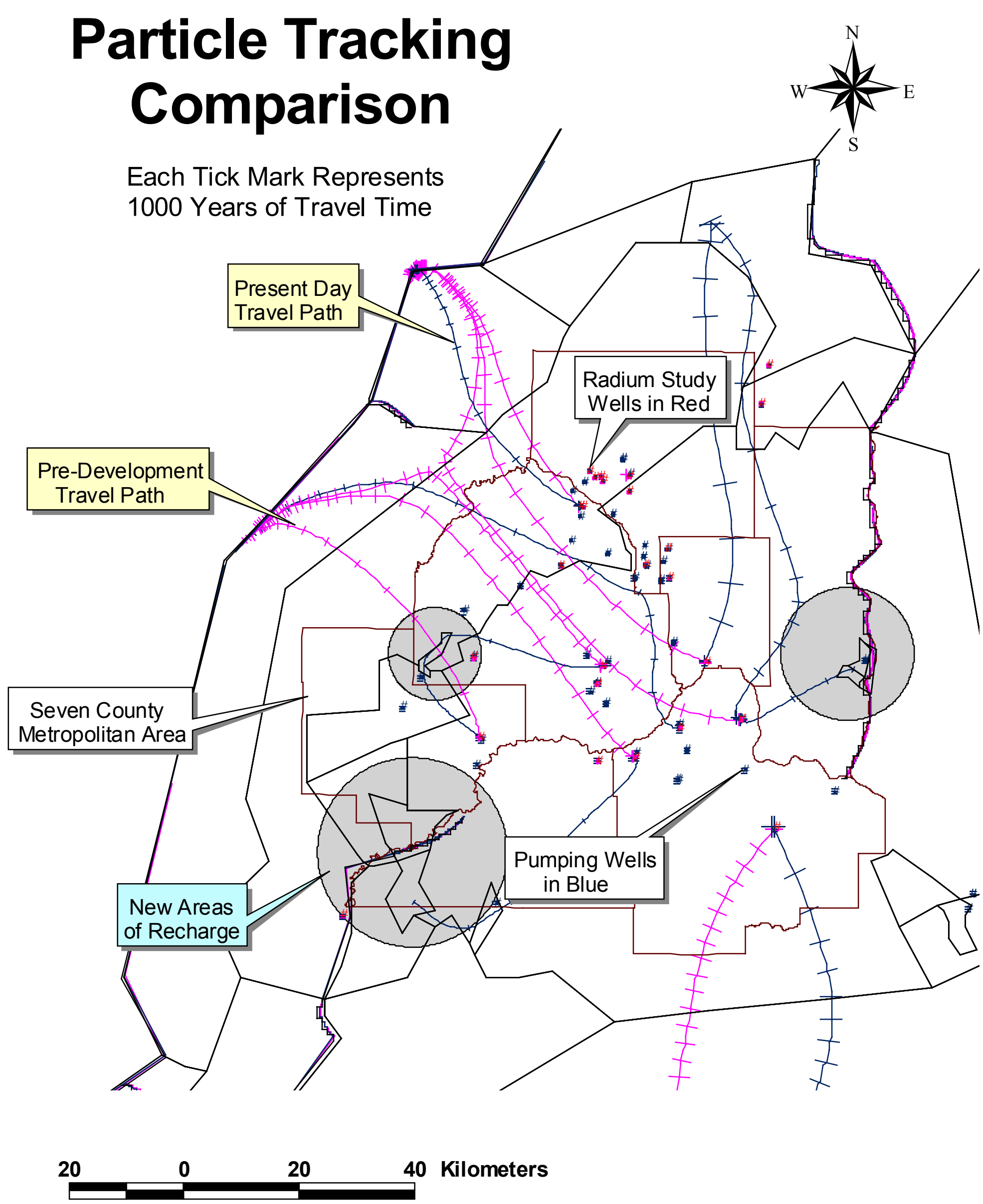

Figure 36 – Particle Tracking Comparison in Layer 5

Figure 36, which presents both pre-development and present day scenarios of particle path lines to selected wells presented in Lively et al. (1992). As stated, the particle tracking begins at the bottom of the aquifer proceeding backward from the well location. The modeled path lines are marked with tick marks that designate 1,000 years of travel between each.

The particle tracks show how the capture zones of these wells have changed with the addition of pumping wells in Layer 5. In general, the pre-development hydraulic gradient across the seven-county metropolitan area was from northwest to southeast. The cone of depression created by pumping has altered this gradient, especially to the north and east. The flow paths for some of the well locations have changed very little since pre-development time, and even indicate essentially the same aquifer residence times. In other cases, the stress of pumping has altered the flow regime so that significant recharge occurs in other areas of the aquifer that had previously served as discharge zones. A consequence of this change is a reduction in travel times to some of the wells.

The new areas of recharge predicted by the model surround the cone of depression and occur within the seven-county metropolitan area. These areas are highlighted in Figure 36, and indicate much shorter travel times to nearby wells. They coincide with locations where overlying bedrock units have been eroded away exposing the Mt. Simon-Hinckley bedrock units beneath drift material.

Changes in the zone of recharge of the Mt. Simon-Hinckley Aquifer may have implications for management and protection of this aquifer. Protection of the groundwater resource requires that we understand how and where the aquifer receives its recharge. Improved understanding of this aquifer will provide the technical basis needed to make informed decisions regarding its use and protection. The Layer 5 model may be useful in determining sensitive zones for the aquifer, as well as for determining special data needs and guiding further investigation.

Head Differences and Resistance

Although the current given-strength approach to modeling leakage on a regional basis allows for water to move vertically through the aquifer system, it does not permit simulation of the interactions that occur between aquifers. For example, the effects of pumping in one aquifer will not induce greater leakage from another aquifer with this approach. This type of simulation can be achieved by replacing given-strength VARELS with leaky VARELS. In a real system, flow between aquifers is driven by the head difference between them. However, the given-strength approach does not constrain the model in such a way that groundwater necessarily flows from higher head to lower head between aquifers.

Leakage between aquifers in this version of the Layers 4 and 5 model is entered as being downward, but there are instances where upward leakage is prescribed on top of Layer 4. The upward leakage occurs in three separate areas, where erosion, geologic structure, or river interaction appears to play a role. Figure 37 shows the location of upward leakage in the polygon mesh on top of Layer 4 and the associated geologic structure, where it is available.

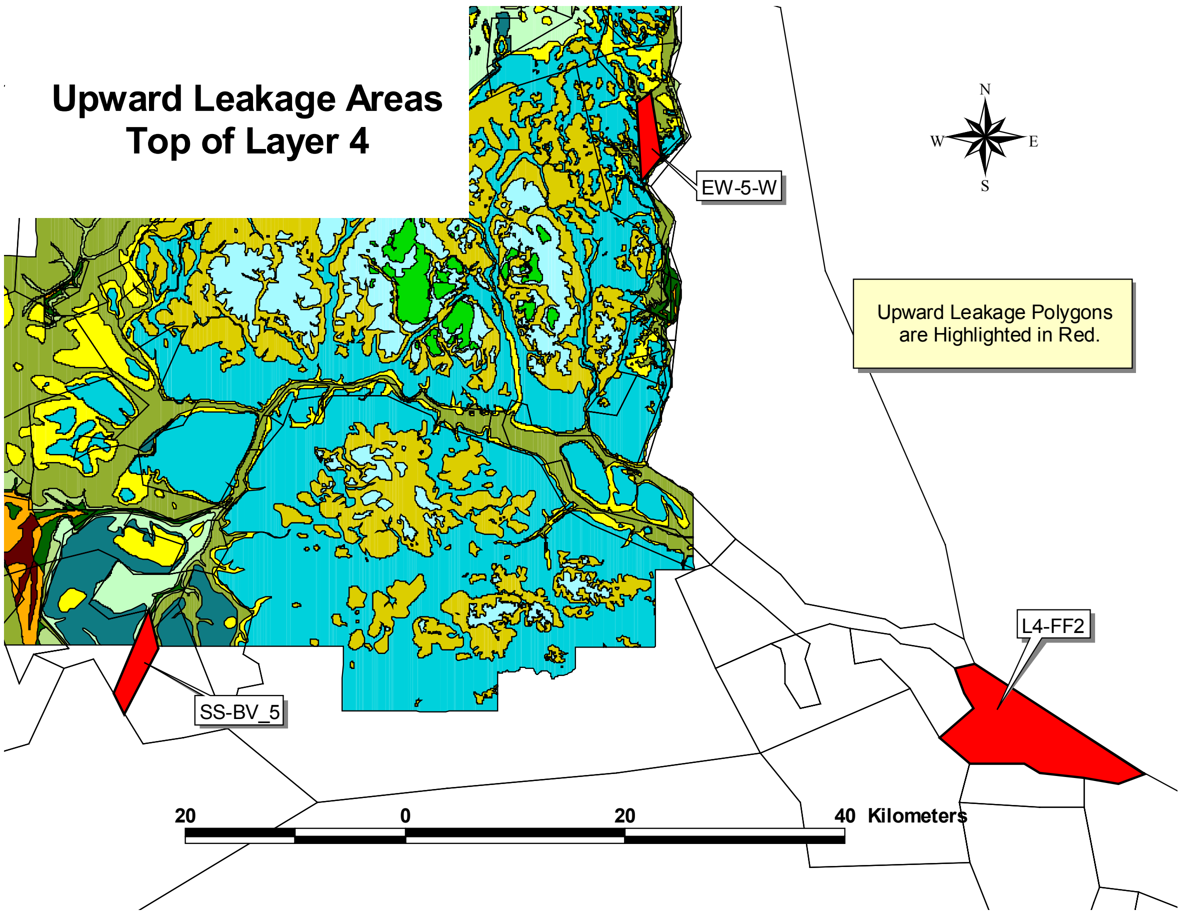

Figure 37 – Upward Leakage Areas Top of Layer 4

Plotting the head difference between layers at specific grid points allows one to check on consistency between the sign of the head difference and the specified leakage direction. Zones where the model head difference and leakage direction are not congruent are indicators of possible problem areas within the model. Evaluation of the head differences provides a good internal check for the model.

A grid has been constructed at a density that readily allows depiction of the head differences, which is plotted in Figure 38 using a color scheme that was chosen to indicate positive (downward) differences in head between aquifer layers (greater than 3 m), and negative (upward) differences in head (less than –3 m). Head differences implying downward leakage are represented by the pale green to dark blue color scheme, and head differences indicating upward leakage are represented by the yellow to red color scheme. Increasing color intensity indicates increasing magnitude in the head differences. The gray color represents zones of relatively small head difference (+/-3 m). Zones represented by gray are not considered to be problematic, because the model does not generally represent an accuracy level much better than +/-3 m on a regional scale. Where necessary, zones of small head differences will be replaced by site-specific modeling calibrated to better match local field conditions. Outside the modeled area of interest, small head differences, even those indicative of upward leakage, are not generally considered consequential.

Since all the leakage is downward to Layer 5 there should not be an occurrence of yellow to red colors in the modeled area, indicating an upward vertical head gradient between Layers 4 and 5. Figure 37 shows this is not the case. Comparing these results with the locations of upward leakage out of Layer 4 in Figure 30 shows some correlation. In these instances, discharge from Layer 4 is concentrated, where it is losing water both to Layer 5 and discharge to surface water bodies simulated with head-specified line-sinks. This would simulate a zone of reduced head in Layer 4, which could fall below that in Layer 5 indicating a vertical upward gradient.

Other yellow to red zones fall where there is considerably more leakage to Layer 5 than to Layer 4 or where erosion has removed the bedrock units overlying the Mt. Simon Sandstone (Layer 5). These occur near or in recharge areas for Layer 5, where calibration to measured heads has indicated small net leakage to Layer 4 while larger net leakage is required to the underlying Layer 5. The greatest focused recharge to Layer 5 in these areas can result in a head increase that could effect a vertical upward gradient to Layer 4.

Another check on model results can be made with resistance values as shown in Figure 39. Resistance in this case refers to resistance to vertical flow between aquifers and is calculated by dividing the modeled head differences shown in Figure 38 by the given leakage rates. Positive leakage is in a downward direction although indicated by the negative sign in the input data, the negative sign implies direction of flow. Resistance is measured in units of time and therefore cannot be negative, but negative values appear in Figure 39 generally where a negative head difference appears.

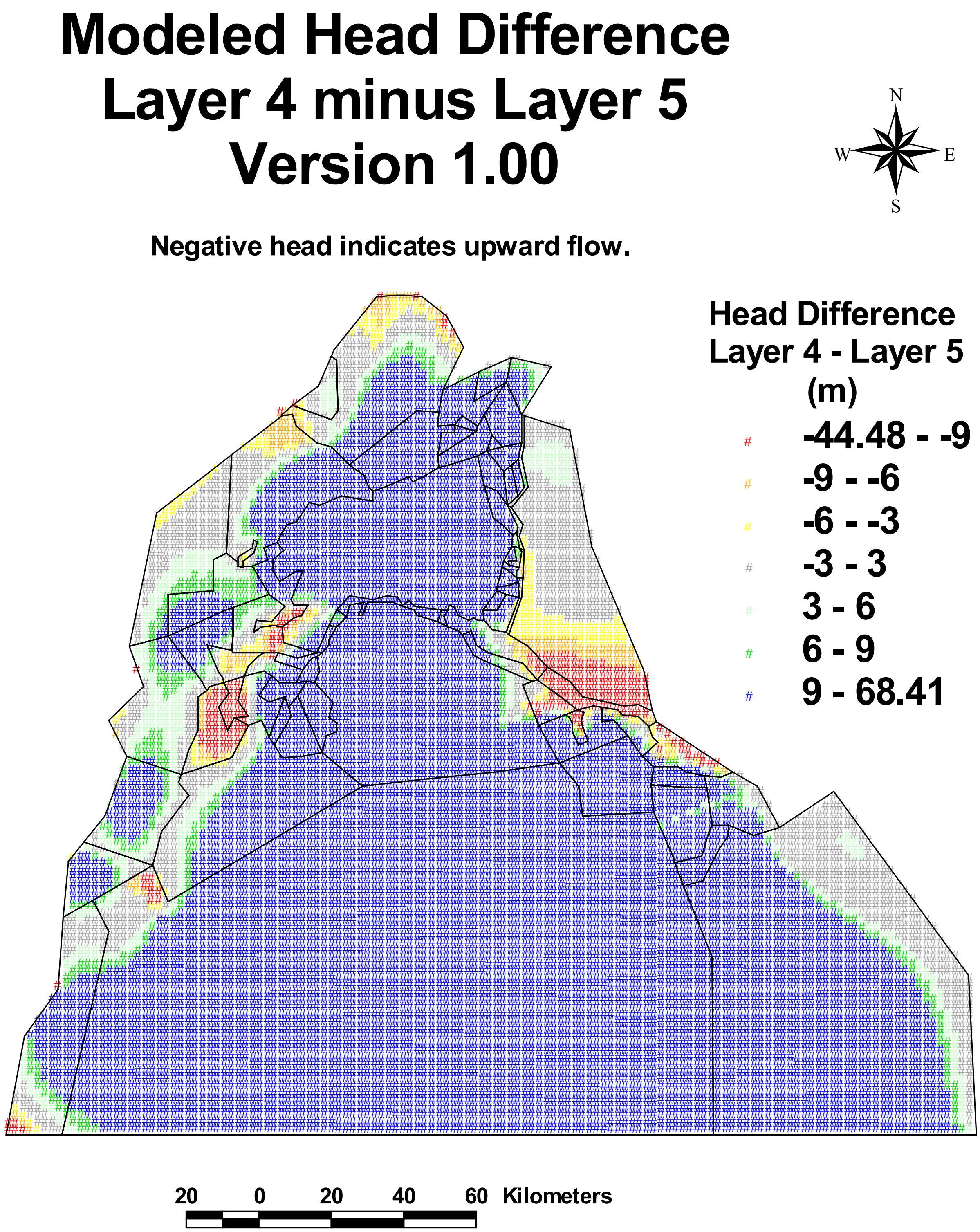

Figure 38 – Modeled Head Difference Layer 4 minus Layer 5

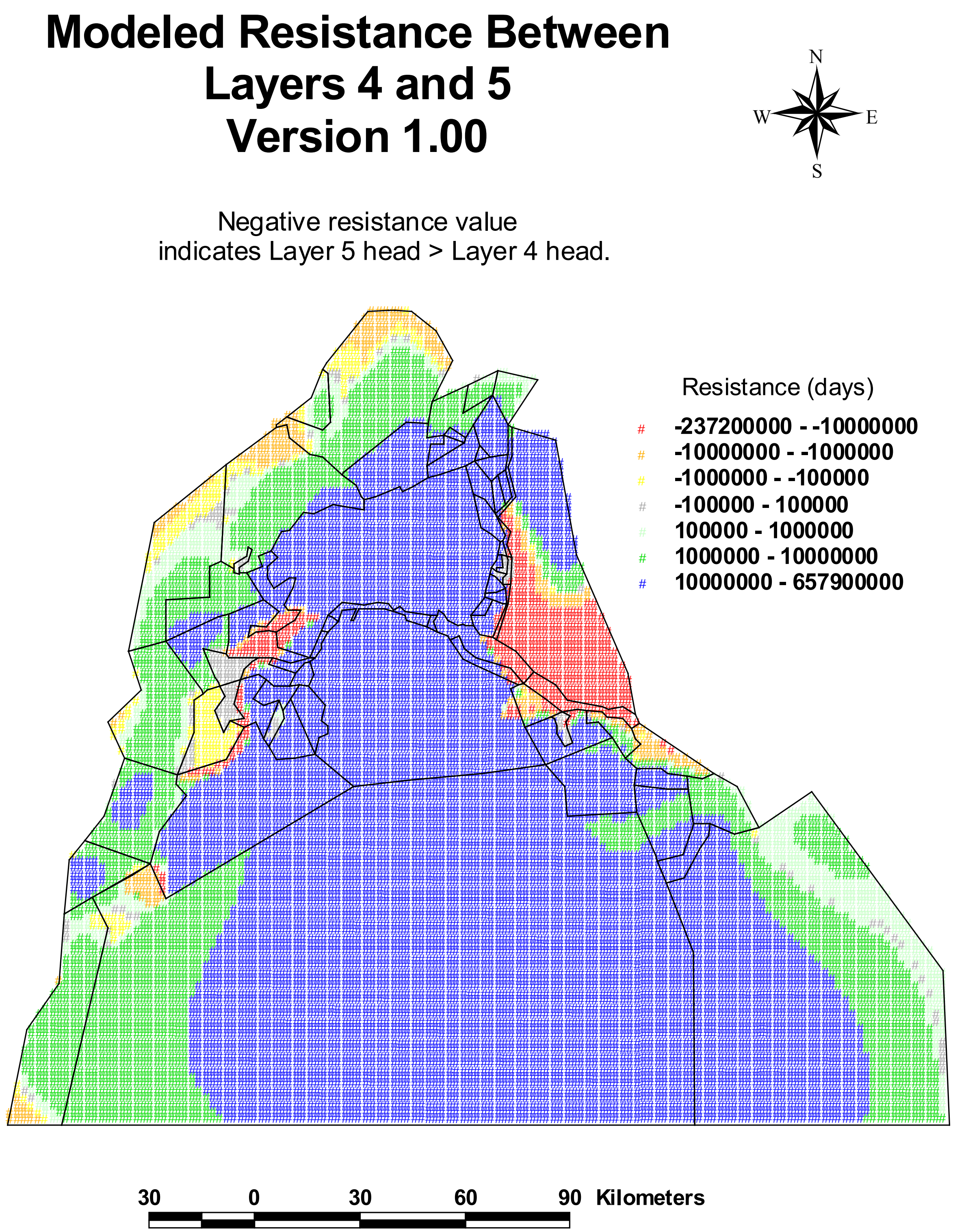

Figure 39 – Modeled Resistance between Layers 4 and 5

Figures 38 and 39 were constructed as internal checks on the consistency of the Layers 4 and 5 model, and to indicate potential problem areas. Future work should include investigations that will help confirm or refute the findings from this analysis of modeled head differences and resistance, and help to resolve internal inconsistencies. Site specific modeling efforts should be conducted in the context of this analysis so that leakage and modeled head differences are consistent with each other.

Water Budgets

Because the Layer 4 and 5 portion of the Metro Model simulates recharge and flow to the lower aquifers over the entire domain that impacts flow to the Twin Cities metropolitan area, it provides an opportunity to evaluate the overall water budgets of these aquifers. In this section we look at the distribution of leakage to each layer between the subcrop zones and zones where the aquifers are covered by other bedrock units. This analysis was conducted to better understand the relative contribution of these areas to aquifer recharge, as well as to make a first-cut quantification of total aquifer recharge. Each layer is evaluated separately and discussed in this section.

Layer 4 was subdivided into four areas--a subcrop zone, a metro north zone, and a metro south zone, which constitute our area of interest, and a far-field zone (Figure 40). The subcrop zone includes given-strength polygons to the west and north of the metropolitan area covering most of the aquifer where bedrock overlying Layer 4 is absent or is assumed to have undergone some erosion. The metropolitan area is divided into a north and a south zone. The metro north zone includes the portion of the seven county metropolitan area south and east of the subcrop zone, and north of the Minnesota and Mississippi Rivers, where numerous bedrock units overlie Layer 4 (Figures 4 and 5). The metro south zone lies south of the Minnesota and Mississippi Rivers, and generally includes most of Scott and Dakota Counties. It is assumed that a northward flow is induced in the aquifer by the two rivers and metropolitan pumping wells. To the south and east is the far-field zone. For purposes of this analysis, the contribution of leakage from the far-field zone to the metropolitan area is assumed to be negligible.

Layer 5 was similarly subdivided, except that the north and south metro zones were lumped together and an additional zone was defined. Three of the zones define our area of interest. The first is the subcrop zone that includes areas where the Mt. Simon Sandstone is exposed beneath drift material and also includes the eroded portion of the overlying Eau Claire Formation aquitard. The second zone is the transition zone, which is directly east of the subcrop zone and includes most of the Layer 4 subcrop zone. This additional zone was defined to determine the leakage contribution to Layer 5 from the area that is overlain by only those bedrock units that comprise Layer 4. However, the transition zone includes some small areas where Layer 5 is exposed beneath drift material due to past structural geologic activity and subsequent erosion. The third zone includes the remaining seven-county metropolitan area, where additional bedrock units overlie both Layers 4 and 5. A far-field zone incorporates all other areas, where less detail is included in the model and leakage is assumed to have negligible effects on the area of interest (Figure 41).

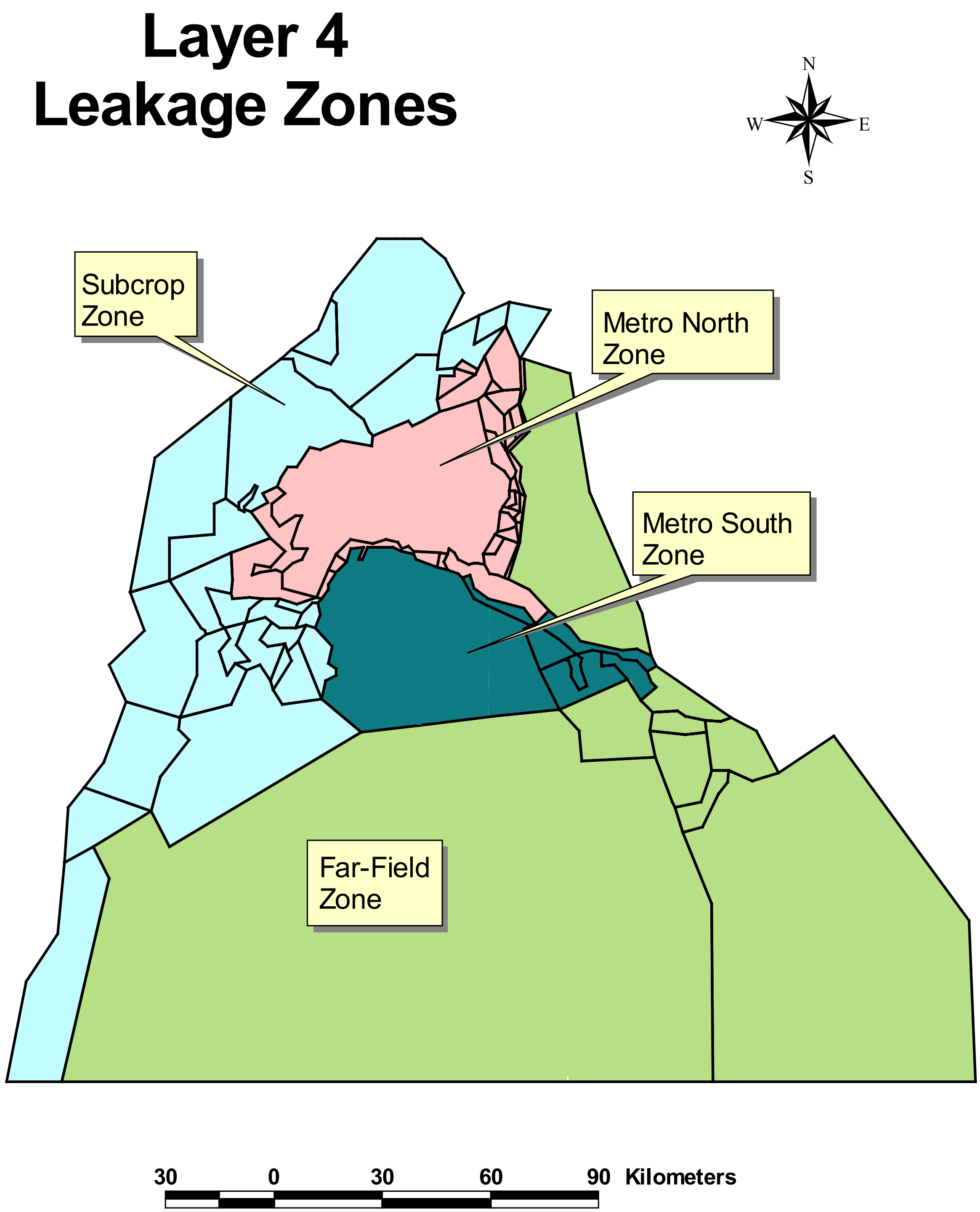

Figure 40 – Layer 4 Leakage Zones

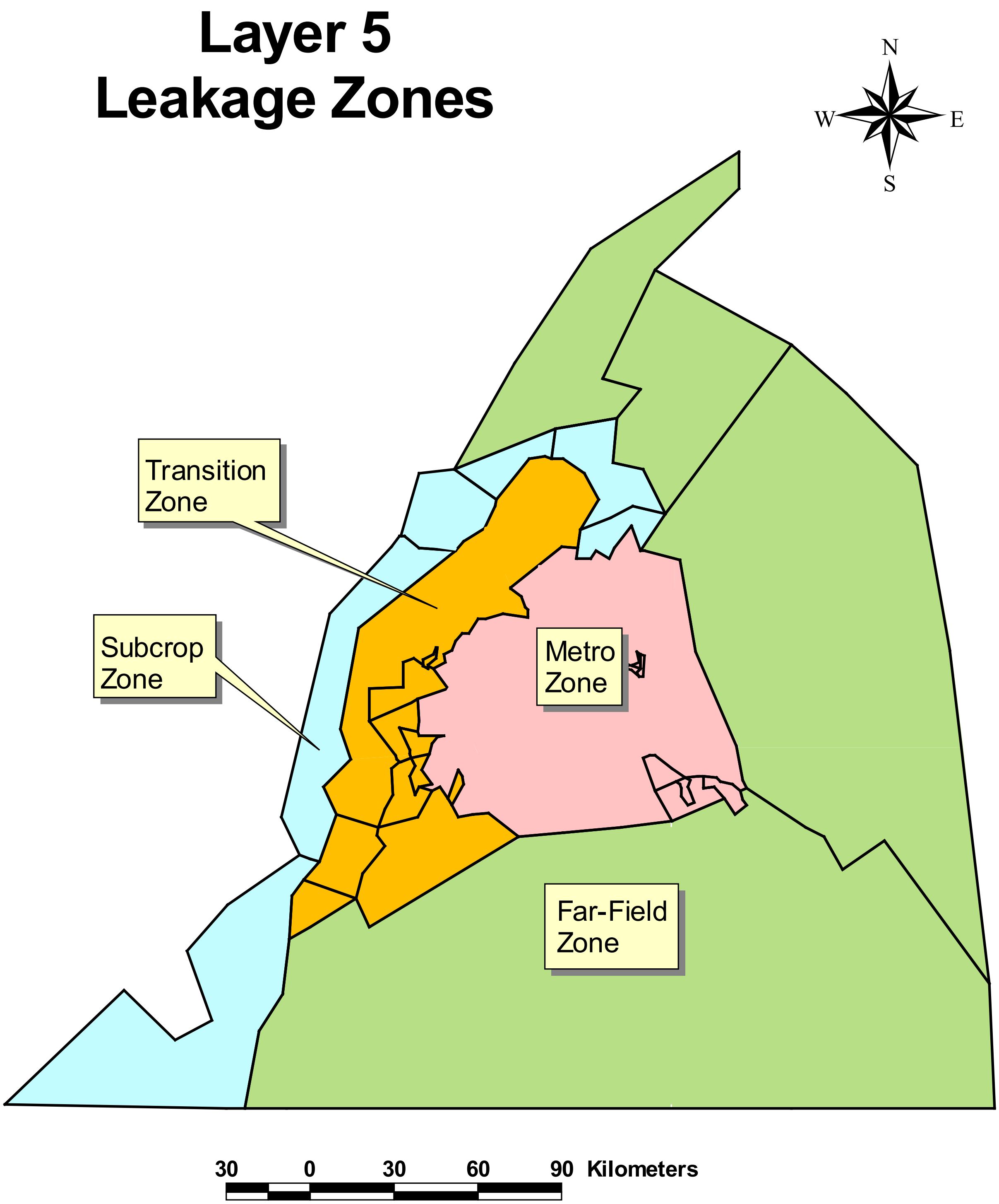

Figure 41 – Layer 5 Leakage Zones

The model recharge values given in Tables 10 and 11 show that the subcrop zones for each layer contribute more than half the total amount of water supplied in the areas of concern. In Layer 4 this zone also includes nearly 60 percent of the total area extending west and north from the Prairie du Chien-Jordan Formations and covering a large portion of Scott, Carver, Hennepin, and Anoka Counties (See Figures 3, 4, and 5).

Recharge to Layer 4 is fairly evenly distributed, being roughly proportional to the relative areas of each zone (Table 10). However, the analysis for Layer 5 (Table 11) indicates a less balanced distribution of recharge. Its subcrop zone covers less than a third of the total area, but provides nearly 60 percent of the total recharge. Most of the remaining recharge occurs in the transition zone, where the included areas of structural geologic activity provide pathways for recharge through Leaky Layer 4-5. Beneath the metropolitan area, which covers almost 40 percent of the area, this leaky layer is assumed to be continuous and to provide a resistance to vertical flow that is orders of magnitude greater than in overlying leaky layers. The total model percentage of recharge through this area is less than 10 percent.

Table 10: Layer 4 Recharge Percentages

Zone Name	Area (km^2)	Percent Total Area	Model Recharge (m^3/d)	Percent Total Recharge
Subcrop	8420	57.5	261700	52.1
Metro North	3314	22.7	138500	27.6
Metro South	2897	19.8	101900	20.3
Total	14631	100	502100	100
Far-Field	23250	N.A.	168700	N.A.

Table 11: Layer 5 Recharge Percentages

Zone Name	Area (km^2)	Percent Total Area	Model Recharge (m^3/d)	Percent Total Recharge
Subcrop	6851	31.09	191300	57.28
Transition	6390	28.99	113900	34.11
Metro	8797	39.92	28800	8.61
Total	22038	100	334000	100
Far-Field	42662	N.A.	57400	N.A.

Groundwater flow for the metropolitan area in Layers 4 and 5 cannot readily be separated out in terms of aquifer recharge since individual polygons may supply water to areas both within and outside of the metropolitan area. The difficulties inherent with isolating metropolitan area groundwater flow in Layers 4 and 5 underscore the fact that the numbers presented above reflecting actual and relative recharge rates to these two aquifers are associated with a high degree of uncertainty. However, we present the results of this analysis to serve as a springboard for additional discussion and future investigation.

In order to begin to understand the role that groundwater extraction plays in both the Franconia-Ironton-Galesville and Mt. Simon-Hinckley Aquifers, we will compare overall pumping rates from high-capacity wells used in the Metro Model datasets that were extracted from SWUDS data for 1995 (MNDNR, 2000b) to the overall modeled recharge rates in the areas of interest for both aquifer layers. Summing up the reported well discharge values for Layer 4 as seen in Table 2 yields a total discharge value of 13655 cmd. This value represents 2.7 percent of the total recharge in the area of interest for Layer 4 (502100 cmd). Using the sum of the modeled discharges reported in Table 3 for Layer 5, a total discharge rate of 80713 cmd was computed, constituting 24.2 percent of the total recharge to the Layer 5 area of interest given in Table 11 (334000 cmd).

To put these numbers into better context it is perhaps more proper to look at the overall water balance for each layer. This was accomplished by subtracting modeled river discharges found in Table 8 and modeled well discharges from the total recharge numbers in Tables 10 and 11. For this mass balance certain river sections were considered part of the far field and excluded.

In Layer 4 the total modeled discharge for all the curvilinear strings is 450720 cmd. Six of twenty strings are assumed to lie in the far-field to the south of the metropolitan area. They are named MISSR_SOUTH, ZUMBRO,WELLS_CREEK, BLUE_EARTH_RIVER, WATONWAN_RIVER, and LE_SUEUR-MAPLE_RIVER. The total discharge for the remaining 14 strings is 337430 cmd. The combined discharge from these strings and the wells is 351085 cmd, constituting 70 percent of the total recharge to Layer 4.

In Layer 5 the total modeled discharge for all the curvilinear strings is 313450 cmd. One string, MISSR_SOUTH, is assumed to lie in the far field to the south of the metropolitan area. The total discharge for the remaining 5 strings is 249850 cmd. The combined discharge from these strings and the wells is 330563 cmd, constituting 99 percent of the total recharge to Layer 5.

Uncertainty is associated with these numbers that can be attributed to several factors. First, there is uncertainty inherent to the regional model as well as the well discharge values reported in SWUDS and the river discharges included are subject to interpretation. Also, the fact that the model represents a transient system as a steady-state model introduces a degree of uncertainty to the numbers. Additionally, the effects of local-scale pumping from lower capacity and multi-aquifer wells are not included in the model. Therefore, as previously stated, it is necessary to emphasize that these numbers must be used judiciously, given the uncertainty surrounding them. They are intended to give a sense for the water budget and the impact of groundwater extraction, and serve as a starting point for future discussion and analysis that ultimately will lead to better understanding of the water budgets of these two aquifers.

Summary

The Layers 4 and 5 model provides a regional flow simulation within the Franconia-Ironton-Galesville and Mt. Simon-Hinckley Aquifers across the seven-county metropolitan area and beyond. The model produced heads that match well to water elevations that exist in the aquifers, and provided discharges to major rivers that are plausible. Flow path simulations indicate residence times that, generally agree with existing age data for Mt. Simon-Hinckley groundwater samples. The results for the metropolitan area are generally consistent with those determined by Schoenberg (1990) indicating the presence of a cone of depression in Layer 5.

The purpose of this report is two-fold: 1) to provide necessary documentation to end-users who choose to apply the Metro Model of the lower aquifer layers, and 2) to contribute to the on-going discussion regarding these important lower aquifers. By treating the aquifers with a systems approach, we have attempted to gain better understanding of the nature of their groundwater flow. These efforts have allowed us to make interpretations regarding water budgets, recharge zones, and how the recharge has changed from pre-development to the present conditions. Additionally, this study may be helpful in identifying sensitive recharge zones to ensure the long-term integrity of water quality in these aquifers. We present these results and interpretations with the hope that they will help spur further investigation into the flow systems of these deeper aquifers.

Data Files, Version 1.00

A brief description of the data files that comprise the Layers 4 and 5 model is presented below. A list of other relevant supporting files such as regional head calibration datasets is found after the model datasets. All of these files can be downloaded from the Metro Model web page.

General Model Datasets:

l_setup.dat	Commands to MLAEM software, and specification of graphical window.
l_aq.dat	Global aquifer parameters for Layers 1, 2, 3, 4, and 5.
l_poly.dat	Polygon mesh for Lower Layers, including both infiltration and leakage polygons.
l_msr_cu.dat	Curvilinear strings for Mississippi River and associated seepage faces.
l_mnr_cu.dat	Curvilinear strings for Minnesota River and associated seepage faces.
l_scr_cu.dat	Curvilinear strings for St. Croix River and associated seepage faces.
l_msc_cu.dat	Curvilinear strings for Crow, Rum, Zumbro, Blue Earth, Le Sueur, Watonwan, and Cannon Rivers, for Hays and Wells Creeks, and for faults and impermeable zones.

Franconia-Ironton-Galesville Aquifer—Layer 4 Data sets

L4_ntop.dat	Infiltration rates for polygons on top of Layer 4; can be considered the total infiltration for the two-layer aquifer system.
L4_msr.dat	Boundary conditions (elevation heads) for relevant portions of Mississippi River and associated seepage faces.
L4_mnr.dat	Boundary conditions (elevation heads) for Minnesota River.
L4_scr.dat	Boundary conditions (elevation heads) for St. Croix River and associated seepage faces.
L4_msc.dat	Boundary conditions (elevation heads) for Crow, Rum, Zumbro, Blue Earth, Le Sueur, Watonwan, and Cannon Rivers, for Hays and Wells Creeks, fault conditions, and impermeable zones.
l4_nbot.dat	Leakage out of bottom of Layer 4 specified for each polygon—same as leakage into the top of Layer 5.
L4_well.dat	Discharge wells used in Layer 4.

Mt. Simon-Hinckley Aquifer—Layer 5 Data sets

l5_ntop.dat	Leakage into top of Layer 5 specified for each polygon—same as leakage out of the bottom of Layer 4.
l5_msr.dat	Boundary conditions (elevation heads) for relevant portions of the Mississippi River and associated seepage faces.
l5_mnr.dat	Boundary conditions (elevation heads) for Minnesota River.
l5_scr.dat	Boundary conditions (elevation heads) for St. Croix River and associated seepage faces.
l5_msc.dat	Boundary conditions for impermeable zones.
l5_well.dat	Discharge wells used in Layer 5.

Call File for Layers 4 and 5 Model

CallL45.dat	Version 1.00 call file dataset for the Layers 4 and 5 model; calls the model datasets described above.

The files described above are all that are needed to run the Layers 4 and 5 model. Head calibration data sets are discussed separately below.

Regional Calibration Data sets

Calibration datasets that were constructed to calibrate the model on a regional basis are included below. As described in the report, "Preparation of Supporting Databases for the Metropolitan Area Groundwater Model" (Streitz, 2000), these data were geostatistically winnowed from the CWI database for Layer 4 and from MDNR's observation well network for Layer 5 to provide head calibration targets over a very large area. As such, these data can only be appropriately applied to regional model development and calibration. Site-specific data are necessary for calibrating the locally refined model. The datasets are separated according to model layer:

L4_cal.dat Head calibration dataset for Layer 4, zones 1, 2, 3, 4, 5, 6, and 7 developed from measured static water levels in the Franconia-Ironton-Galesville Aquifer.

L5_cal.dat Head calibration dataset for Layer 5, developed from MDNR observation well network in the Mt. Simon-Hinckley Aquifer.

Application and Use of the Metro Model

The Layers 4 and 5 portion of the Metro Model has been presented as a starting point for constructing models on a more local scale. A regional system has been developed that will require modification to local scale models for two reasons. First, on a regional basis, the model will not provide a correct coarse representation of the flow system in all areas. Use of all available data on a more local basis will help lead to a better representation. Second, local detail will need to be incorporated to properly simulate local groundwater flow conditions.

Model elements themselves will require modification and/or replacement for more site-specific modeling. For example, order and overspecification values will likely need to be increased on curvilinear elements in the area of interest to provide sufficient control to model the groundwater system. Also, multi-aquifer systems will require replacement of given-strength areal elements with leaky elements, which can actually propagate hydraulic interactions between aquifers. Additionally, control point placement is critical to properly simulate leakage effects between aquifers. Metro Model staff can provide guidance for applications of the model.

Changes and improvements are expected to the model. They will be periodically posted on this web site. To ensure that you are using the latest version of the Metro Model, be sure to frequently check it. The version currently posted is 1.00. The version number for future releases will be incrementally increased and will readily allow users to determine if they are using the most current version available.

Future Work

Data and information regarding the lower two aquifers tend to be sparse, owing in large part to the expense of invasive techniques such as drilling and well construction. As a result, many gaps remain in our knowledge of these aquifers. One advantage to constructing a model of these aquifers is that it helps us to better define our weaknesses in understanding. Therefore, this model and analysis are presented as a contribution to help guide future work. Used mindfully and with discretion, the Layer 4 and 5 portion of the Metro Model and its results can be a useful tool in helping groundwater scientists understand these deeper flow systems. Additionally, it helps us to identify gaps in our knowledge and understanding of flow in the lower aquifers. Some needs for information have been identified during the modeling process and are included in the following list:

- More complete and accurate pumping records
- Additional high-quality head monitoring points, such as those maintained by MDNR, particularly within the metropolitan area for the Franconia-Ironton-Galesville Aquifer, and anywhere in the Mt. Simon-Hinckley Aquifer.
- Any data relating to aquifer hydraulics including parameters such as values of infiltration rates, hydraulic conductivity, and storativity.
- Information regarding the nature of inter-aquifer flow occurring through erosional apertures incised into bedrock units.

As data become available, Metro Model staff will incorporate it into the model, resources permitting.

References Cited

Delin, G.N., and D.G. Woodward, 1984, Hydrogeologic Setting and the Potentiometric Surfaces of Regional Aquifers in the Hollandale Embayment, Southeastern Minnesota, 1970 - 80, U.S. Geological Survey Water-Supply Paper 2219, 56 p.

Jirsa, M.A., B.M. Olsen, and B.A. Bloomgren, 1986, Bedrock Map of the Seven-County Twin Cities Metropolitan Area, Minnesota, Minnesota Geological Survey Miscellaneous Map Series M-55, 2 plates.

Lively, R.S., Jameson, R., Alexander, E.C., and Morey, G.B., 1992, Radium in the Mt. Simon-Hinckley Aquifer, East-Central and Southeastern Minnesota, Information Circular 36, Minnesota Geological Survey, University of Minnesota.

MDNR, 2000a, Minnesota Department of Natural Resources (MDNR), Division of Waters Observation Well Program, accessible through website URL http://www.dnr.state.mn.us/waters/programs/gw_section/obwell/watlevs.html.

MDNR, 2000b, Minnesota Department of Natural Resources (MDNR), Division of Waters, State Water Use Data System (SWUDS) database for high-capacity permitted wells.

Mossler, J.H., and R.G. Tipping, 2000, Bedrock geology and structure of the seven-county Twin Cities metropolitan area, Minnesota, Miscellaneous Map series M-104, Minnesota Geological Survey.

Reeder, H.O., 1966, Fourteen maps of parts of the groundwater reservoir in the Minneapolis-St. Paul Metropolitan Area: U. S. Geological Survey Open-File Maps, 14 pls., scale 1:125,000.

Schoenberg, M.E., 1990, Effects of Present and Projected Ground-Water Withdrawals on the Twin Cities Aquifer System, Minnesota, U.S. Geological Survey Water-Resources Investigations Report 90-4001, prepared in cooperation with Minnesota Department of Natural Resources, and Metropolitan Council of the Twin Cities, 165 p.

Seaberg, J.K., 2000, Overview of the Twin Cities Metropolitan Groundwater Model, Ver. 1.00.

Streitz, A.R., 2000, Preparation of Supporting Databases for the Metropolitan Area Groundwater Model, Ver. 1.00, in preparation.

Appendix A

Calibration Test Using Multi-Aquifer Wells

Appendix A Table of Contents

Figures

Tables

Appendix A

Calibration Test Using Multi-Aquifer Wells

Calibration Test

New pumping data became available toward the end of this model's development, which allowed us to explore the use of a larger set of pumping wells in Layer 5. MDNR's SWUDS database was reviewed for the years 1995 through 1998 for wells associated with the Mt. Simon-Hinckley aquifer and a total of 148 wells throughout the portion of Minnesota covered by this aquifer were selected for use in this test. The current model contains 47 wells in Layer 5. An average daily pumping rate based upon the total annual pumping was calculated from the 1995 through 1998 data and initially used in this test. These average daily rates as well as a maximum daily pumping rate for the years of record are reported in Table A-1.

The reason for this test was to attempt to reduce or eliminate the discharge to pumping wells that was added during the model calibration process. It was hoped that looking at more than one year's pumping data would provide better estimates of the average discharge of high capacity wells from the aquifer and add wells in areas where the model wasn't as well calibrated to the observation well data. This area is generally located in southeastern Hennepin and northern Scott and Dakota Counties where MDNR's observation well data indicates a cone of depression in the Mt. Simon-Hinckley aquifer system. The Mt. Simon-Hinckley aquifer is synonymous with Layer 5.

This was not the result however, as most of the additional wells were located outside of the seven-county metropolitan area (See Figure A-1). The discharges within the seven-county area still required higher rates than the calculated average pumping rates to calibrate the model. The adjusted daily pumping rates assigned to individual wells were increased to no more than a rate that would produce the maximum total annual output that was reported for the years 1995 to 1998. This did not improve the model's calibration.

Finally, in addition to the larger set of Layer 5 wells, 67 multi-aquifer wells open to both Layers 4 and 5 were used, as well as the existing set of wells in Layer 4. As mentioned in this report, the use of multi-aquifer wells caused Layer 4 to become drier and Layer 5 to become wetter in the model. This is probably because the multi-aquifer wells allow the transfer of water between layers to equalize the head at the well. The locations of the multi-aquifer wells are shown in Figure A-2 and the particulars of these wells are reported in Table A-2.

Although the multi-aquifer wells did not produce the desired effect within the system they were kept in this test to allow users to see how the model reacts to this type of well. One point that is necessary to highlight is most of the well data was used rather than only selecting multi-aquifer wells in problem areas for inclusion in this regional model. It was

Table A-1

Test Case Layer 5 Discharge Wells

UTME 83	UTMN 83	Unique Number	Discharge Rates (cmd) 1995-98 Average Daily	Maximum Average Daily	Modeled Average Daily
477004	5004971	110469	265	444	444
608225	4879059	110484	1068	1217	1068
482939	4992641	110485	135	280	280
583527	4840052	110496	186	215	186
604247	4879781	112210	689	848	689
448375	4984155	112238	9	15	9
473594	5047716	114488	72	72	72
468275	4996624	122250	36	72	36
442564	5017674	126505	242	293	242
438496	5019651	126508	154	268	154
427090	4931153	132296	228	309	228
615133	4845743	150341	163	175	163
631794	4845784	150345	143	149	143
478563	4958697	150359	2130	2740	2740
497079	4958623	151553	7	8	7
502360	5058681	151559	716	789	716
536607	4931349	151565	1837	3649	1837
485696	4991861	151568	170	170	170
392782	4901432	154609	105	125	105
497002	4956269	161421	8391	9020	9020
484518	4987445	161432	187	247	247
451069	4963042	161435	1823	1996	1996
440681	5020296	163648	295	530	295
450035	4976036	165595	396	621	396
455051	5018302	167972	40	156	40
472246	5007495	171011	751	1116	1116
479345	4995780	180920	1413	1928	1928
472910	5026061	184885	806	913	806
417030	4889540	191916	163	174	163
484472	4978488	200177	29	87	87
480040	4992092	201158	2562	3197	3197
467898	5005768	201191	1046	1697	1697
468929	4974007	203614	2129	3136	3136
472962	4967878	206184	2788	3206	3206
471865	4979094	206424	3151	4735	4735
471052	4977505	206439	553	1720	1720
472030	4974481	206456	3272	4318	4318
471309	4971574	206588	2579	4181	4181
479943	4992093	206670	1669	2183	2183
479947	4991793	206674	1376	2249	2250
480250	4992086	206675	1699	2040	2040
483772	4994764	206716	53	108	108
482644	4989281	206794	0.2	0.2	0.2
509548	4963154	208001	17	42	17
496850	4957123	208394	386	510	510
408965	4957540	210312	271	299	271
408965	4957540	210313	308	310	308
408565	4957749	210324	820	1013	820
408565	4957749	210412	627	1005	627
440858	4972581	212279	264	375	264
440858	4972581	212280	300	347	300
386395	4878389	213559	954	1145	954
496850	4956923	213584	1816	3891	3891
433087	5017368	214549	160	192	160
384676	4853581	217107	28	71	28
486343	5062774	217883	296	312	296
484338	5052463	217885	115	177	115
522986	5037268	217893	634	691	634
499941	5019878	217901	521	612	521
500153	5020281	217902	482	562	482
519763	5026013	217905	66	127	66
512146	5026573	217911	338	371	338
513072	5025890	217913	764	862	764
501429	5026909	217915	247	336	247
501375	5049591	217923	10	10	10
455859	5021386	217941	540	635	540
442171	5020651	217948	252	314	252

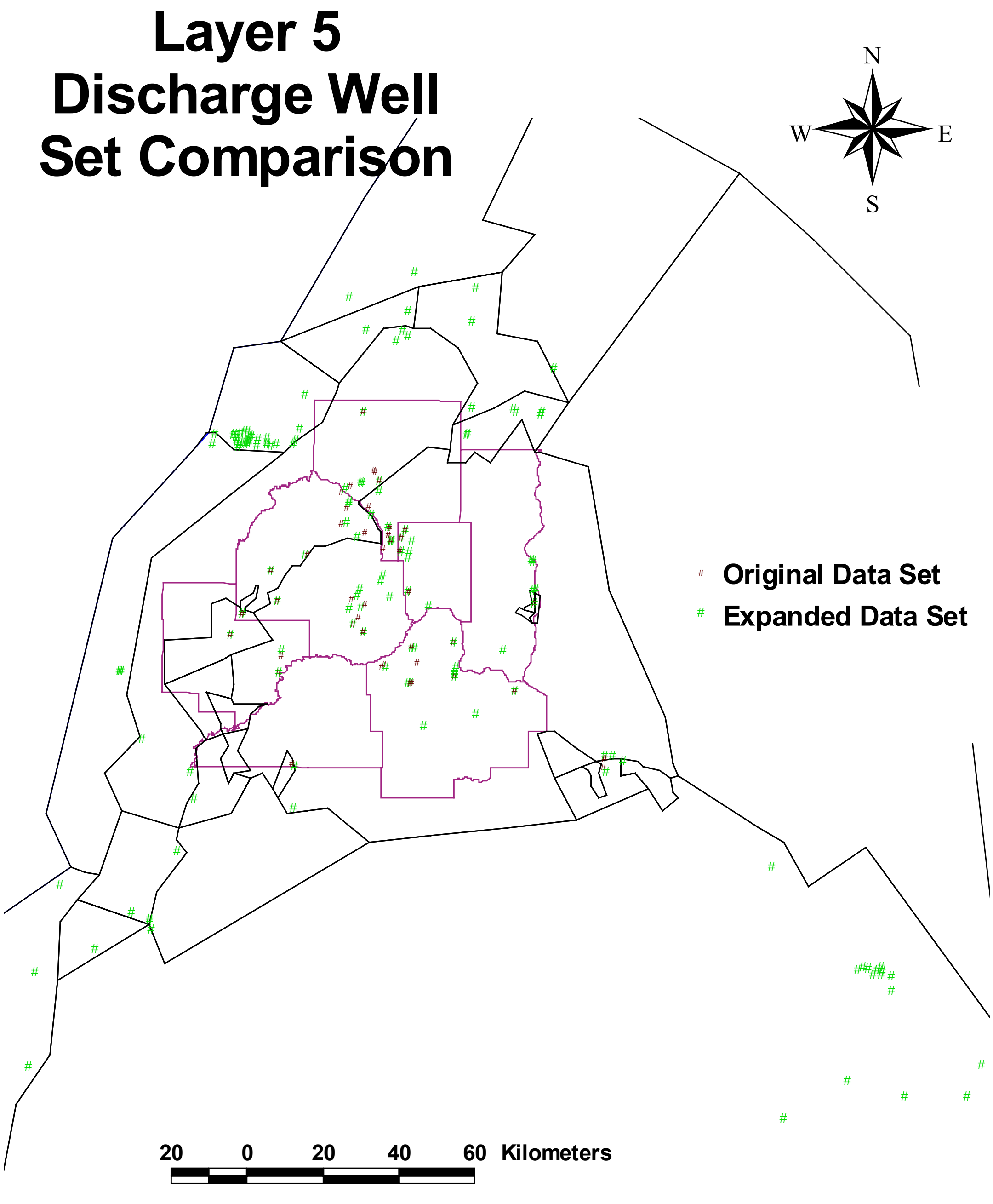

Figure A-1 – Layer 5 Well Data Set Comparison

found that Layer 5 calibration could be improved when only certain multi-aquifer wells were added, generally in the area of the suspected cone of depression. This may be how a local model should be modeled, but on a regional basis the effect of all known multi-aquifer wells provides the best picture of regional leakage.

Table A-2

Multi-Aquifer Well Discharge Rates (cmd)

UTME 83	UTMN 83	Unique Number	Discharge Rate
450287	4946652	207133	640
496444	4957225	208391	4502
471307	4958150	208836	489
458953	4959461	205978	1316
491965	4960688	208388	1
451550	4961669	200809	3666
451349	4961675	110453	1822
472418	4965022	222912	8668
441254	4970489	208860	168
446589	4972068	161408	80
440858	4972581	212279	133
450035	4976036	224642	201
446996	4977862	208864	154
536267	4935182	218622	845
518953	4945540	171732	292
536329	4902146	226952	111
517502	4985651	208790	1681
514398	4990814	208038	113
509352	4982578	208448	397
499955	4987878	222880	666
516427	4985986	208791	263
515251	4989436	236085	30
465730	4925326	220922	2
425500	4918108	211802	123
422899	4903504	211797	169
416466	4892566	112207	1215
423289	4955124	219000	121
420419	4947689	218056	115
449713	4989388	240631	28
450133	5001848	114358	36
466172	4991839	223350	24
466216	4994566	207018	83
471060	4993005	203265	3
473251	4994003	203022	31
475651	4993593	203026	209
468533	5000417	160019	49
467122	5004833	202754	2693
479333	4993405	206657	2284
480060	4990491	206685	61
479594	4995372	206638; 223294	1968
479293	4995607	206637	71
486834	4997478	233109	301
483776	4994363	206121	820
497041	5009424	208989	672
503591	5009636	208560	210
501158	5014220	208558	1564
500956	5014518	201157	1287
480650	5037790	114383	352
514532	5026807	217914	103
481528	5016186	209224	161
484300	5010993	107442	23
470114	5008414	224625	4054
480566	5007085	208594	318
479820	5003559	208615	791
478583	5002340	202930	3507
478385	5002535	202932	3724
472159	5001776	228438	173
474306	5001204	161413; 110460	1230
474505	5000997	110461	5284
474890	4999975	202965	386
475706	4999941	168721	136
479786	5001147	208628	1542
479373	5000742	208629	1796
478338	4999528	202951	48
488475	5000463	209209	24
488076	5000474	208634	1581
488079	5000673	208633	1954

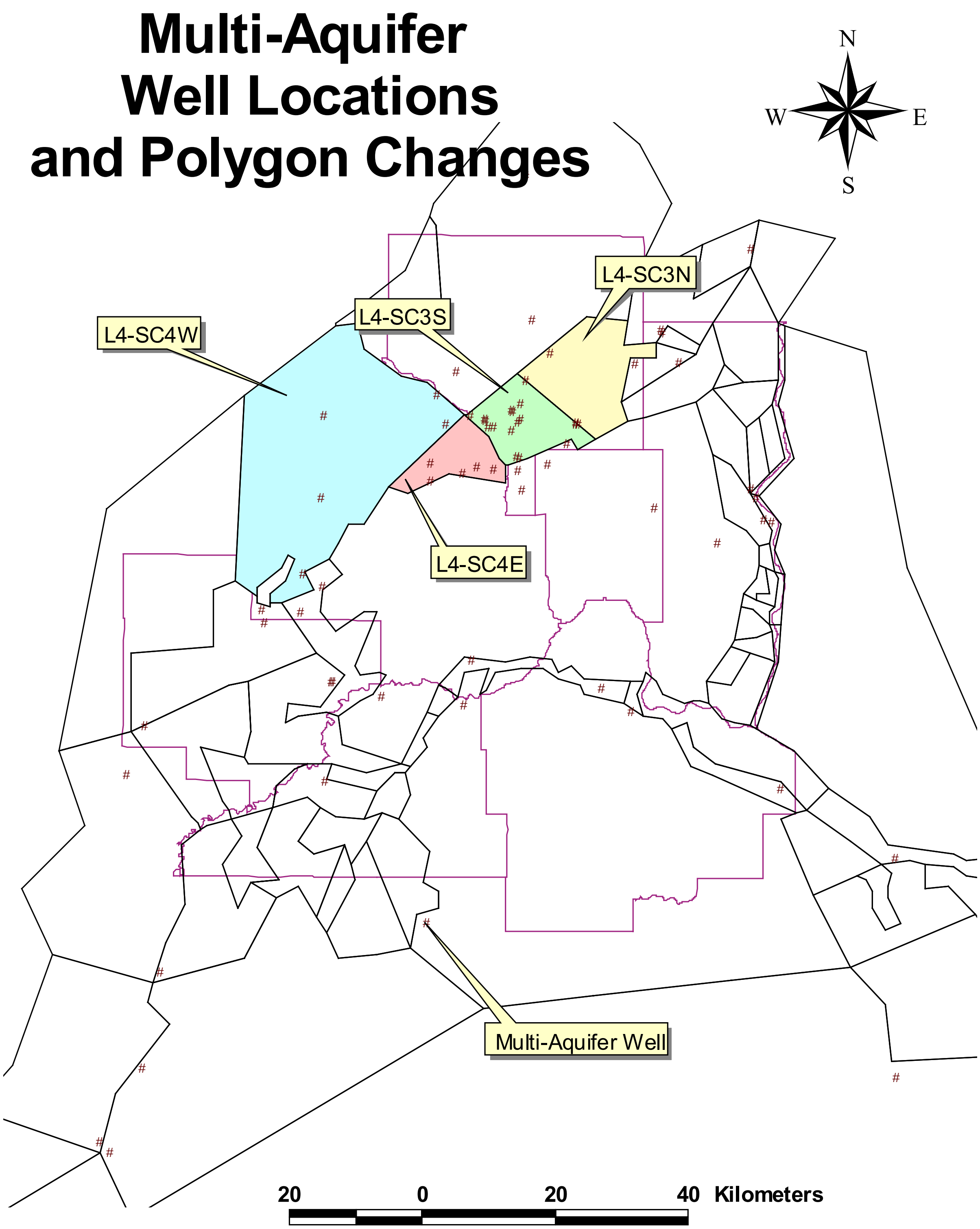

Figure A-2 – Multi-Aquifer Well Locations and Polygon Changes

Table A-3
Layer 4 Leakage Inputs
Test Case

POLYGON	Layer 4 Top (Total Infiltration) (m/day)	Top (Total Infiltration) (in/year)	Bottom (m/day)	Net (Top - Bottom) (m/day)	Net (Top - Bottom) (in/year)	Corresponding Layer 5 POLYGON
L4-SC1	-2.38E-05	-0.34	-1.00E-07	-2.37E-05	-0.341	L4-SC-W
L4-SC2	-5.21E-05	-0.75	-1.00E-07	-5.20E-05	-0.747	L4-SC-W
L4-SC3S	-2.00E-04	-2.88	-1.00E-07	-2.00E-04	-2.874	L5-LKG
L4-SC3N	-3.14E-05	-0.45	-1.00E-07	-3.13E-05	-0.450	L5-LKG
L4-SC4E	-7.01E-05	-1.01	-1.00E-07	-7.00E-05	-1.006	L4-SC-W
L4-SC4W	-3.14E-05	-0.45	-1.00E-07	-3.13E-05	-0.450	L4-SC-W
L4-SC5	-3.70E-06	-0.05	-1.70E-06	-2.00E-06	-0.029	L4-SC5
L4-SC6	-1.05E-04	-1.50	-1.00E-07	-1.04E-04	-1.500	L5-LKG
L4-SC7	-5.55E-05	-0.80	-5.00E-07	-5.50E-05	-0.790	L4-SC7
L4-SC8	-1.40E-07	0.00	-1.00E-07	-4.00E-08	-0.001	L5-LKG
L4-SC9	-4.13E-05	-0.59	-1.00E-07	-4.12E-05	-0.593	L5-LKG
L4-SC10	-3.13E-05	-0.45	-1.10E-06	-3.02E-05	-0.435	L4-SC10
L4-SC11	-5.70E-05	-0.82	-1.10E-06	-5.59E-05	-0.803	L4-SC11
L4-SC12	-1.40E-05	-0.20	-2.50E-06	-1.15E-05	-0.165	L5-FF3
L5-SC1	-1.09E-03	-15.66	-1.08E-03	-1.00E-05	-0.144	L5-SC1
L5-SC2	-1.24E-04	-1.78	-1.74E-04	5.00E-05	0.719	L5-SC2
WC-1	-8.11E-06	-0.12	-1.00E-07	-8.01E-06	-0.115	L4-SC-W
W-FF2	-1.75E-05	-0.25	-1.00E-07	-1.74E-05	-0.250	L4-SC-W
SLS-1	-2.61E-05	-0.38	-4.87E-05	2.26E-05	0.324	SLS-1
SLS-2	-2.10E-06	-0.03	-1.00E-07	-2.00E-06	-0.029	SLS-2
SS-8	-7.34E-04	-10.55	-8.35E-04	1.01E-04	1.451	SS-8
SS-9	-1.39E-04	-2.00	-1.00E-07	-1.39E-04	-1.997	L5-LKG
SS-10	-8.36E-05	-1.20	-1.00E-07	-8.35E-05	-1.200	L5-LKG
SS_SAND_S1	-3.01E-05	-0.43	-1.00E-07	-3.00E-05	-0.431	L5-LKG
SS-BV_1	-2.00E-04	-2.88	-1.00E-07	-2.00E-04	-2.874	L5-LKG
SS-BV_2	-1.00E-07	0.00	-1.00E-07	0.00E+00	0.000	L5-LKG
SS-BV_3	-3.01E-05	-0.43	-1.00E-07	-3.00E-05	-0.431	L5-LKG
SS-BV_4	-3.49E-05	-0.50	-1.00E-07	-3.48E-05	-0.500	L5-LKG
SS-BV_5	1.17E-04	1.69	-1.50E-04	2.67E-04	3.843	SS-BV_5
MNR_BV_2	-5.00E-04	-7.19	-1.00E-07	-5.00E-04	-7.185	L5-LKG
SD-BV_2	-4.00E-04	-5.75	-1.00E-07	-4.00E-04	-5.748	L5-LKG
L4-BV1	-4.00E-04	-5.75	-1.00E-07	-4.00E-04	-5.748	L5-LKG
L4-BV2	-2.00E-07	0.00	-1.00E-07	-1.00E-07	-0.001	L5-LKG
L4-BV3	-1.10E-06	-0.02	-1.00E-07	-1.00E-06	-0.014	L5-LKG
L4-BV4	-3.00E-07	0.00	-1.00E-07	-2.00E-07	-0.003	L5-LKG
L4-LKG-S	-5.20E-06	-0.07	-1.00E-07	-5.10E-06	-0.073	L5-LKG
L4-LKG-N	-7.10E-06	-0.10	-1.00E-07	-7.00E-06	-0.101	L5-LKG
L4-FF1	-5.20E-06	-0.07	-1.00E-07	-5.10E-06	-0.073	L5-LKG
L4-FF2	4.84E-04	6.96	-2.50E-06	4.87E-04	6.993	L5-FF3
L4-FF3	-8.65E-05	-1.24	-2.50E-06	-8.40E-05	-1.207	L5-FF3
L4-FF4	-4.90E-04	-7.04	-2.50E-06	-4.88E-04	-7.005	L5-FF3
L4-FF5	-2.00E-05	-0.29	-2.50E-06	-1.75E-05	-0.251	L5-FF3
L4-FF6	-1.40E-04	-2.01	-2.50E-06	-1.38E-04	-1.976	L5-FF3
L4-FF7	-7.50E-06	-0.11	-2.50E-06	-5.00E-06	-0.072	L5-FF3
L4-FF8	-1.77E-04	-2.54	-2.50E-06	-1.75E-04	-2.508	L5-FF3
L4-FF9	-5.20E-06	-0.07	-2.50E-06	-2.70E-06	-0.039	L5-FF3
SG-1-E	-1.87E-04	-2.69	-2.00E-06	-1.85E-04	-2.658	SG-1-E
SG-3-M	-3.50E-04	-5.03	-2.00E-06	-3.48E-04	-4.999	SG-3-M
SG-3-E	-2.09E-05	-0.30	-1.39E-05	-6.98E-06	-0.100	SG-3-E
SG-3-BV	-3.22E-04	-4.63	-6.96E-04	3.74E-04	5.374	SG-3-BV
E-FF5	-2.10E-05	-0.30	-7.00E-06	-1.40E-05	-0.201	L5-RE3
E-FF6	-6.20E-05	-0.89	-7.00E-06	-5.50E-05	-0.790	L5-RE3
E-CHISAGO_L	-3.70E-05	-0.53	-7.00E-06	-3.00E-05	-0.431	L5-RE3
E-B-MARINE_L	-7.01E-05	-1.01	-1.00E-07	-7.00E-05	-1.006	L5-LKG
E-FOREST_L	-2.01E-05	-0.29	-1.00E-07	-2.00E-05	-0.287	L5-LKG
EW-1	-2.01E-05	-0.29	-1.00E-07	-2.00E-05	-0.287	L5-LKG
EW-2	-1.21E-05	-0.17	-1.00E-07	-1.20E-05	-0.172	L5-LKG
EW-3	-9.51E-05	-1.37	-1.00E-07	-9.50E-05	-1.365	L5-LKG
EW-4	-4.00E-04	-5.75	-1.00E-07	-4.00E-04	-5.748	L5-LKG
EW-5-E	-5.50E-04	-7.90	-1.00E-07	-5.50E-04	-7.904	L5-LKG
EW-5-W	9.99E-05	1.44	-1.00E-07	1.00E-04	1.437	L5-LKG
EW-6N	-1.00E-04	-1.44	-1.00E-07	-1.00E-04	-1.437	L5-LKG

Table A-4

Layer 5 Leakage Inputs

Test Case

POLYGON	Layer 5 Top (m/day)	Layer 5 Top (in/year)
E-FF1	-1.00E-07	-0.001
E-FF4	-1.20E-04	-1.724
L5-RE1	-2.50E-05	-0.359
L5-RE2	-4.00E-05	-0.575
L5-RE3	-7.00E-06	-0.101
L5-RE4	-3.10E-05	-0.445
L5-RE5	-1.55E-05	-0.223
L5-SC1	-1.08E-03	-15.520
L5-SC2	-1.74E-04	-2.500
L5-LKG	-1.00E-07	-0.001
L4-SC-W	-1.00E-07	-0.001
L5-FF1	-1.00E-07	-0.001
L5-FF2	-5.00E-08	-0.001
L5-FF3	-2.50E-06	-0.036
L4-SC5	-1.70E-06	-0.024
L4-SC7	-5.00E-07	-0.007
L4-SC10	-1.10E-06	-0.016
L4-SC11	-1.10E-06	-0.016
SLS-1	-4.87E-05	-0.700
SLS-2	-1.00E-07	-0.001
EW-15SE	-2.09E-04	-3.003
EW-16N	-6.26E-04	-8.996
SCX2	-5.57E-04	-8.004
SS-8	-8.35E-04	-11.999
SS-BV_5	-1.50E-04	-2.156
SG-1-E	-2.00E-06	-0.029
SG-3-M	-2.00E-06	-0.029
SG-3-E	-1.39E-05	-0.200
SG-3-BV	-6.96E-04	-10.002

Also note another important item regarding the use of multi-aquifer wells with MLAEM. In this regional model test case if two or more multi-aquifer wells had the same X and Y coordinates, MLAEM would not produce a solution. To overcome this problem the discharges of multi-aquifer wells with the same coordinates were added together. If it is important in a local scale model to separate discharges, then the wells will require better locating procedures.

The use of a greater number of wells in Layer 5 and the multi-aquifer wells required adjustment to leakage rates from those shown in Tables 4 and 5. The polygons' net leakage for each layer in this test is given in Tables A-3 and A-4. In addition, more polygons were required in the subcrop zones of Layer 4 because of the presence of the multi-aquifer wells in clusters especially along the Mississippi River. The new polygons are highlighted on Figure A-2.

The Layers 4 and 5 calibration results shown in Figures A-3 and A-4 respectively reflect the model discharge rates given in Tables A-1 and A-2, and the Layer 4 discharge well rates given in Table 2. This is a similar situation to what was encountered when no multi-aquifer wells were used. Namely, that the averaged discharges of high capacity wells modeled in Layer 5 does not account for all the drawdown in the aquifer as indicated by the Layer 5 calibration data set. Maintaining our initial assumption that Leaky Layer 4-5 characteristics remain the same away from eroded surfaces and past geologic structural zones, then additional pumping at existing wells must be added to produce a better calibration.

Data Files, Test Case

Modelers interested in using the expanded Layer 5 discharge well and/or the multi-aquifer well data sets can find them in the following files along with files of adjusted leakage rates.

Test Case files.

L5_wellx.dat	Expanded Layer 5 well discharges file using SWUDS 1995-1998 pumping data.
L45_multi.dat	Multi-aquifer well discharges file-using SWUDS 1995 pumping data.
polytest.dat	Polygon file containing the additional polygons shown in Figure A-2.
L4_ntopx.dat	Infiltration rates for polygons on top of Layer 4; can be considered the total infiltration for the two-layer aquifer system.
l4_nbotx.dat	Leakage out of bottom of Layer 4 specified for each polygon—same as leakage into the top of Layer 5.
l5_ntopx.dat	Leakage into top of Layer 5 specified for each polygon—same as leakage out of the bottom of Layer 4.

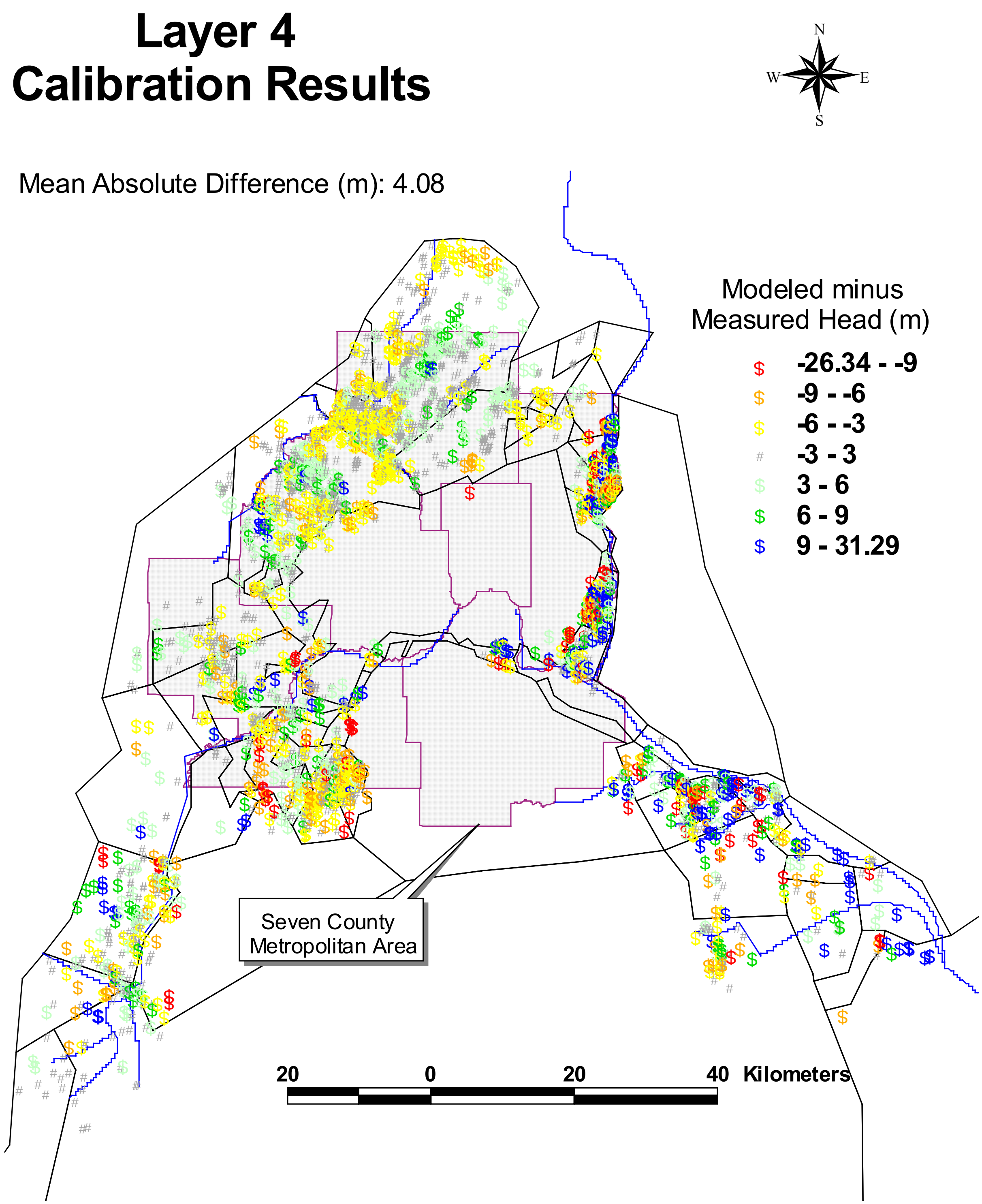

Figure A-3 – Layer 4 Calibration Plot

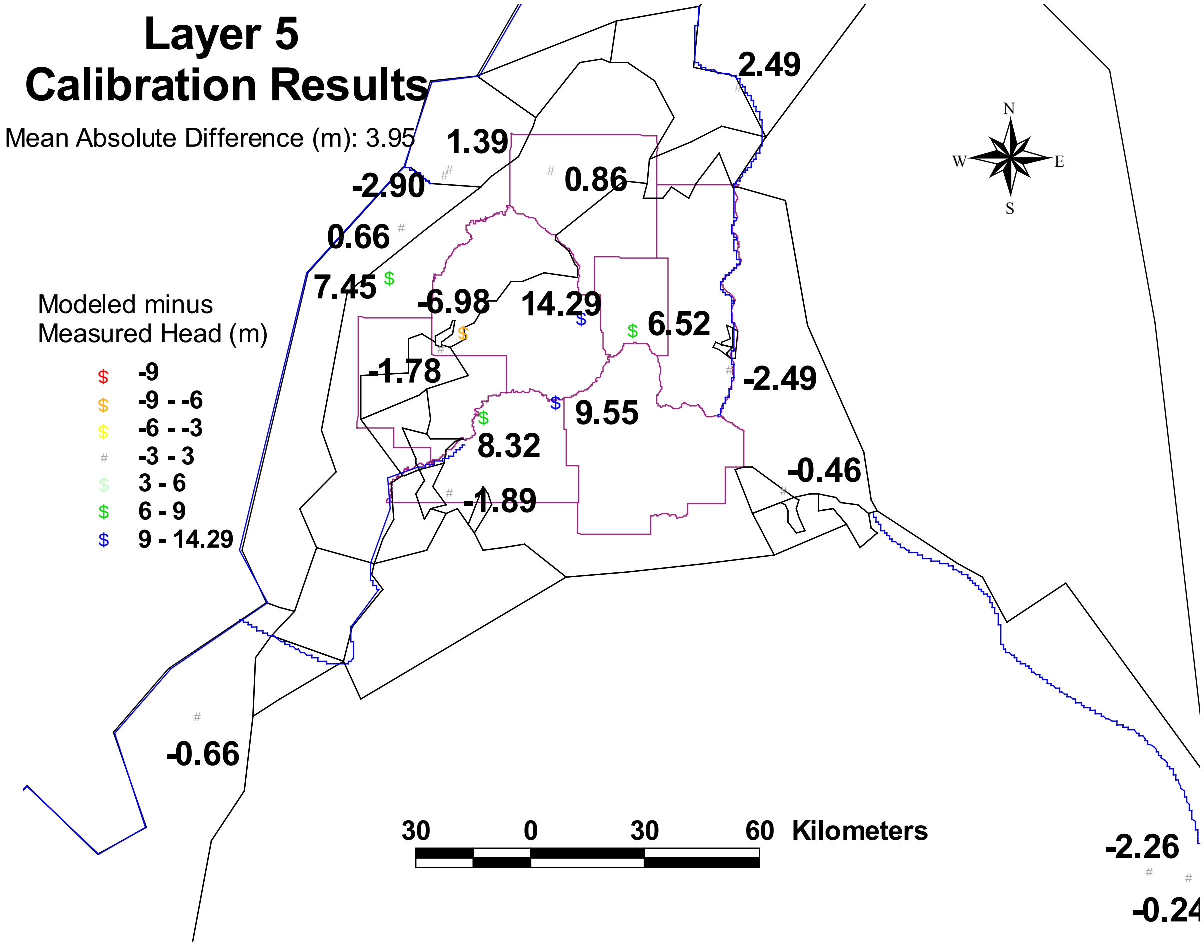

Figure A-4 – Layer 5 Calibration Plot

Appendix B

Statistical Analysis of Modeled and Measured Age Dating Samples

Appendix B Table of Contents

Figures

Tables

Appendix B

Statistical Analysis of Modeled and Measured Age-Dating Samples

The first step is to generate a list of ratios based on the age of modeled versus observed for each groundwater monitoring point. The values can then be analyzed statistically to trim outliers and produce a smoothed calibration data set.

Judging the quality of a well-modeled system depends upon the ratios (a form of residual) being:

1) Normally distributed,
2) Exhibiting a mean close to zero, and
3) Possessing a random spatial distribution

The data will be presented and analyzed with these goals in mind.

A. The Wells

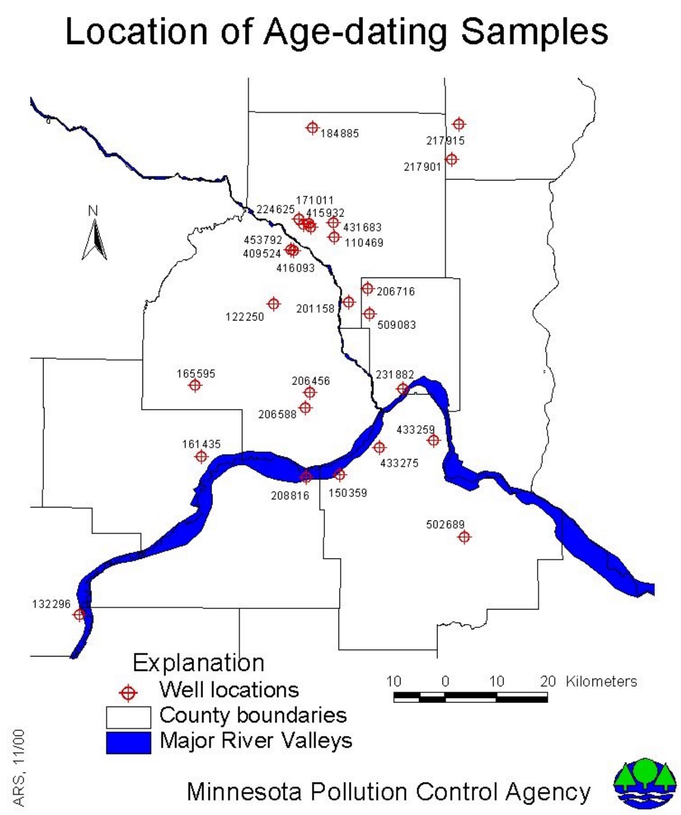

Figure B-1 – Location of Age-dating Samples

B. The Analysis

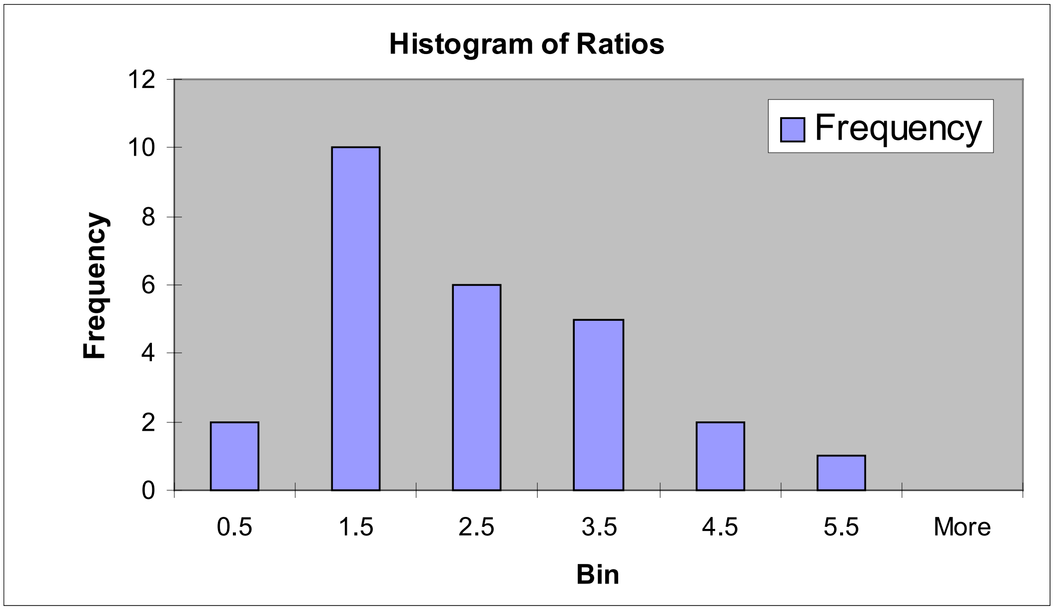

Figure B-2 - Histogram of Ratios

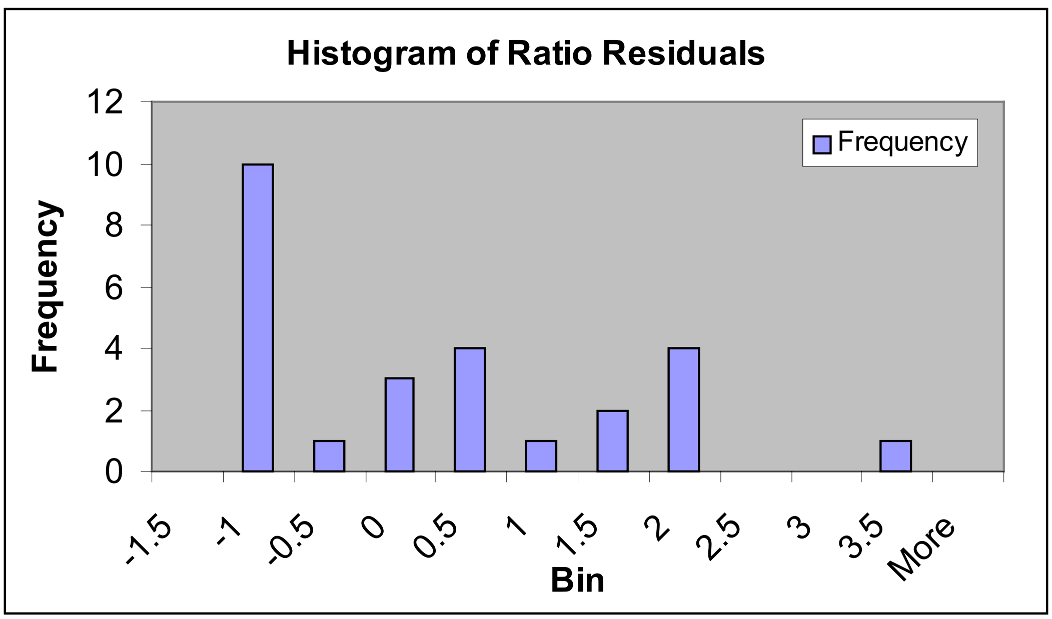

Figure B-3 - Histogram of Ratio Residuals

Both the histogram of the straight ratios and the histogram of the ratio residuals show a "normal-ish" behavior. Generating a mean of the ratio and then subtracting it from each ratio forms the ratio residual.

B. Data Analysis (Continued)
Descriptive Statistics

Table B-1 Age Date Ratios Summary Statistics

UNIQUE	Measured Age of GW	Modeled Age of GW	Ratio of Modeled to Measured	Ratio Residuals
453792	35,000	16,000	0.46	-1.45
161435	23,000	11,000	0.48	-1.43
132296	15,000	8,000	0.53	-1.38
206456	35,000	20,000	0.57	-1.34
208816	35,000	20,000	0.57	-1.34
231882	35,000	21,000	0.60	-1.31
171011	24,000	16,000	0.67	-1.24
433259	35,000	27,000	0.77	-1.14
206588	23,000	18,000	0.78	-1.13
150359	28,000	23,000	0.82	-1.09
224625	16,000	15,000	0.94	-0.97
433275	16,000	24,000	1.50	-0.41
415932	10,100	16,000	1.58	-0.33
509083	9,200	16,000	1.74	-0.17
184885	6,500	14,000	2.15	0.24
502689	35,000	76,000	2.17	0.26
217915	3,200	7,000	2.19	0.28
217901	2,700	6,000	2.22	0.31
206716	7,000	18,000	2.57	0.66
122250	5,600	17,000	3.04	1.13
165595	3,300	11,000	3.33	1.42
201158	5,200	18,000	3.46	1.55
409524	4,600	16,000	3.48	1.57
110469	4,400	17,000	3.86	1.95
431683	4,100	16,000	3.90	1.99
416093	3,600	19,000	5.28	3.37

Ratio Descriptive Statistics	
Mean	1.91
Median	1.66
Standard Deviation	1.36
Range	4.82
Minimum	0.46
Maximum	5.28
Count	26
Mean of Residuals	0.00
Filter	
Within 1 Std. Dev.	0.56 - 3.27
Mean + 1 Std. Dev.	3.27
Mean - 1 Std. Dev.	0.56
Within 2 Std. Dev.	-0.8 - 4.62
Mean + 2 Std. Dev.	4.62
Mean - 2 Std. Dev.	-0.80

Histogram of Ratios

Bin	*Frequency*
0.5	2
1.5	10
2.5	6
3.5	5
4.5	2
5.5	1

Because the residuals have been identified as normal, it is possible to use parametric functions such as standard deviations, which can be used to rank the data points according to their representativeness. Plus or minus one standard deviation in a normally distributed data set should contain about 67% of the data, which is what the age-dating data set contains (65.4%). Approximately 95% should be contained within +/- 2 standard deviations, which compares with 96% of this data set. The data set can then be trimmed to contain just the well locations that have been statistically identified as "representative" of the underlying population.

The mean of the residuals of the ratios is <0.01.

That leaves the spatial distribution. The next figure shows the location of those data points that lie within 1 standard deviation of the residual mean. The wells that lie outside of 1 standard deviation appear to be clustered along the Anoka-Hennepin county line on both sides of the Mississippi river. The lack of good spatial distribution of the residuals suggests that the data is not well fit to the assumptions used in this analysis, even though other measures looked fine. Close inspection of the Anoka-Hennepin cluster reveals large discrepancies in age between geographically proximate wells. This may be due to pumping which is drawing younger water into the aquifer and mixing it with the older water. This artificial recharge of younger water significantly affects some of the age-dated samples.

C. The Trim

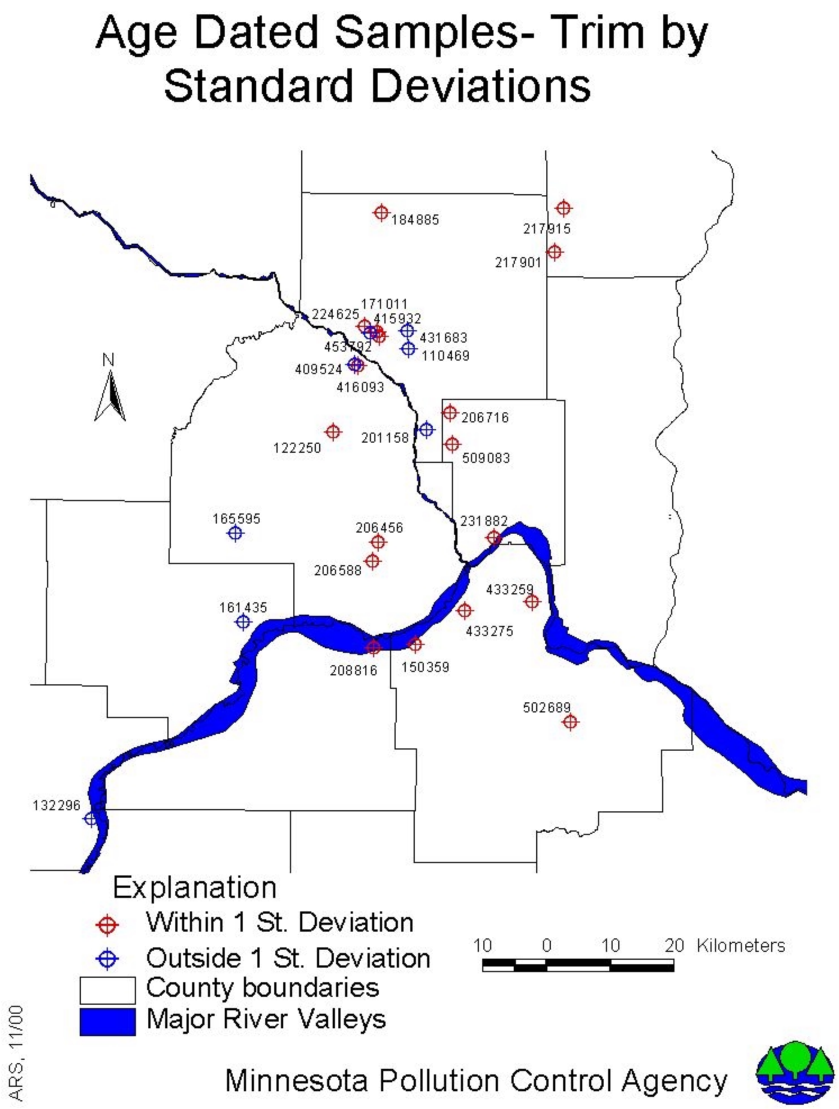

Figure B-4 – Age Dated Samples Trim by Standard Deviations